GCA Technical Report No. 63-23-N

ELECTRON DENSITY IN THE IONOSPHERE

L. G. Smith

Final Report
Contract No. NASw-98

July 1963

GEOPHYSICS CORPORATION OF AMERICA
Bedford, Massachusetts

Prepared for

NATIONAL AERONAUTICS AND SPACE ADMINISTRATION
Washington 25, D. C.

TABLE OF CONTENTS

TABLE OF CONTENTS (continued)

LIST OF ILLUSTRATIONS

LIST OF ILLUSTRATIONS (continued)

LIST OF ILLUSTRATIONS (continued)

INTRODUCTION

This Final Report is in two parts. Part I begins with a discussion of probe theory as developed by Langmuir and others. The next section is devoted to the application of the probe for rocket and satellite measurements in the ionosphere. In the following section the instrument used for probe measurements is described in some detail.

Part II of this report gives further details of the three pairs of rocket flights that comprised the main part of the experimental program. The first two rockets (Nike-Asp 3.12 and Nike-Cajun 10.25) were designed to test certain aspects of the theory and use of the Langmuir probe technique in the ionosphere. The second two (Nike-Cajuns 10.51 and 10.52) were used to study the structure of the nighttime E region of the ionosphere. The last two (Aerobee 4.48 and Nike-Apache 14.31) involved instruments "hitch-hiked" onto payloads containing other types of experiments. The launch dates and times and main results of the flights follow. All launches were from Wallops Island, Virginia.

(1) Nike-Asp 3.12, 1240 EST, 22 August 1960 -- The vehicle malfunctioned and failed to attain sufficient altitude for the scientific purposes of the flight. However, the instrumentation continued to operate

throughout the flight and it was possible to determine the cause of the malfunction: the coupling ring between payload and second stage gave way during second stage burning.

(2) Nike-Cajun 10.25, 1152 EST, 8 December 1960 -- This flight, a backup for the unsuccessful Nike-Asp flight established that the transmitter had no effect on the measurements and that the nose tip electrode was a simple and convenient probe. It was also shown that data could be obtained in the D-region where the probe was operating as a conductivity device.

(3) Nike-Cajun 10.51, 2206 EST, 17 August 1961 -- The experience of the previous flight led to an improvement in the technique, particularly suitable for examination of find structure in the electron density profile. This resulted in the penetration of a Sporadic E-layer on this flight.

(4) Nike-Cajun 10.52, 0435 EST, 27 October 1961 -- This was a further examination of the structure of the nighttime E-region and definitely established the value of the Langmuir probe technique for small sounding rockets.

(5) Aerobee 4.48, 0743 EST, 25 May 1962 -- In this case the instrument was included in a payload which was primarily a test of a recovery system. The instrument was, in fact, recovered in perfect condition. The flight was notable for the occurrence of a Sporadic E-layer.

(6) Nike-Apache 14.31, 1006 EST 16 October 1962 -- This payload carried, in addition to the Langmuir probe instrument, a C.W. propagation experiment, giving an independent method of measuring electron density. Data was lost for a ten-second period in the D-region due to RF breakdown at the antennas. This flight provided a significant comparison of the two techniques.

The scientific significance of the first two nighttime flights has been discussed in a technical report issued earlier.*

In addition to these flights a study was made of an ionospheric experiment for the satellite E.G.O. This phase of the project has been discussed in a separate report.**

*Smith, L.G., "Rocket Measurements of Electron Density and Temperature in the Nighttime Ionosphere", GCA Technical Report 62-1-N, (January 1962).
**Smith, L.G., "Ionospheric Experiment for the Eccentric Geophysical Observatory", GCA Technical Report 61-10-N, (December 1961).

PART I

THEORY AND USE OF THE LANGMUIR PROBE IN THE IONOSPHERE

NOMENCLATURE

A	probe area
e	electron charge
h	Debye length
i	current
i_e	electron random current
i_+	positive ion random current
j	current density
j_e	electron random current density
j_+	positive ion random current density
k	Boltzmann constant
m_e	electron mass
m_+	positive ion mass
M	molecular weight
n_e	electron density
T_e	electron temperature
T_+	positive ion temperature
v	vehicle velocity
$\overline{v_e}$	electron mean velocity
$\overline{v_+}$	positive ion mean velocity
V	probe potential
V_e	electron energy (volts)
V_f	floating potential
σ	area ratio
η	potential ratio

SECTION 1

LANGMUIR PROBE THEORY

1.1 RETARDING POTENTIAL ANALYSIS

The use of a probe in studying plasmas was originally put on a sound theoretical basis by Langmuir and his colleagues more than thirty years ago. [1-1] Experimentally, an electrode is inserted into the plasma and the current to it is determined as a function of the potential of the electrode. From the resulting current-voltage characteristic the electron energy distribution and the electron density are obtained.

When the electrode is exactly at the potential of the plasma the electron current to it is determined by the random thermal motions of the electrons in the gas. From kinetic theory the number of electrons striking unit area per second is $n_e\overline{v}_e/4$ where n_e is the electron density and $\overline{v}_e$ the mean electron velocity. Since each electron carries a charge e, the electron random current density j_e is given by

$$j_e = n_e e \overline{v}_e/4 \qquad (1\text{-}1)$$

The mean electron velocity $\overline{v_e}$ is related to the electron temperature T_e by

$$\overline{v_e} = (8kT_e/\pi m_e)^{\frac{1}{2}} \qquad (1\text{-}2)$$

where k is the Boltzmann constant and m_e is the electron mass. The use here of electron temperature implies a Maxwellian distribution, i.e., thermal equilibrium. Numerically,

$$\overline{v_e} = 6.21 \times 10^5 \, T_e^{\frac{1}{2}} \text{ cm/sec} \qquad (1\text{-}3a)$$

or

$$\overline{v_e} = 6.69 \times 10^7 \, V_e^{\frac{1}{2}} \text{ cm/sec} \qquad (1\text{-}3b)$$

where V_e is the electron energy in volts.

The variation of electron random current density as a function of electron density is shown in Figure 1-1 for three values of electron energy.

As the electrode is made negative with respect to the plasma, only those electrons with energies greater than the retarding potential can strike the electrode. For retarding potentials the electron current density j is given by

$$j = j_e \exp(eV/kT_e) \qquad (1\text{-}4)$$

where V is the retarding potential.

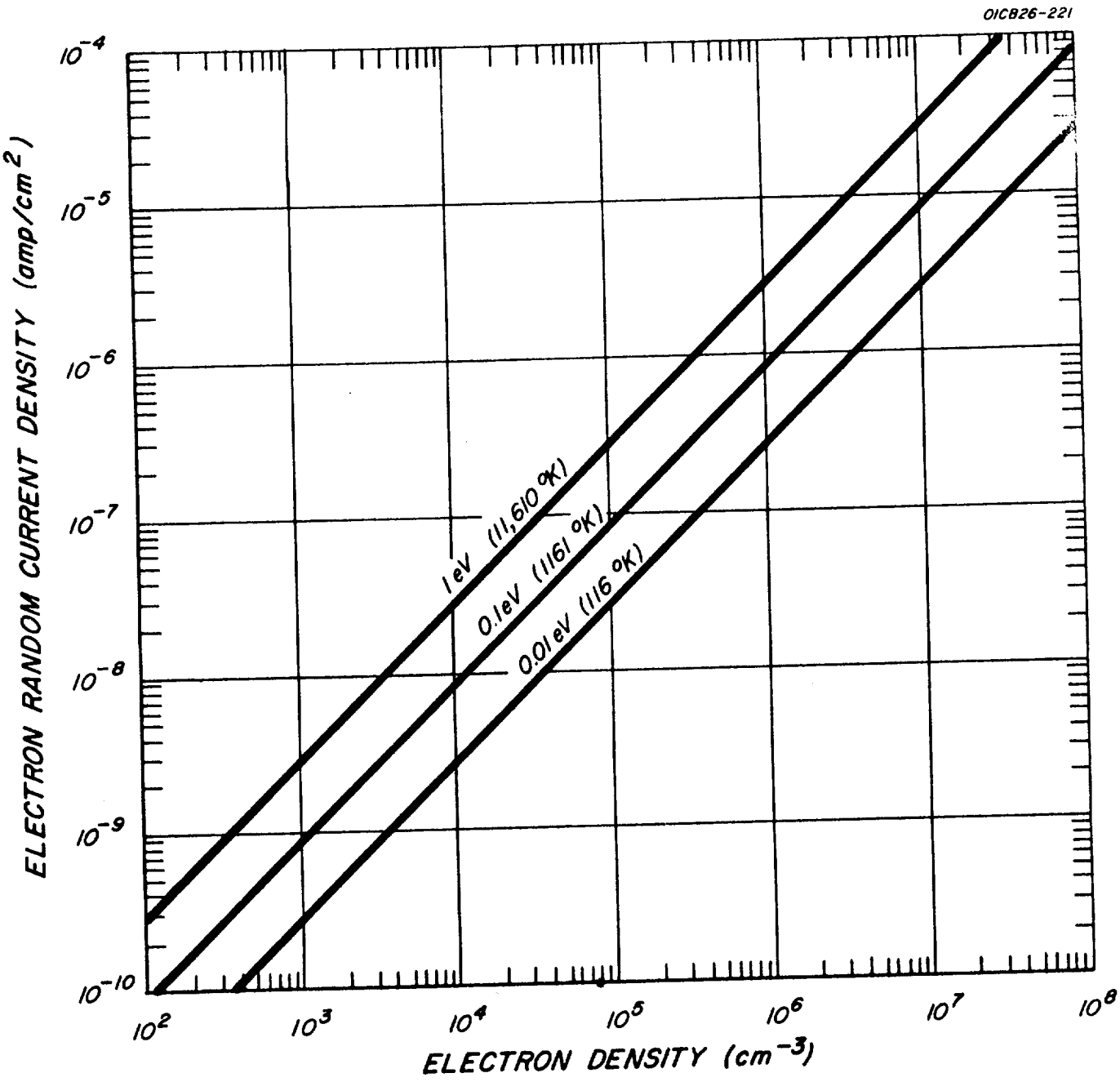

Figure 1-1. Electron random current density as function of electron density for three values of electron energy.

Equations (1-1), (1-2) and (1-4) above, define the theory of the Langmuir probe technique in its simplest possible terms.

1.2 PLASMA SHEATH

Important to the basic theory of the Langmuir probe, though not appearing explicitly in the formulae quoted above, is the concept of the plasma sheath--the space charge region adjacent to the electrode. It will be realized that the sheath has zero thickness (i.e., does not exist) when the electrode is at plasma potential. The concept of the sheath is important in two respects: (1) it provides a criterion for the validity of the technique; namely, that the mean free path be large compared with the sheath thickness, and (2) it provides a method of computing the current-voltage curves for accelerating potentials. Such calculations have been given in detail by Mott-Smith and Langmuir.(1-2)

The thickness of the plasma sheath varies with the potential of the electrode, but the scale of thickness can conveniently be expressed in terms of the plasma properties by the Debye shielding length h, defined by the equation

$$h = \left(\frac{kT_e}{4\pi\, n_e e^2} \right)^{\frac{1}{2}} = 6.90\ (T_e/n_e)^{\frac{1}{2}} \text{ cgs units} \qquad (1\text{-}5)$$

The variation of Debye shielding length with electron density is shown in Figure 1-2 for three values of electron energy.

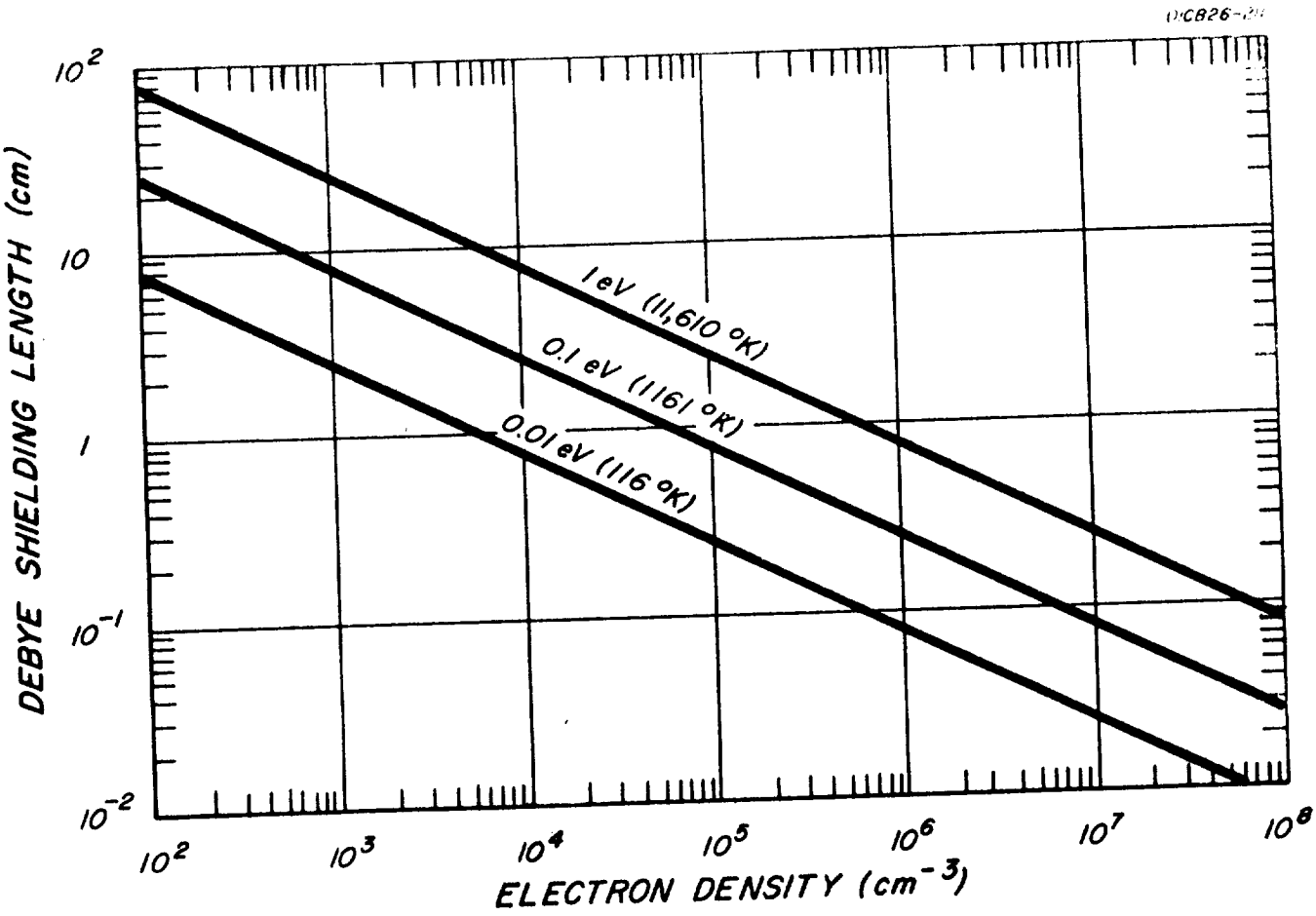

Figure 1-2. Debye shielding length as a function of electron density for three values of electron energy.

The current-voltage characteristic for accelerating potentials is a function of the shape and size of the electrode. Exact expressions are available when the dimensions of the electrode are very large or very small compared with the Debye shielding length:

(1) Large plane

$$j = j_e \tag{1-6}$$

(2) Long thin cylinder

$$j = j_e \left\{ \frac{2}{\pi^{\frac{1}{2}}} \left(\frac{eV}{kT_e}\right)^{\frac{1}{2}} + \exp\left(\frac{eV}{kT_e}\right) \operatorname{erf} \left(\frac{eV}{kT_e}\right)^{\frac{1}{2}} \right\} \tag{1-7}$$

(3) Small sphere

$$j = j_e \left(1 + \frac{eV}{kT_e}\right) \tag{1-8}$$

A normalized semi-log plot of electron current versus voltage is shown in Figure 1-3 for these three electrode configurations. The large plane and small sphere are limiting cases; all other electrode shapes result in plots falling within the region between these two curves. As noted before, for retarding potentials the current density is independent of electrode shape and the semi-log plot results in a straight line where slope gives the electron temperature. The point at which the electrode is at plasma potential is readily identified by the change in slope on this semi-log plot.

1.3 NON-MAXWELLIAN ENERGY DISTRIBUTION

When the electron energy distribution is not Maxwellian the log j-V plot is not linear in the retarding potential region. The

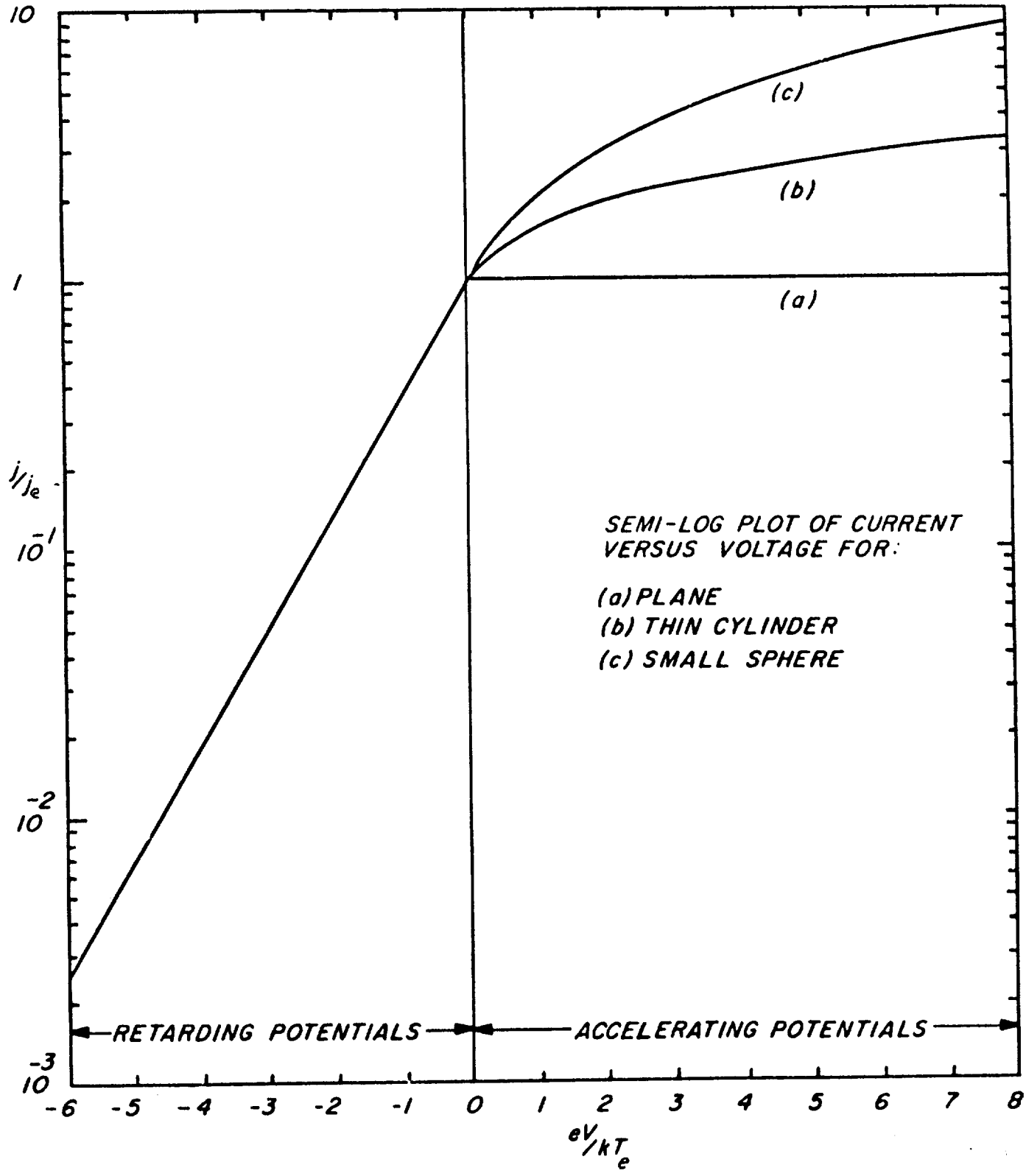

Figure 1-3. Theoretical semi-log plot of electron current.

current-voltage curve may still be analysed, however, to give the actual electron energy distribution. A convenient method, due to Druyvesteyn,[1-3] uses the second derivative d^2j/dV^2. Expressed in terms of the electron energy in volts, V_e, the distribution function $F(V_e)$ is given by

$$F(V_e) = \frac{1}{n}\frac{dn}{dV_e} = \frac{(8m)^{\frac{1}{2}}}{e^{3/2}} V^{\frac{1}{2}} \frac{d^2j}{dV^2} \qquad (1\text{-}9)$$

Several methods are available for obtaining the second derivative electrically though only recently has the theory of such methods been discussed generally.[1-4] The automatic technique was not incorporated in the instrument described in this report.

1.4 POSITIVE ION CURRENT

The current to the electrode is the sum of currents due to positive ions as well as electrons. (Here and later we postulate the absence of negative ions.) The positive ion component of the current is given by Equations (1-1), (1-2) and (1-4) when the sign of the potential is reversed and j_+, T_+, $\overline{v_+}$ and m_+ are substituted for the corresponding quantities j_e, T_e, $\overline{v_e}$ and m_e. Because of the much greater mass of the positive ion (for atomic oxygen $m_+/m_e = 16 \times 1836$), the positive ion random current density is smaller than the electron random current density by a factor of about 170. This has two important consequences: (1) correcting the observed current to obtain the electron current involves a small quantity, and (2) because the ion

current is small it is not practical to use the technique to obtain positive ion densities and temperatures.

1.5 FLOATING POTENTIAL

The potential at which the total electrode current is zero is of considerable significance in rocket and satellite measurements. This is a negative potential V_f known as the floating (or wall) potential, because any isolated conductor or insulator will come to this potential under electron and positive bombardment. Since the positive ion and electron currents must be equal in magnitude, the value of V_f is given by

$$j_+ = j_e \exp\left[-(eV_f/kT_e)\right]$$

or

$$eV_f = kT_e \log_e (j_e/j_+) = 5.1\ kT_e$$

for $(j_e/j_+) = 170$. Thus the floating potential is almost equal to five times the electron energy when both are expressed in volts. This value is very insensitive to the particular values assumed for ion mass and ion temperature.

1.6 BI-POLAR PROBE

An important development of the Langmuir probe technique is known as the floating double-probe method. (1-5) Two probes are inserted in the plasma and the current flowing between them is measured

as a function of the voltage difference without reference to the actual potential of the plasma. The method was originally developed to minimize the reaction of the probes on the plasma under investigation. It is also used on rockets and satellites where no reference potential is available.

The two probes comprising the bi-polar arrangement are not necessarily equal in size or shape. If the inequality in size of the two probes is considerable then the smaller can be treated as a single probe, the other providing a constant reference potential. An analysis of the current-voltage characteristic as a function of the area ratio (σ) is given in the appendix.

Three modes of operation of a bi-polar probe are determined by the magnitude of the area ratio of the probes σ and the ratio of electron to ion random current density j_e/j_+:

(1) $1 \leqslant \sigma < j_e/j_+$. In this mode of operation neither probe can be driven positive with respect to the plasma. Hence the electron random current density is not measured. In addition the value of electron temperature that is obtained is representative of these electrons with energies greater than a certain value. There is very little to recommend this mode of operation.

(2) $j_e/j_+ \leqslant \sigma < 10\ j_e/j_+$. Electron and ion random current densities are measured. The electron temperature is obtained for a complete spectrum of electron energies and it is possible to test for a Maxwellian distribution.

(3) $10j_e/j_+ \leqslant \sigma$. The merits of the previous mode are present with the advantage that the data evaluation is somewhat simplified. It has the disadvantage that, for a given total probe area, the probe current is rather small.

The optimum area ratio for the bi-polar probe is considered to be $\sigma = 10j_e/j_+$.

Another result of this analysis is that the value of electron temperature that is obtained is not affected by the area ratio of the electrodes.

1.7 LIMITATIONS OF PROBE THEORY.

There are restrictions on the use of the Langmuir probe. The following criteria must be met when applying the probe to the study of discharges in gases:

(1) The probe dimensions must be small in comparison to significant changes in potential over the space it occupies.

(2) The current drawn by the probe must not disturb the plasma.

(3) There must be no collisions within the sheath (i.e., the mean-free path must be large compared with the sheath thickness).

(4) There must be no production of electrons by impact, photoemission, etc., at the probe surface.

(5) Contact potential differences must be constant.

(6) Radio-frequency fields must be absent (because of the possibility of exciting plasma oscillations).

(7) The geometry of the probe arrangement must be clearly defined.

Within the limitations imposed by these criteria, the Langmuir probe has proved an elegant and powerful tool for the study of low pressure discharges. Attempts have been made to extend the use of the probe to other conditions, particularly to higher pressures, (i.e., short mean free paths) but the interpretation under these conditions is uncertain.

SECTION 2

THE PROBE IN THE IONOSPHERE

2.1 USEFUL ALTITUDE RANGE

The ionosphere in the E region provides an almost ideal plasma for application of the Langmuir probe technique. Values of some of the relevant quantities are given in Table 2-1. The theory of the probe is invalid at heights below about 90 km because two important factors do not meet the criteria previously given: (1) the mean free path is not large compared with the Debye length and (2) negative ions are present in significant numbers.

The use of the probe in the F region is limited by photoemission. The photoelectric current density from a tungsten surface exposed to unattenuated solar radiation is about 4×10^{-9} amp/cm^2. This is equal to the random current for a value of electron density of about 4×10^3 cm^{-3} (at a temperature of 10^{3o}K). This gives an upper limit to the height range for daytime measurements of about 1000 km.

TABLE 2-1

SELECTED QUANTITIES RELEVANT TO THE LANGMUIR PROBE IN THE IONOSPHERE

Height, h Km	150	250	350	700
Electron Concentration, n_e cm^{-3} (noon)	2×10^5	1×10^6	2×10^6	2×10^5
*Temperature, T^oK	1031	1415	1445	1812
Molecular Weight, M (ions)	28	16	16	16
Ratio, $\overline{v_e}/\overline{v_+}$ $(= j_e/j_+)$	228	170	170	170
Electron Mean Velocity, $\overline{v_e}$ cm sec^{-1}	2.0×10^7	2.3×10^7	2.4×10^7	2.7×10^7
Ion Mean Velocity, $\overline{v_+}$ cm sec^{-1}	8.8×10^4	1.4×10^5	1.4×10^5	1.6×10^5
Electron Random Current Density, j_e amp cm^{-2}	1.6×10^{-7}	9.2×10^{-7}	1.9×10^{-6}	2.1×10^{-7}
Ion Random Current Density, j_+ amp cm^{-2}	7.0×10^{-10}	5.4×10^{-9}	1.1×10^{-8}	1.2×10^{-9}
Floating Potential, V_f volt	-0.48	-0.63	-0.64	-0.80
Debye shielding length, h cm	0.50	0.26	0.19	0.66

*Values up to 700 km from 1959 ARDC Model Atmosphere

2.2 ENVIRONMENT OF THE VEHICLE

The atmosphere in the vicinity of a rocket or satellite is disturbed from its quasi-equilibrium state. The electron density, probably more than any other property, is susceptible to considerable modification. If a probe is to succeed in measuring ambient electron density it is of the utmost importance that the interaction of the vehicle and the ionosphere be understood. Considered to be of potential importance are:

(1) Ionization by R. F. excitation, increasing the electron density.

(2) Absorption of R. F. energy, increasing the electron temperature.

(3) Rectification at the antennas, modifying the vehicle potential.

(4) Escaping gas and outgassing, tending to dilute the plasma.

(5) Vehicle motion, modifying the spatial density distribution.

(6) Shock wave ionization, increasing the electron density.

(7) Photo emission from the vehicle, modifying the vehicle potential.

(8) Magnetic fields (including the geomagnetic field) modifying the probe current.

Effects associated with the R. F. transmitters, when, as usually is the case, the data is telemetered, with gas contaminating the environment and with vehicle motion can, in practice be made negligible by suitable design of the experiment. Photoemission (in daytime) and the geomagnetic field are left as being inherent limitations on a probe measurement of electron density. The theory of operation of the probe should be modified to incorporate these effects.

2.3 VEHICLE MOTION

It is in the nature of rocket and satellite-borne instruments they are moving with significant velocity relative to the plasma. It is important to consider the effect of this relative motion on the operation and interpretation of the probe. Two separate aspects of the motion can be distinguished.

2.3.1 Effect of Motion on Ion Current. The velocity of a sounding rocket (say 1 km/sec) is comparable with, and the velocity of a satellite (say 8 km/sec) is appreciably greater than, the mean velocity of the ions (of the order of 1 km/sec), although both are very small compared with the mean velocity of electrons (about 200 km/sec). The ion current to an electrode is increased due to relative motion whereas the electron current is not appreciably changed. An exact expression has been given by Sagalyn, Smiddy and Wisnia[2-1] for a spherical electrode. This is shown graphically in Figure 2-1. When the vehicle velocity, v, equals the mean ion velocity, $\overline{v_+}$, the current is increased about 40 percent above the value with no relative motion. For a satellite having a velocity of 8 times the mean ion velocity the current is increased by a factor of about 8. Since the ion current is still small compared with the electron current the motion of the vehicle does not affect the retarding potential analysis for electrons.

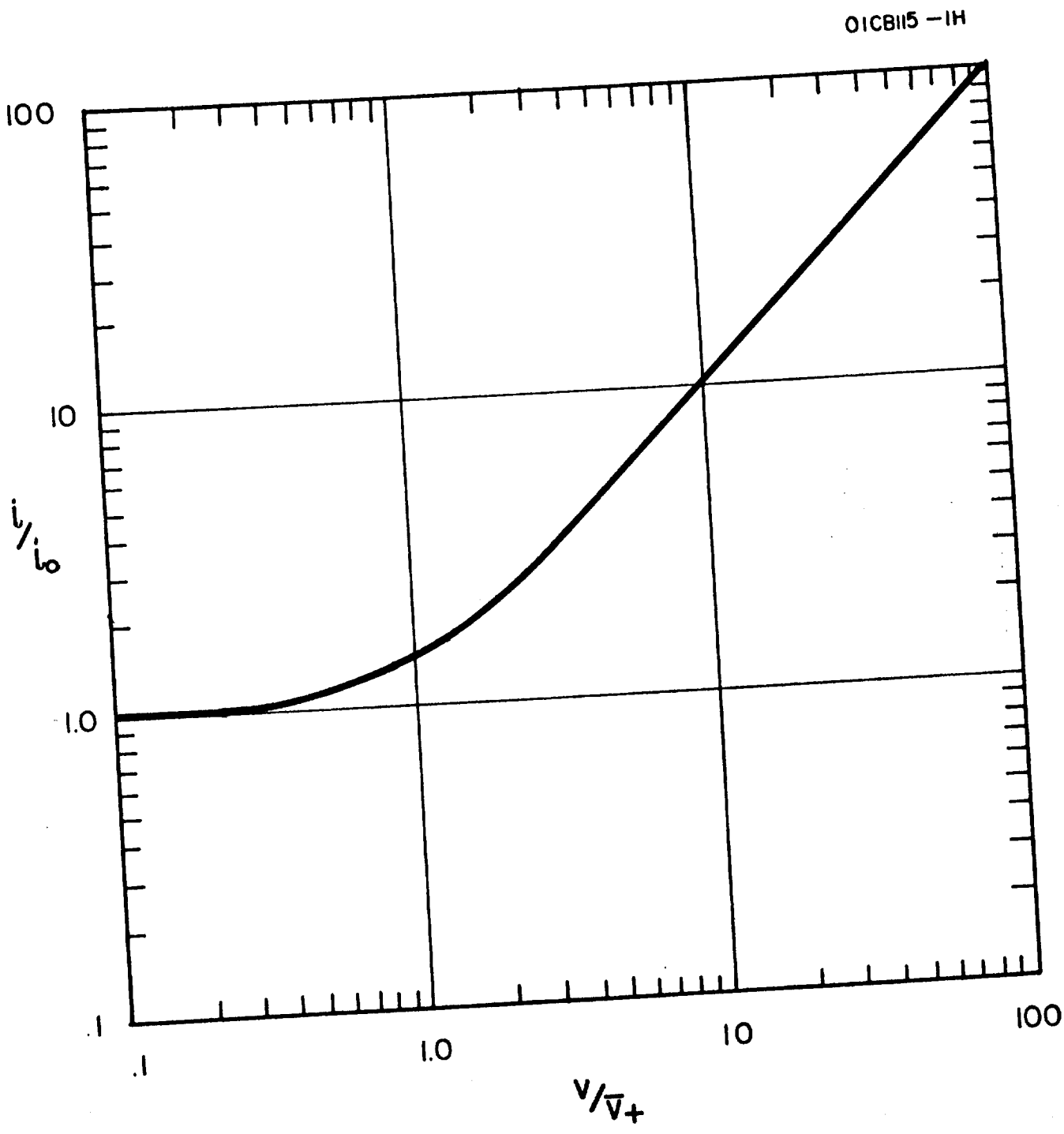

Figure 2-1. Effect of vehicle velocity on ion current.

2.3.2 Rarefaction in the Vehicle Wake. A further factor affecting the design of a probe experiment results from the local disturbance of ion and electron density due to rarefaction in the wake of a body traveling through the plasma with a velocity comparable with or greater than the mean ion velocity.[2-2] Although the electrons have sufficient velocity individually to penetrate this region the absence of a neutralizing positive space charge prevents the build up of an appreciable electron concentration with the result that the electron density distribution also shows a rarefaction in the wake of the vehicle. This effect showed up clearly in an early flight (Nike-Cajun 10.25) which included in the payload an electrode in the form of a disc flush-mounted in the cylindrial section of the payload housing. This rocket slowly executed a large precession cone while spinning more rapidly on its longitudinal axis. It was found that the current to this probe was modulated in synchronism with the spin, being a minimum with the electrode at the trailing side of the payload. The probe on a rocket or satellite should therefore be located so as to minimize the probability of its passage through the rarefied vehicle wake.

2.4 MAGNETIC FIELD

A factor which is not considered in simple probe theory is the effect of a magnetic field. In the E region the radius of gyration (Larmor radius) for electrons in the geomagnetic field is about 1 cm. Since this dimension is less than the mean free path of the electrons and comparable with the size of the probe normally used, the motions of electrons into or away from the probe must be profoundly affected.

In some unpublished lecture notes F. F. Chen states that in a magnetic field weak enough that the ion Larmor radius is large compared with the probe radius and the Debye length and hence that j_+ is not affected, but strong enough that the electron Larmor radius is comparable to or smaller than the relevant dimensions, the ratio j_e/j_+ falls to 10 or 20. In the absence of a magnetic field the ratio j_e/j_+ has a value of about 200. Thus the geomagnetic field would tend to decrease the observed value of j_e by an order of magnitude. There is some evidence that this is the case. Chen also states that, in the presence of a weak magnetic field the retarding potential analysis would not be affected and the resulting value of electron temperature should be correct. It should be pointed out however, that there exists no comprehensive mathematical treatment of the Langmuir probe theory in the presence of even a weak magnetic field. This is of no particular concern in respect of the use of the probe to measure electron density where other methods (such as radio-frequency techniques) can be used to check and calibrate the equipment. There is no direct method of measuring electron temperature, however, which is not based on Equation (1-4).

2.5 MEASUREMENT OF IONOSPHERIC IRREGULARITIES

An important aspect of probes carried by rockets and satellites is their ability to resolve the fine structure of the medium. This is most important initially in respect to electron density where less direct methods, e.g., radio star scintillations, have indicated that

significant variations exist having typical dimensions as small as 200 meters.

A basic weakness of the conventional Langmuir probe technique is its poor time resolution. This follows because a complete sweep of potential of the electrode leads to only a single value of electron density and of electron temperature. In practice, the sweep duration is limited by two factors: (1) a bandwidth of the measuring device, and (2) the bandwidth of the telemetry system. A sweep duration of the order of one second is generally convenient for rocket and satellite measurements although this can be reduced to about 0.1 sec at the expense of elaborating the instrument. However, an alternative method has been developed and used with considerable success.(2-3)

The method is experimentally very simple but somewhat more difficult to justify on theoretical grounds. It consists in changing the program of the voltage applied to the probing electrode from one of consecutive sweeps to a program in which occasional sweeps are separated by periods of fixed voltage. In recent flights using the technique, the program consists of a sweep voltage of -2.7 to +2.7 volt (duration 0.5 sec) alternating with a fixed voltage of +2.7 volt (duration 1.5 sec), Figure 2-2.

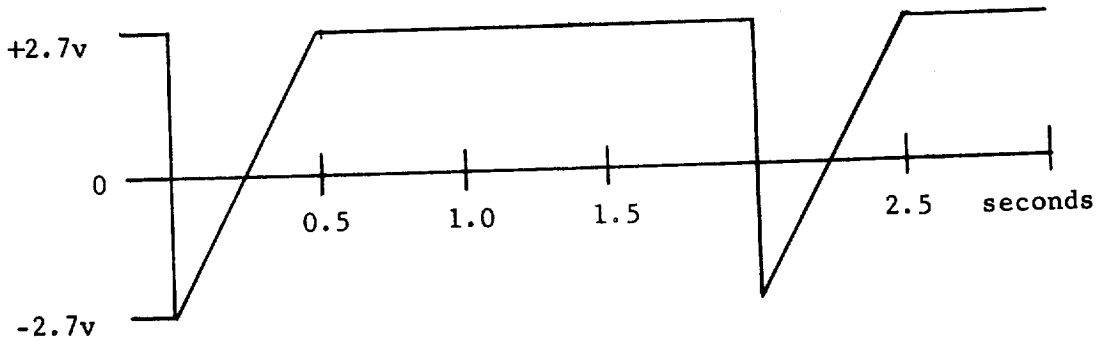

Figure 2-2. Probe Voltage Program.

The probe current at fixed potential is proportional to electron density. The only assumption made is that electron temperature is constant; the current is proportional to the average velocity of the electrons and hence varies as $(T_e)^{\frac{1}{2}}$. The proportionality of current to electron density has been verified in the flight of a rocket (Nike-Apache 14.31) which carried a D.C. probe and a C.W. propogation experiment, the latter prepared by S. J. Bauer.

The distance resolution of the instrument used in this way depends on the vehicle velocity and the bandwidth of the system (including telemetry). For a rocket with a velocity of 1 km/sec and a bandwidth of 1 kc/sec the distance resolution is 1m, more than adequate for present applications. In a satellite having a velocity of 8 km/sec the bandwidth required to give a distance resolution of 80m would be 100c/sec.

2.6 TELEMETRY REQUIREMENTS

The bandwidth required in the telemetry channel is principally determined by the lower limit of electron temperatures. In the lower E region values of electron temperature as low as $300^{o}K$ have been measured and it is probably desirable that the limit for the measurement be set at $100^{o}K$. This corresponds to a mean electron energy of about 0.01 volt. Now the sweep voltage applied to the probe has a slope of 10 volts/sec which is equal to an increment of 0.01 volt in 1 msec. This indicates that the bandwidth should be about 1 kc/sec if the exponentially rising current in the retarding potential region is to be transmitted.

The output of the instrument is an analog voltage and may be transmitted by any standard telemetry system. It has been found that the FM/FM system is the most convenient manner of telemetering for this instrument when used on sounding rockets.

2.7 CONTACT POTENTIAL

A feature of the current-voltage plots obtained on rocket flights using the bi-polar arrangement is that they do not pass through the origin of coordinates. Thus with zero potential applied to the electrode (either nose or side) the current is not zero. Similarly the electrode must be made positive with respect to the rocket body to reduce the probe current to zero. Comparison of actual and theoretical plots shows that the curve is displaced along the voltage axis rather

than the current axis. Thus the effect is due to a bias voltage appearing in the probe circuit. This bias voltage usually lies between 0.5 and 1.0 volt and may change slowly with time, Figure 2-3.

The bias is believed to be an effect produced by contact potential though no complete explanation can be given. It has been observed in laboratory tests that, while there is no bias voltage when an ohmic (carbon) resistor is used as a load, the bias appears when a very dilute solution of common salt is used. This was also noticed on one occasion (Nike-Cajun 10.108) the bias voltage appeared as salt spray accumulated on the rocket during the pre-launch period. (Incidentally, the leakage current due to the salt spray disappeared at launch).

The contact potential presumably arises from the use of dissimilar metals for the two electrodes of the bi-polar arrangement. The change during flight is believed to be due to the heating of the electrodes during the launch phase.

The actual value of the contact potential is of no consequence in the normal retarding potential analysis since the potentials are automatically referred to plasma potential. It does, however, somewhat affect the fixed-voltage mode of operation of the probe since any change in contact potential produces an equal change in the potential of the probe with respect to the plasma. When this effect is important a correction may be obtained from the individual current-voltage plots.

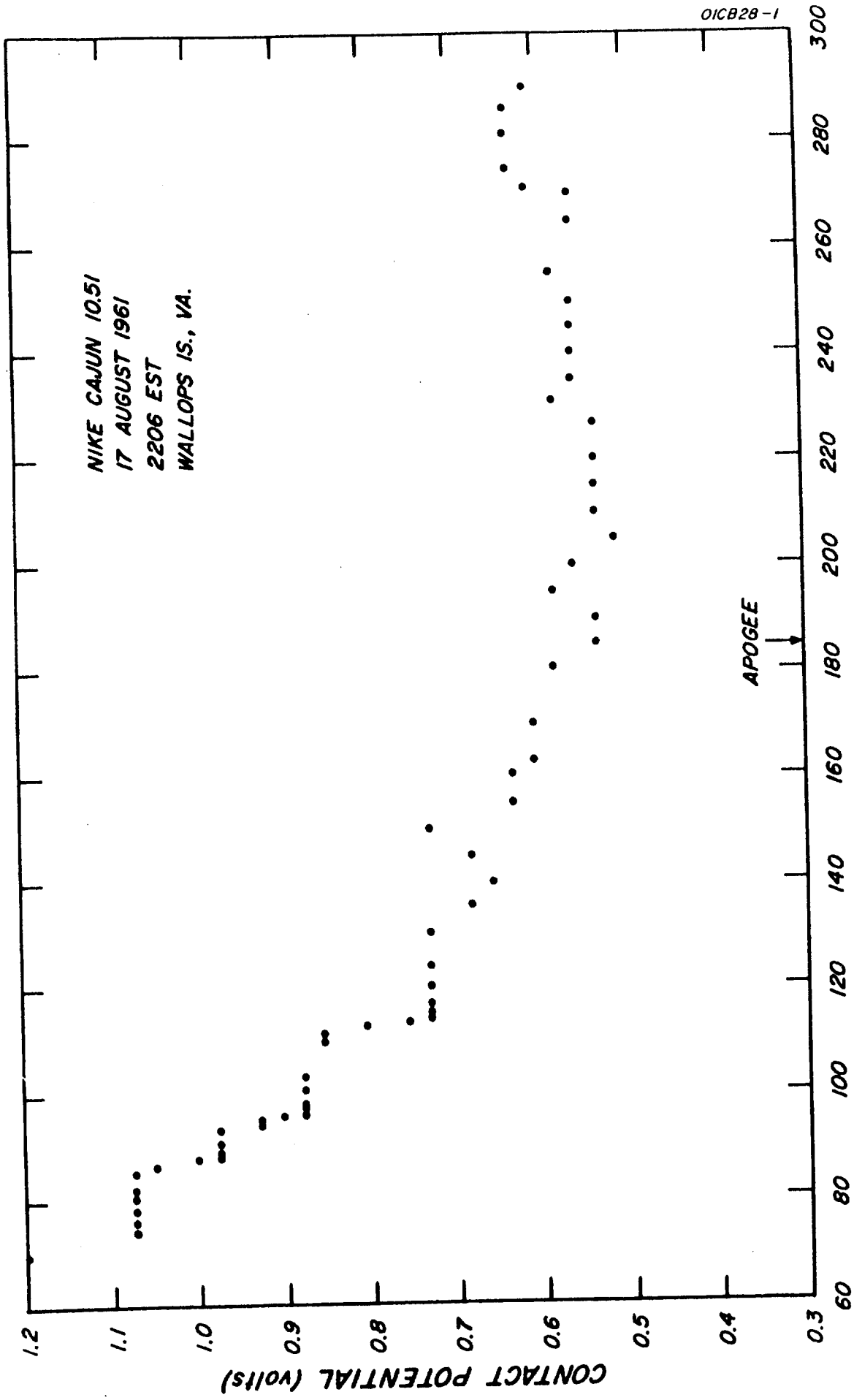

Figure 2-3. Variation of contact potential.

2.8 PROBE IN THE D REGION

In daytime flights probe current is first measured at about 50 km and at night at about 75 km. Profiles obtained on four recent flights are shown in Figure 2-4. Nike-Cajun 10.99 was a pre-dawn flight into a quiet ionosphere with sporadic E present (the bifurcated layer between 98 and 102 km). Nike-Cajun 10.108 was also a pre-dawn flight but into a disturbed ionosphere (indicated by the ionosonde). Nike-Cajun 10.109 was launched at sunset into a quiet ionosphere with sporadic E present (possibly the peak at 110 km). Nike-Apache 14.86 gave a typical daytime profile.

The proportionality of probe current to electron density can be justified on theoretical grounds at heights greater than 90 km. The general appearence of these profiles, however, strongly suggest that this proportionality is also true in the lower portions of the profiles. In the daytime profile the so-called C layer may be identified between 50 and 65 km with the peak at 58 km. The D layer, occurring between 65 and 82 km, corresponds with the absorption of Lyman-α radiation. The nighttime profiles show a generally steeper gradient. Pending further analysis of the operation of the D.C. probe and possible comparison with independent techniques the profile of probe current should be taken to indicate the type of structure that prevails in the D region and the values of electron density disregarded.

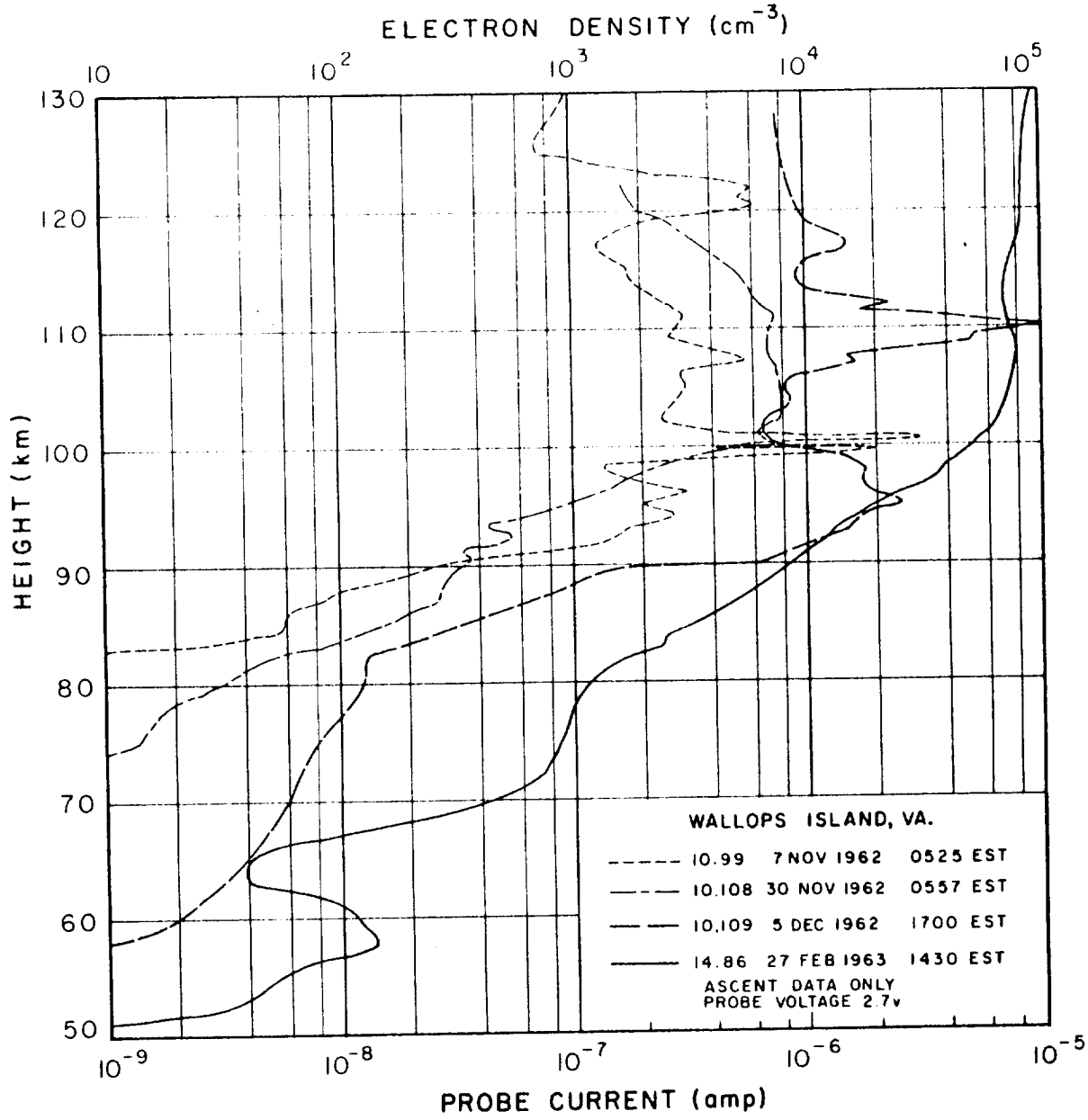

Figure 2-4. Profiles of probe current in the D and lower E region.

SECTION 3

INSTRUMENTATION

3.1 GENERAL ARRANGEMENT

The instrument has been constructed in several models differing in detail but with the same basic circuit arrangement. The instrument has been used most frequently with the nose tip of the rocket as the probing electrode. This may be seen in Figure 3-1 which shows the payload of Nike-Cajun 10.52. The circular electrode on the side of the payload was found to be unsatisfactory and was not used on subsequent flights. Otherwise the external configuration has remained the same. The probe instrumentation occupies the top three decks visible in the figure while the lower part of the instrumentation rack is used for power supplies and telemetering equipment. The upper encapsulated section contains two magnetic aspect sensors.

A different version of the instrument was build to be flown in the nose of an Aerobee. The unit, shown in Figure 3-2 with the heat shield removed from the upper section (program unit), was flown on Aerobee 4.48. The basic method of construction has been retained in subsequent flights of Nike-Apache rockets.

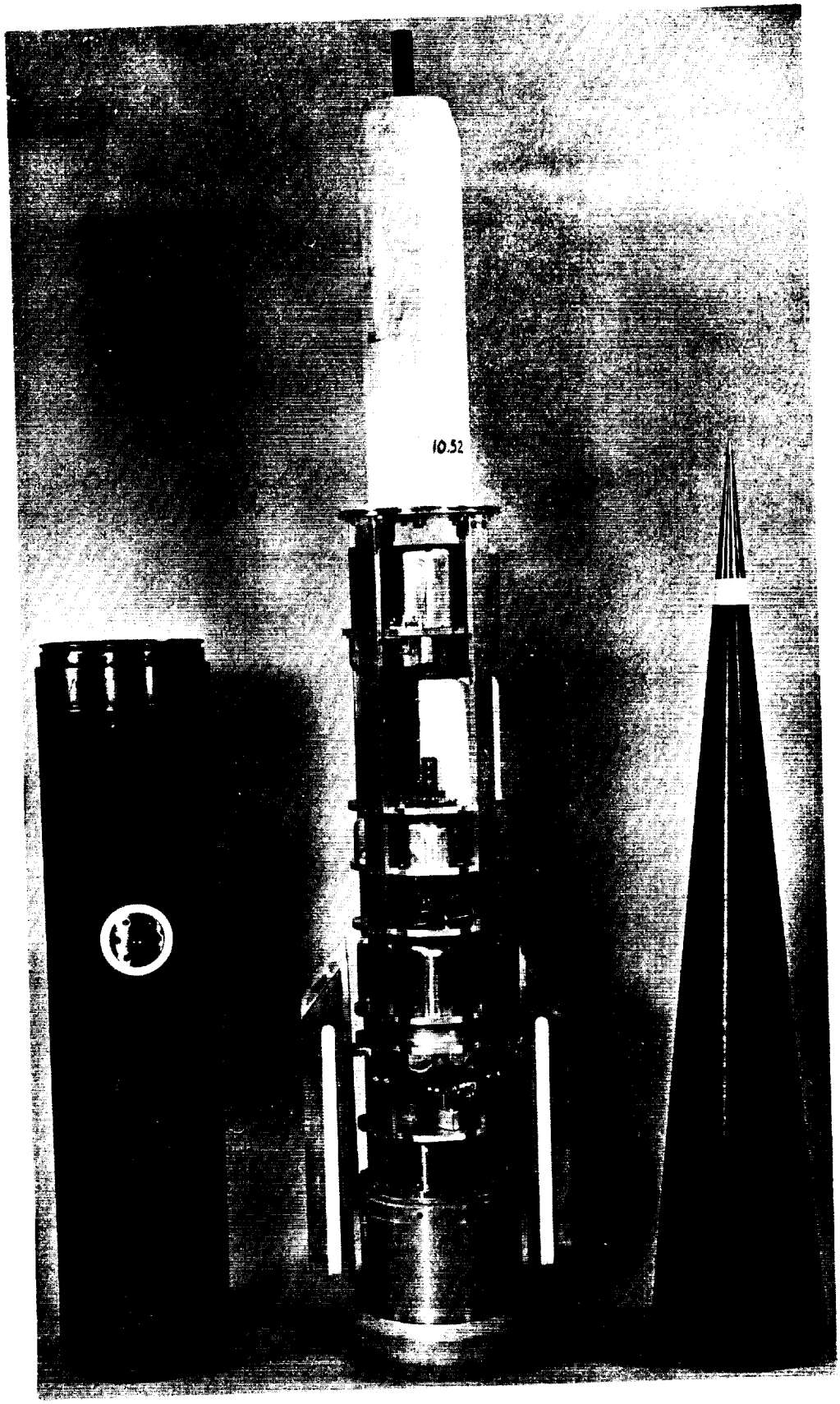

Figure 3-1. Payload of Nike-Cajun 10.52.

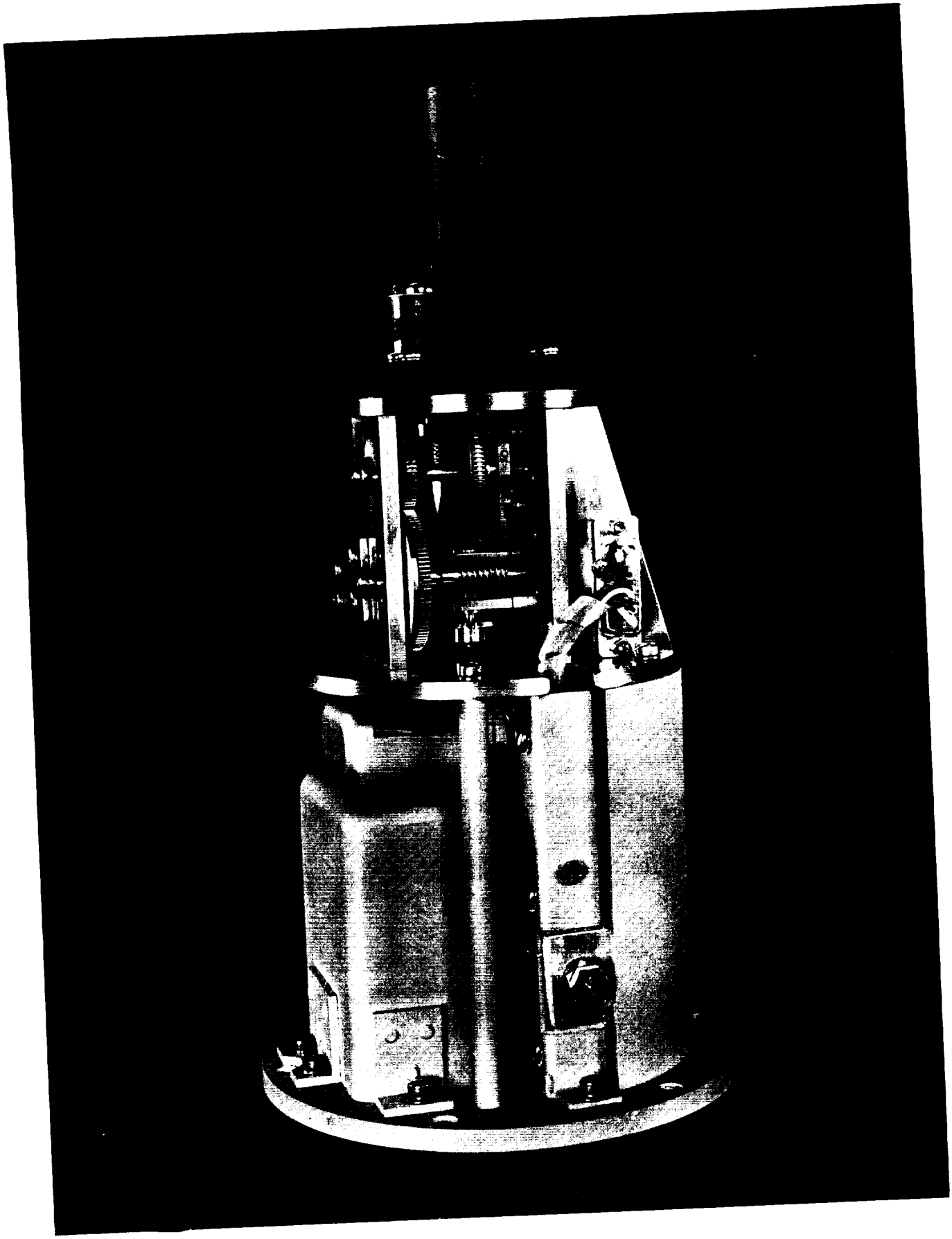

Figure 3-2. Instrument with heat shield removed.

The basic circuit of the probe is shown schematically in Figure 3-3. The two main parts are the electro-mechanical program unit and the electrometer. The program unit is so called because it creates the voltage function applied to the probe. The electrometer converts the probe current to an analog voltage which is the output of the instrument.

The program unit forms the upper part of the complete instrument which is constructed in modular form. The lower part contains a central wiring channel to which four sub-assemblies are attached: the program unit from the top, the electrometer from the front and, from the back, the battery box and the unit containing the thyrite resistor and the calibration resistor. The diameter of the base is 5-1/2 in. and the height 8-1/2 in. The unit can be installed inside a cone having a 6-1/2 in. diameter at the base and a 20° included angle. The weight of the complete instrument is 5 lb.

The instrument is normally used with a conical electrode having an included angle of 11° or 20°. The construction in either case is the same and is shown in Figure 3-4 for an 11° cone. The electrode assembly replaces the standard nose tip and therefore does not add extra weight to the payload. Electrical connection is made through the rod which mates with a special connector on the instrument and allows a limited amount of relative motion (such as results from thermal expansion of the payload housing).

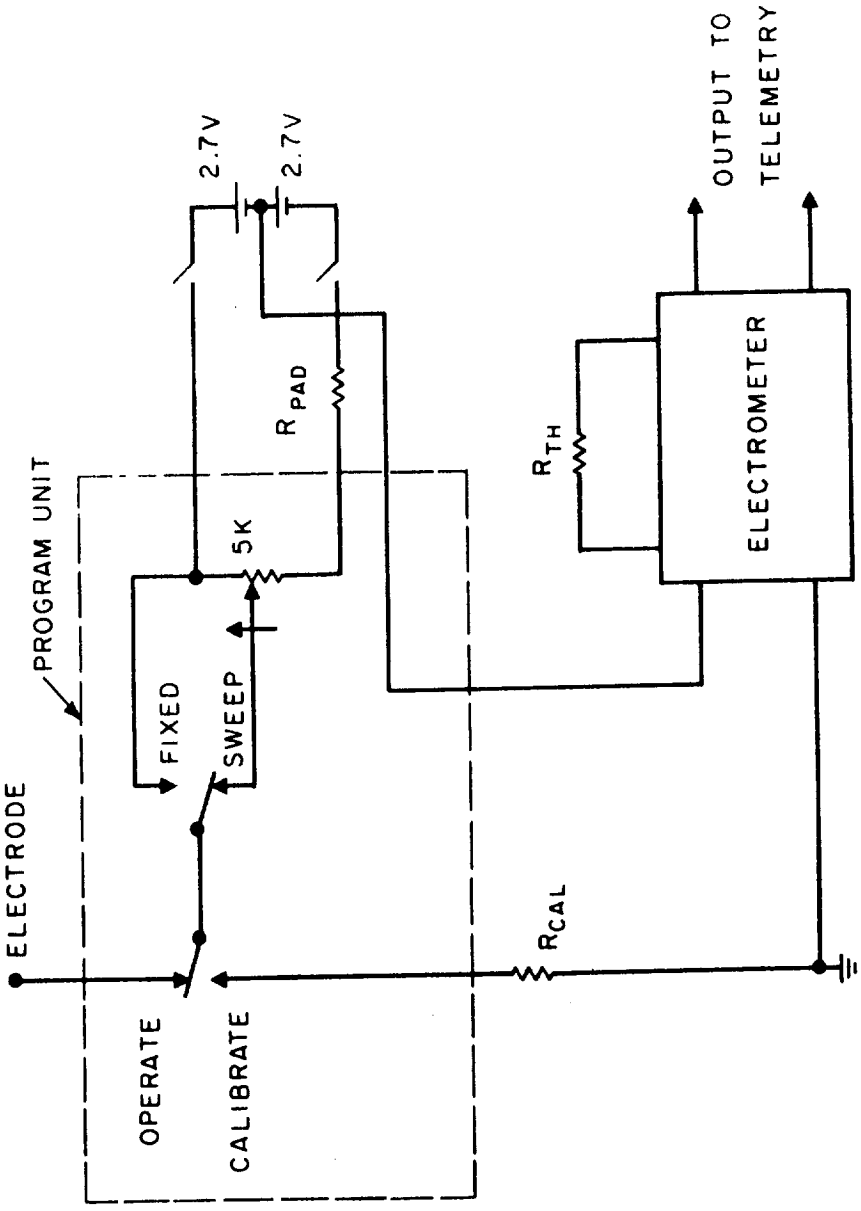

Figure 3-3. Probe circuit schematic.

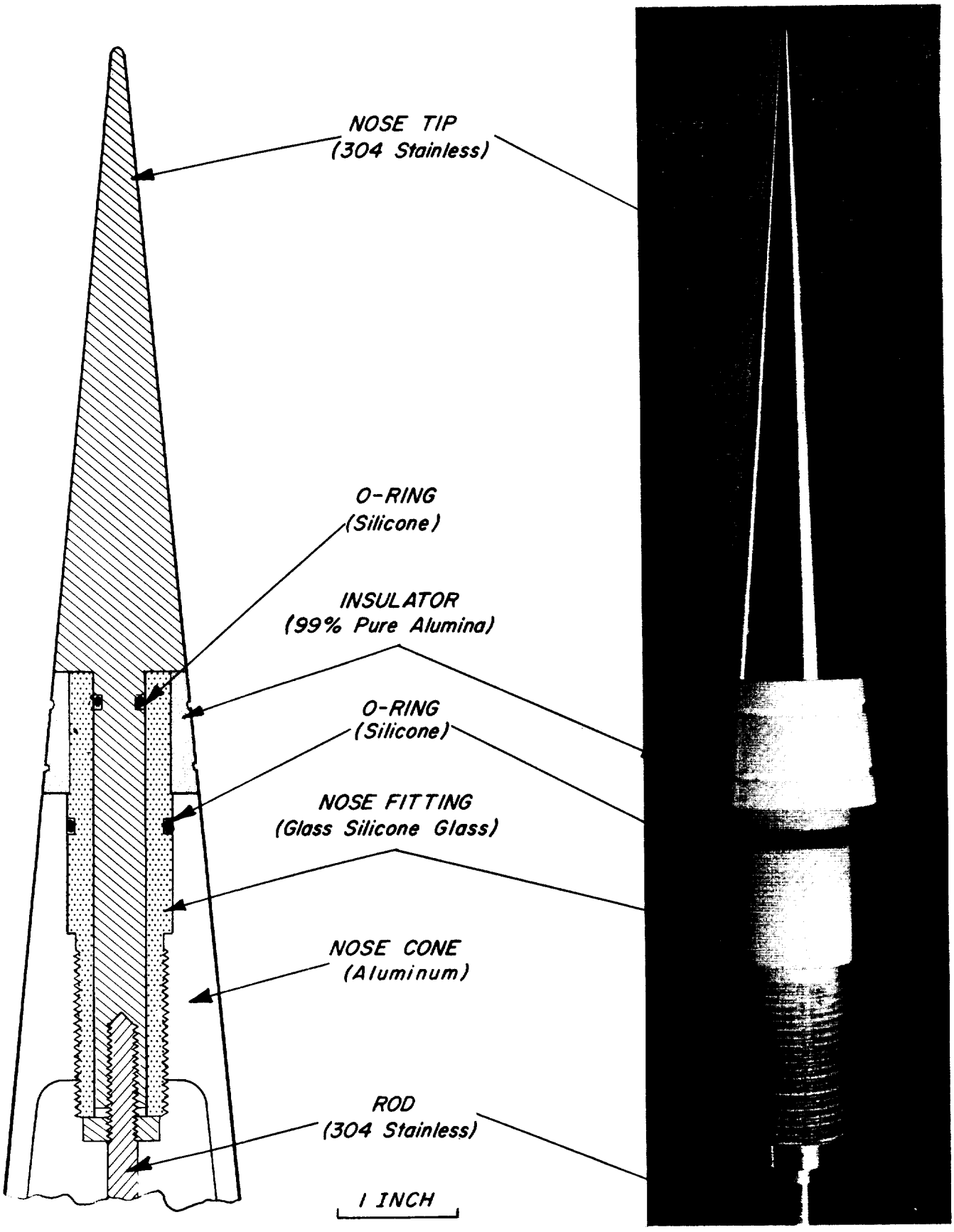

Figure 3-4. Nose tip electrode.

3.2 PROGRAM UNIT

The program unit serves three main functions:

(1) Sweep generator. A linear potentiometer (5k ohm) is driven in continuous rotation at about 2 rps.

(2) Mode Switching. A cam-operated microswitch alternates the mode of operation between a single sweep (-2.7 volts + 2.7 volt, duration 0.5 sec) and a period of fixed voltage (+2.7 volt, duration 1.5 sec).

(3) Calibration. A second cam-operated microswitch inserts a fixed resistor in place of the probe at intervals of 20 seconds for the duration of a single sweep.

The construction of the program unit in the most recent instruments is shown in Figure 3-5. A dc motor (Globe Industries, No. 41A345) with a shaft speed of 100 rps drives the potentiometer at 2 rps. This is followed by the mode-switching cam (#1) at 1/2 rps and the calibration cam (#2) at 1/20 rps. In some applications a commutator has been added on the shaft carrying cam #1. (The commutator was used with magnetic aspect sensors and had no electrical connection with the probe).

Inaccuracies due to variation of motor speed are eliminated by monitoring the speed. A magnetic pick-up is excited by a five-pole generator on the motor shaft giving an ac signal of 500 cycles per second (nominal). Using a small transformer this is added to the output of the instrument at an amplitude of 100 mv (peak-to-peak). Each cycle corresponds to a fixed increment in sweep voltage. A resistor (about 1K ohm)

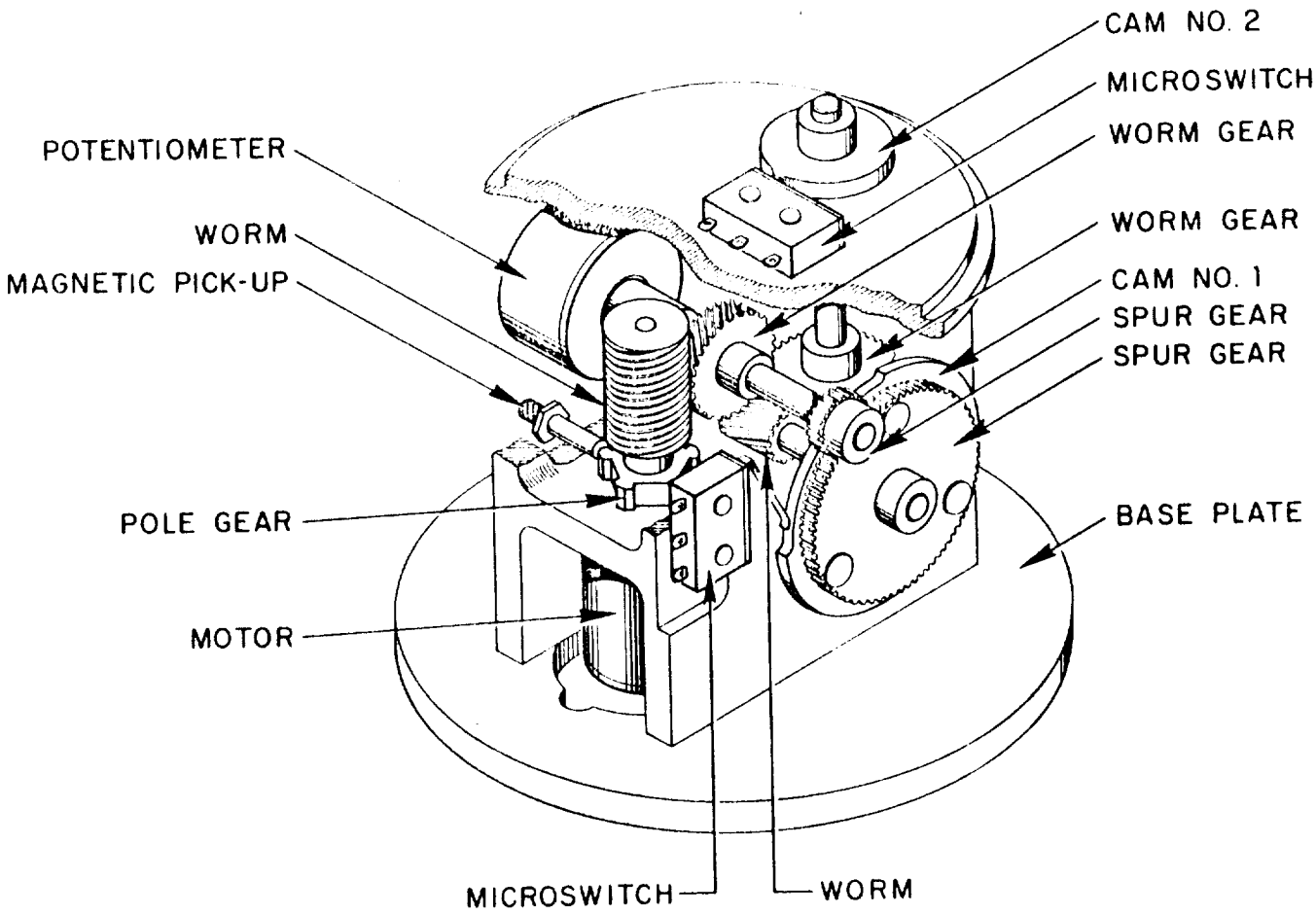

Figure 3-5. Program unit.

is added in series with the sweep potentiometer to give an increment of exactly 0.02 volt per cycle. The presence of these voltage markers on the telemetry record has been found to facilitate date-reduction as well as to increase the accuracy of the measurement. Power for the motor is obtained from the main supply (+28 volt) while the probe voltage is derived from two 2.7 volt mercury cells (Mallory TR-132R). The latter supply is switched on by means of a relay.

3.3 ELECTROMETER

The probe current is measured in the electrometer, Figure 3-6. The tubes in the input stage of this balanced circuit are type 6946 (Sylvania). This is a rugged tube suitable for the severe environment of sounding rockets. Tubes having grid currents less than 10^{-10} amp are selected for use in the electrometer. The electrometer employs 100 percent current feedback. A novel feature is the use of a thyrite resistor (General Electric, Magnetic Materials Division) as the feedback element which results in a compressed scale. The calibration curve of one having a full scale current of about 15 microamp is shown in Figure 3-7. Note that the output of the electrometer is +0.6 volt for zero current at the input of the electrometer. This allows small positive-ion currents to be measured within the limits of 0 and 5 volt prescribed by the standard telemetry systems.

The thyrite resistor alone determines the overall sensitivity of the instrument. With the particular electrode at present in use an electron density of 10^4 cm^3 gives a probe current (at +2.7 volt) of

is added in series with the sweep potentiometer to give an increment of exactly 0.02 volt per cycle. The presence of these voltage markers on the telemetry record has been found to facilitate date-reduction as well as to increase the accuracy of the measurement. Power for the motor is obtained from the main supply (+28 volt) while the probe voltage is derived from two 2.7 volt mercury cells (Mallory TR-132R). The latter supply is switched on by means of a relay.

3.3 ELECTROMETER

The probe current is measured in the electrometer, Figure 3-6. The tubes in the input stage of this balanced circuit are type 6946 (Sylvania). This is a rugged tube suitable for the severe environment of sounding rockets. Tubes having grid currents less than 10^{-10} amp are selected for use in the electrometer. The electrometer employs 100 percent current feedback. A novel feature is the use of a thyrite resistor (General Electric, Magnetic Materials Division) as the feedback element which results in a compressed scale. The calibration curve of one having a full scale current of about 15 microamp is shown in Figure 3-7. Note that the output of the electrometer is +0.6 volt for zero current at the input of the electrometer. This allows small positive-ion currents to be measured within the limits of 0 and 5 volt prescribed by the standard telemetry systems.

The thyrite resistor alone determines the overall sensitivity of the instrument. With the particular electrode at present in use an electron density of 10^4 cm^3 gives a probe current (at +2.7 volt) of

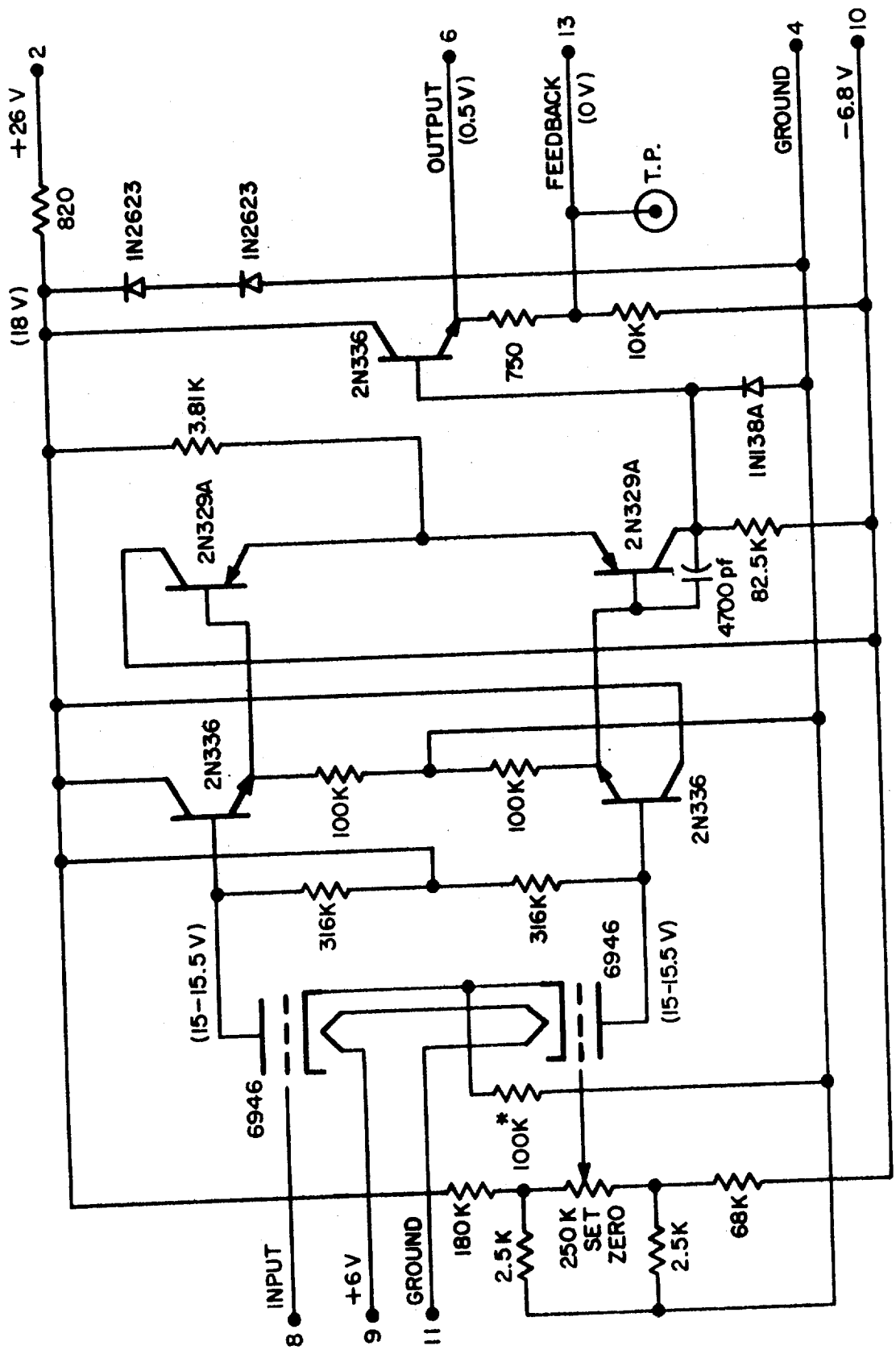

Figure 3-6. ELECTROMETER

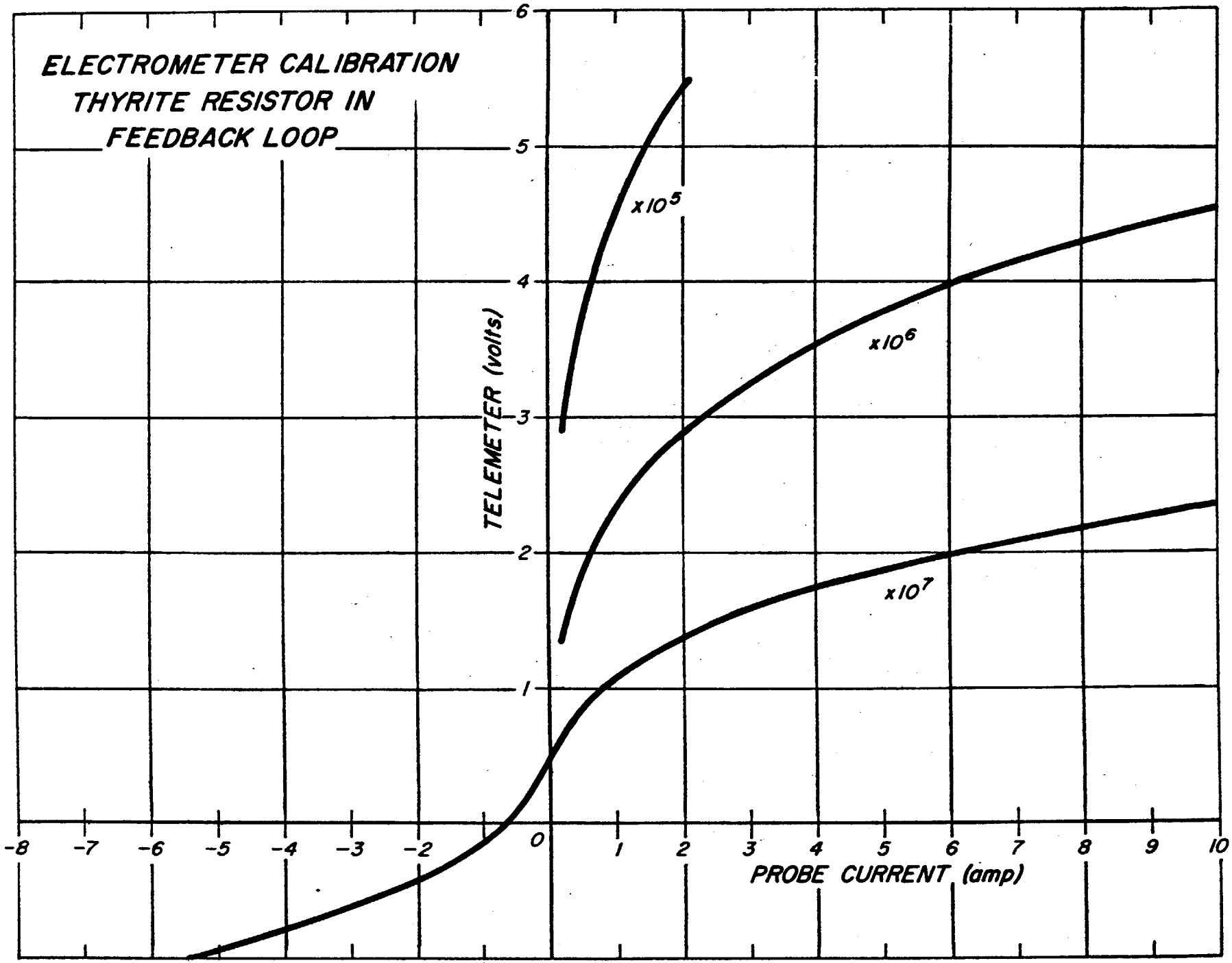
ELECTROMETER CALIBRATION
THYRITE RESISTOR IN
FEEDBACK LOOP
TELEMETER (volts)
PROBE CURRENT (amp)
x10^5
x10^6
x10^7
6
5
4
3
2
1
0
-8
-7
-6
-5
-4
-3
-2
1
2
3
4
5
6
7
8
9
10

about 1 microamp. Thus for daytime E region measurements a thyrite giving a current of 30 micoramp (measured at 5 volt) would be selected while at night one giving a current between 5 and 10 microamp (at 5 volt) would be appropriate. Thyrites which show a marked polarity effect (i.e. the magnitude of the current depends on the polarity of the applied voltage) are rejected. Thyrites are also rather temperature sensitive; they are therefore thermally shielded and in addition are calibrated at regular intervals during the flight.

Power for the instrument is obtained from main supply (200 milliamp at +28 volt). In addition the electrometer required a negative supply (1 milliamp at -6.8 volt) which can conveniently be obtained from mercury cells.

3.4 SPECIAL NOTES

The payload housing and rocket motor casing form the second electrode of the bi-polar system. Any voltages developed across portions of the external surface must be carefully considered to avoid interfering with the operation of the probe. One precaution that has been adopted is to disconnect all signals from the umbilical connector using relays within the payload.

A second possible problem concerns rocket gas which could conceivably disturb the ionosphere in the vicinity of the electrode. Trouble from this cause is avoided by sealing the payload with O-rings at the nose tip and providing vent holes toward the rear: four holes, 0.75 in. diameter equally spaced on the circumference. Venting also permits the

inclusion in the payload of an altitude switch. This is used for arming a door release mechanism (when used) and in determining trajectory.[3-1]

A further precaution which is observed is to limit the power of the telemetry transmitter. It has been found on two occasions that rf breakdown at the antennas supresses the probe current; the vehicle becomes a few volts negative with respect to the plasma potential. Using quadraloop antennas seen in Figure 3-1 with a transmitter developing 5 watts (at 231.4 Mc/sec) breakdown occurred intermittently between 55 and 80 km. No breakdown has been observed at the normal power of 2 watts.

3.5 DATA REDUCTION

The telemetered signal is always tape recorded at two independent ground stations. At the same time a real-time record is obtained at a chart speed of 10 in./sec and a sensitivity of 1 in./volt. This high-speed record is used to obtained electron temperatures. A slow-speed record is also prepared, generally by play-back of the tape, but sometimes in real-time, at a chart speed of 0.25 in./sec and a sensitivity of 1 in./volt. For this record the normal bandwidth of the telemetry channel is reduced to about 100 cycles per second. This eliminates the small ac signal which at the slow speed would merely broaden the trace.

The slow-speed record immediately shows the electron density profile. An example is given in Figure 3-8 which was obtained about one hour before dawn. The record on descent was photographically reversed

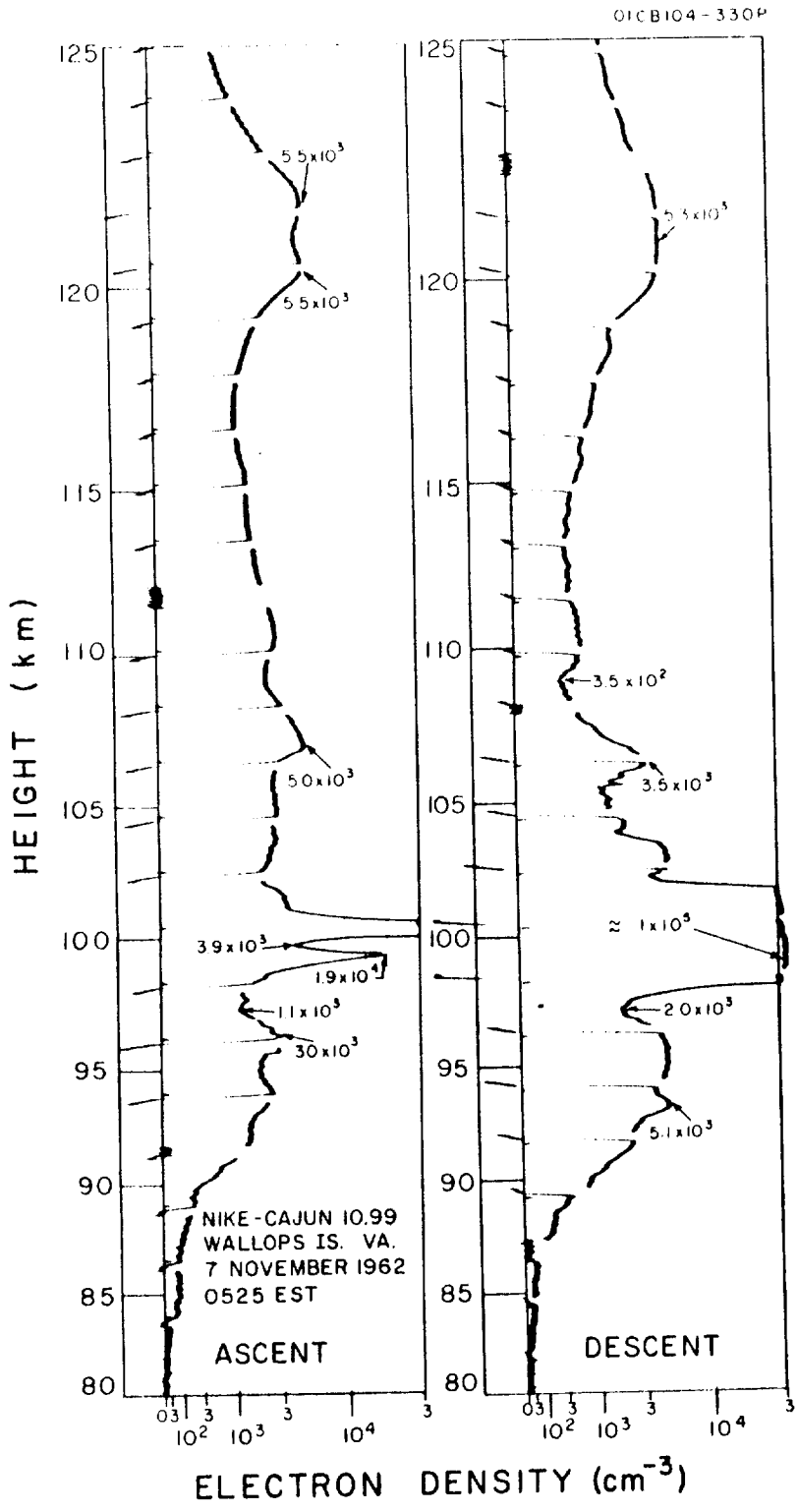

Figure 3-8. Sections of telemetry record showing electron density profile, 7 November 1962, 0525 EST.

for easier comparison with the corresponding portion on ascent. The height scale is obtained directly from radar data. The electron density scale is obtained from the pre-flight or in-flight calibration using a scaling factor obtained from daytime measurements when the absolute value electron density at the peak of the E layer may be obtained from a local ionosonde. The scaling factor used in this case is 1.1×10^{-6} amp equivalent to 1.0×10^{4} cm^{-3}.

The reduction of the data to obtain electron temperature is rather tedious. Individual sweeps of probe voltage must first be measured on the high-speed chart record and a graph prepared of current against voltage. The part of the graph representing collection of positive ions is extrapolated as shown in Figure 3-9 and subtracted from the total probe current to give electron current. This is then plotted on a conventional semi-log plot as shown in Figure 3-10. The slope of the linear part of this semi-log plot gives the electron temperature directly. In principle the absolute value of electron density can also be obtained from this plot by identifying the point at which the probe is at the potential of the plasma; this is normally taken to be the upper limit of the linear portion of the plot. In practice it is difficult to identifying the point accurately due to the gradual curvature of the graph. It is found, in addition, that the absolute values obtained in this way are significantly lower than theory indicates. The discrepancy has not yet been adequately explained and it is recommended that this method of analysis not be used to obtain electron density.

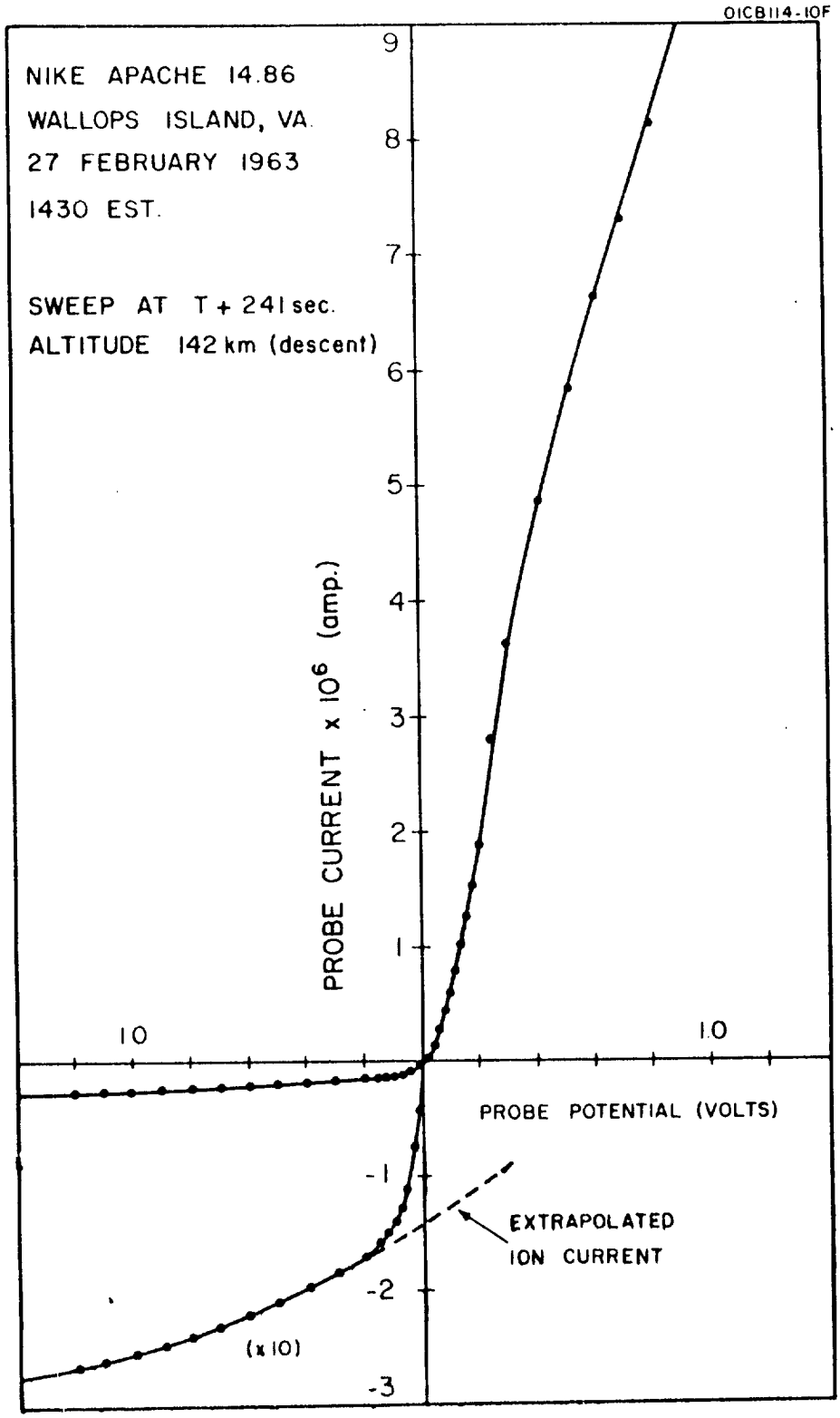

Figure 3-9. Current-voltage characteristic.

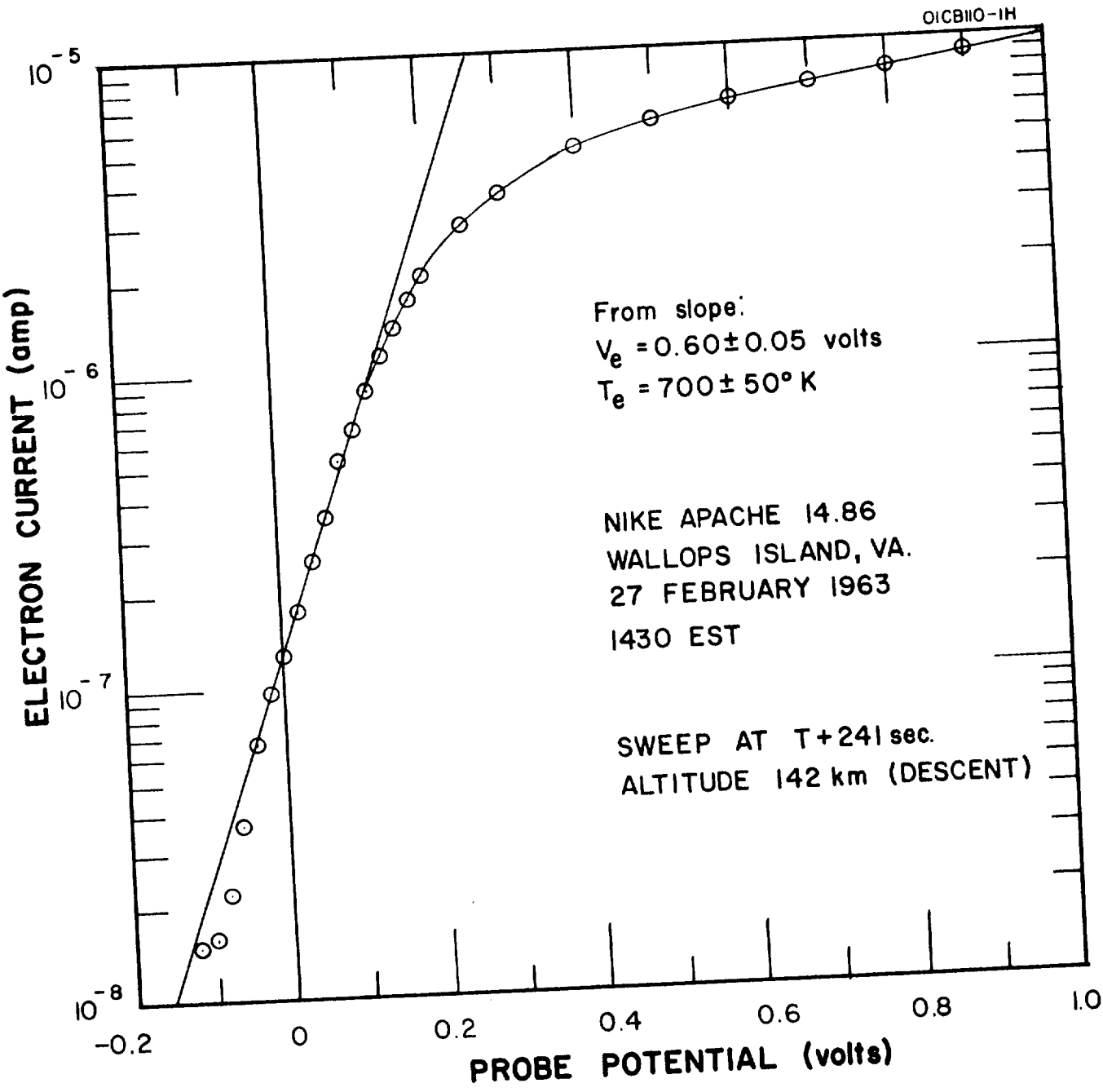

Figure 3-10. Semi-log plot of electron current vs probe potential.

APPENDIX A

THE ASYMMETRICAL BI-POLAR PROBE

Consider an asymmetrical bi-polar probe consisting of two electrodes of unequal surface area between which a potential may be applied and the resulting current measured. It is assumed that (1) the electron velocity distribution is Maxwellian and can be represented by the temperature T and (2) the sheath thickness is small compared with the radius of curvature of the electrodes, so that the current saturates for accelerating potentials.

Initially, with both electrodes at the same potential, the system assumes a negative potential with respect to the plasma, the floating potential, V_f, given by

$$V_f = -(kT_e/e)\log_e (j_e/j_+) \qquad \text{(A-1)}$$

where k is Boltzmann's constant

T_e the equivalent electron temperature

e the electronic charge

j_e the electron random current density

j_+ the positive ion random current density.

A potential V is applied between the electrodes, V being taken to be positive when the smaller (area A_2) is positive with respect to the larger (area A_1). The potentials of the electrodes assume new values V_1 and V_2, where

$$V = V_2 - V_1 \tag{A-2}$$

The electron currents to the electrodes are, for retarding potentials,

$$i_{e1} = A_1 \, j_e \exp[eV_1/kT_e] \tag{A-3}$$

$$i_{e2} = A_2 \, j_e \exp[eV_2/kT_e] \tag{A-4}$$

where the subscripts 1 and 2 refer to the larger and smaller electrode, respectively.

It is convenient at this point to introduce two parameters: the area ratio:

$$\sigma = A_1/A_2 \tag{A-5}$$

and the voltage ratio:

$$\eta = eV/kT_e \tag{A-6}$$

with appropriate subscripts for V being applied to η. Thus η is the potential V expressed as a multiple of the electron energy in voltage units.

Now the positive ion currents to the two electrodes are independent of V_1 and V_2 and have values

$$i_{+1} = A_1 \, j_+ \tag{A-7}$$

and

$$i_{+2} = A_2 \, j_+ \tag{A-8}$$

The total electron current must be numerically equal to the total positive ion current, that is

$$i_{e1} + i_{e2} = i_{+1} + i_{+2} \qquad \text{(A-9)}$$

From (A-3) and (A-4):

$$i_{e1}/i_{e2} = (A_1/A_2)\ \exp[e(V_1 - V_2)/kT_e] \qquad \text{(A-10)}$$

that is

$$i_{e1}/i_{e2} = \sigma\ \exp[-\eta] \qquad \text{(A-11)}$$

and from (A-7) and (A-8):

$$i_{+1}/i_{+2} = \sigma \qquad \text{(A-12)}$$

Finally the probe current i is given by

$$i = i_{+1} - i_{e1} \qquad \text{(A-13)}$$

Therefore, using (A-9), (A-11), (A-12) and (A-13), we find:

$$i/i_{+1} = \left[\frac{\exp(\eta) - 1}{\exp(\eta) + \sigma}\right] \qquad \text{(A-14)}$$

This is the mathematical formulation of the current-voltage characteristic of an asymmetrical bi-polar probe having an area ratio $\sigma(\geq 1)$. It is plotted in Figure A-1 for values of σ of 1, 10, 100, and 1000. The curve for the symmetrical bi-polar probe ($\sigma = 1$) is point symmetric about the origin (only the positive half is shown). For values of σ greater than 100, the curves become point symmetric about the point

$$i/i_{+1} = 0.5 \qquad \text{(A-15)}$$

and

$$\eta = \log_e\ (2 + \sigma). \qquad \text{(A-16)}$$

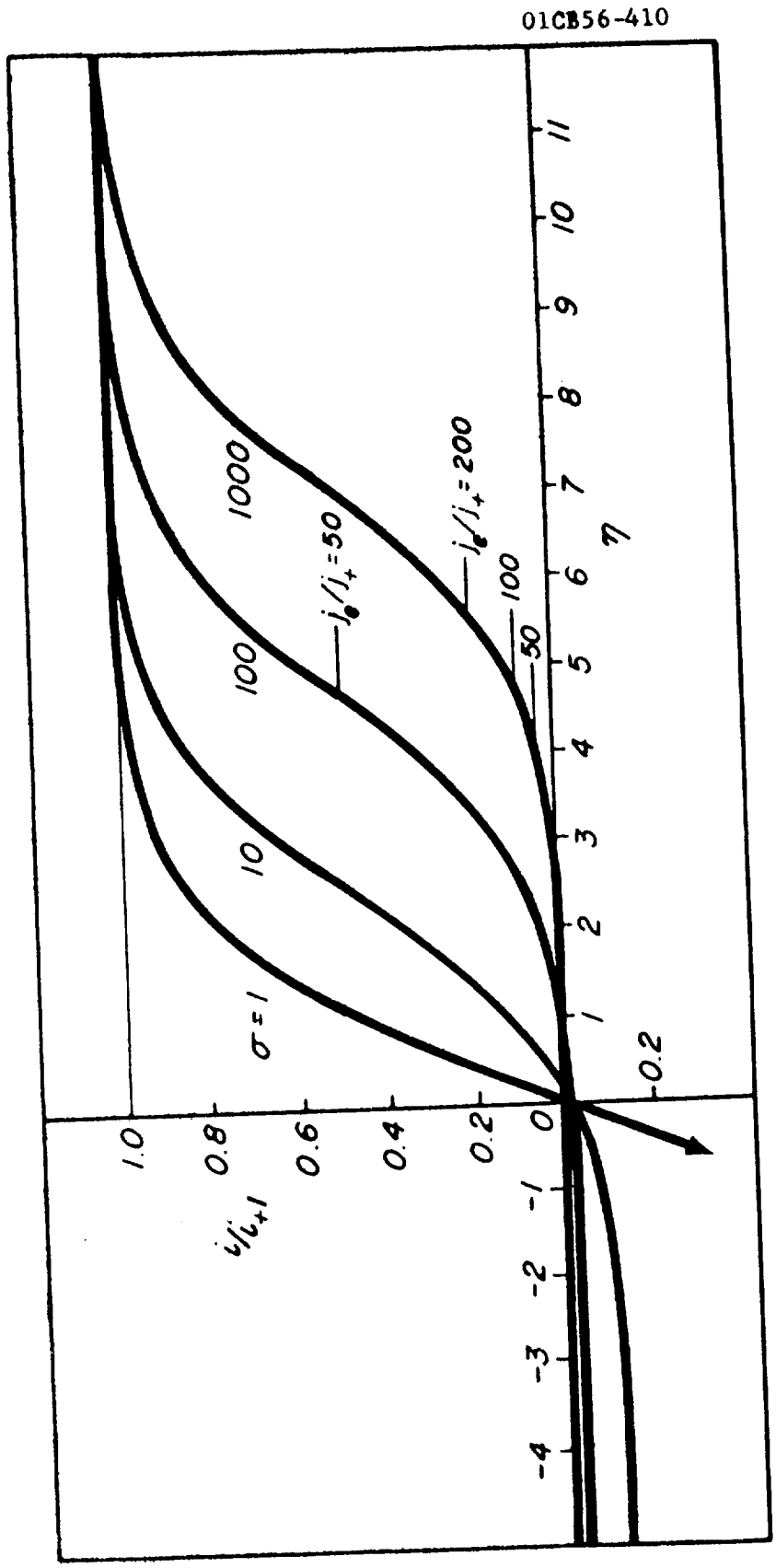

Figure A-1. Current-Voltage Characteristics for Four Values of Area Ratio.

We must now introduce the restriction that the above analysis is valid only for retarding potentials on the electrodes. For accelerating potentials, the electron current is limited to the random current density. Now the potentials of the two electrodes, η_1 and η_2, are given by

$$\exp(-\eta_1) = (j_e/j_+)\,\frac{\sigma + \exp(\eta)}{\sigma + 1} \qquad \text{(A-17)}$$

and

$$\exp(-\eta_2) = (j_e/j_+)\,\frac{\sigma \exp(-\eta) + 1}{\sigma + 1} \qquad \text{(A-18)}$$

Saturation occurs when the smaller electrode reaches space potential ($\eta_2 = 0$) at a value of η given by

$$\exp(\eta) = \frac{\sigma(j_e/j_+)}{\sigma + 1 - (j_e/j_+)} \qquad \text{(A-19)}$$

and a value of i given by

$$i/i_{+1} = (j_e/j_+ - 1)/\sigma \qquad \text{(A-20)}$$

If $\sigma < (j_e/j_+ - 1)$, no electron current saturation occurs.

The point at which electron current saturation occurs is thus determined by the area ratio σ and the random current density ratio j_e/j_+. The short horizontal lines in Figure A-1 indicate electron current saturation. In the ionosphere the value of j_e/j_+ is computed to be about 200.

The floating potential $\eta_f (=eV_f/kT_e)$ is from equation (A-1),

$$\exp(\eta_f) = j_e/j_+ \qquad \text{(A-21)}$$

and therefore, as might be expected, for very large σ ($\gg j_e/j_+$) the smaller electrode saturates when η is equal to the floating potential. In other words, for sufficiently large σ the smaller electrode is essentially a single probe and the larger electrode maintains a constant potential equal to the floating potential. We may determine how large σ must be for such a simplification to be made; it evidently must be several times the value of j_e/j_+. In Figure A-2 the curves of Figure A-1 are replotted on semi-log paper in the manner used on deriving electron temperature. On this plot the ordinate is

$$\Delta i/i_{+1} = (i + i_{+2})/i_+1 \qquad \text{(A-22)}$$

The single Langmuir probe is characterized by a linear plot on semi-log paper. It is seen in Figure A-1 that for all values of σ the plots are very close to linear for $\Delta i/i_{+1} \leqslant 0.1$. Now electron saturation occurs at $\Delta i/i_{+1} = (j_e/j_+)/\sigma$. Therefore the condition that the asymmetrical bi-polar probe may be analyzed as a single probe is

$$\sigma \geqslant 10\ (j_e/j_+). \qquad \text{(A-23)}$$

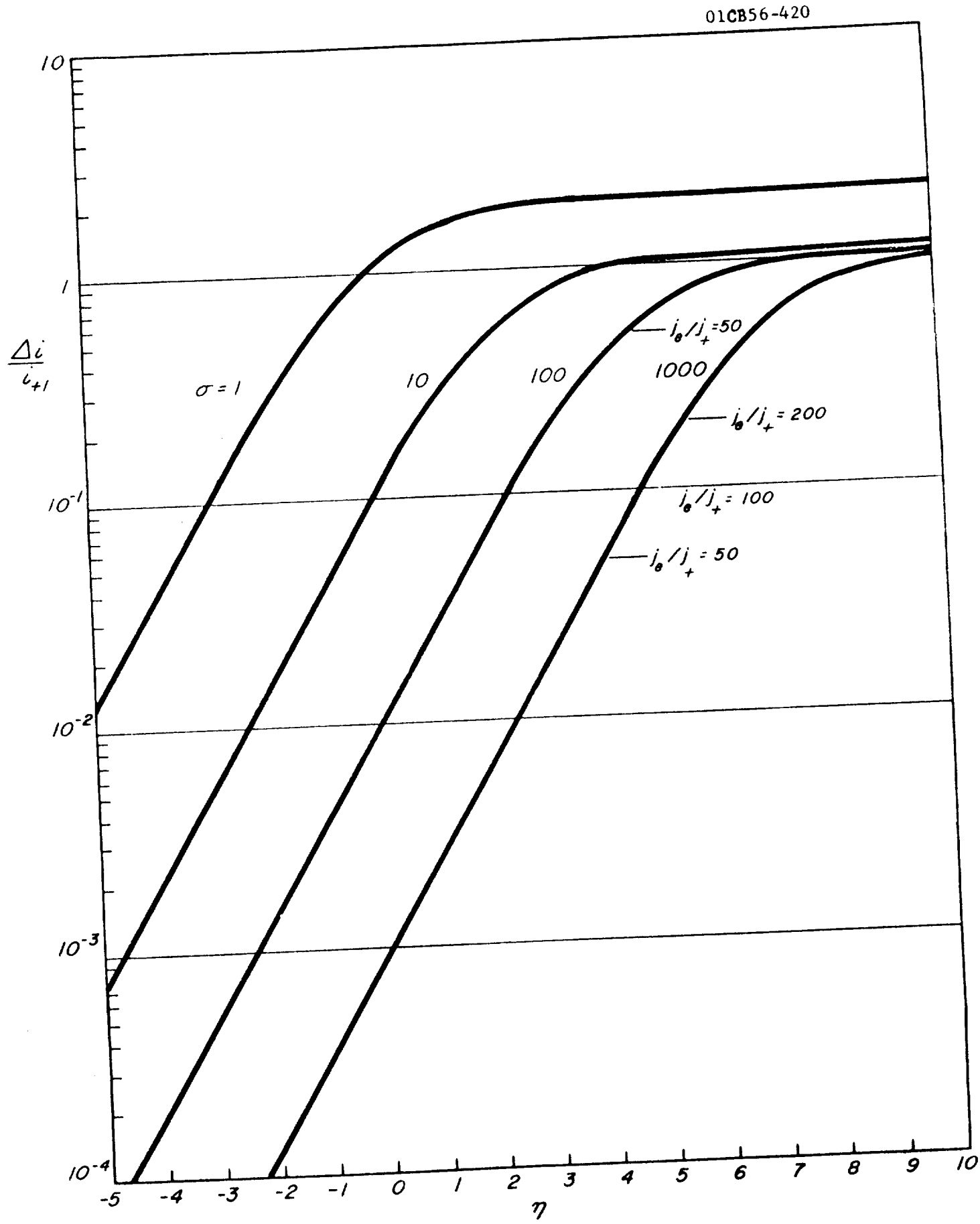

Figure A-2. Semi-log Plot of Current-Voltage Characteristics for Bi-polar Probes.

REFERENCES

1.1 Langmuir, I. and H. M. Mott-Smith, "Studies of Electric Discharges in Gases at Low Pressures," General Electric Review 27, 449-455, 538-548, 616-623, 762-771, 810-820 (1924).

1-2 Mott-Smith, H. M. and I. Langmuir, "The Theory of Collectors in Gaseous Discharges," Phys. Rev. 28, 727-763 (1926).

1-3 Druyvesteyn, M. J., Z. Physik. 64, 781-798 (1930).

1-4 Branner, G. R., E. M. Friar and G. Medicus, "Automatic Plotting Device for the Second Derivative of Langmuir Probe Curves," Rev. Sci. Inst. 34, 231-237 (1963).

1-5 Johnson, E. O. and L. Malter, "A Floating Double Probe Method for Measurements in Gas Discharges," Phys. Rev. 80, 58-68 (1950).

2-1 Sagalyn, R. C., M. Smiddy, and J. Wisnia, "Measurement and Interpretation of Ion Density Distributions in the Daytime F Regions," J. Geophys. Rev. 68, 199-211 (1963).

2-2 Gurevich, A. V., "Perturbations in the Ionosphere Caused by a Moving Body," TRUDY Nr. 17(27), 173-186 (1960).

2-3 Smith, L. G., "Rocket Measurements of Electron Density and Temperature in the Nighttime Ionosphere," GCA Technical Report 62-1-N (January 1962).

3-1 Smith, L. G., "A Simple Method of Trajectory Determination for Sounding Rockets," GCA Technical Report No. 63-9-N (March 1963).

PART II

THE EXPERIMENTAL PROGRAM

SECTION 4

NIKE-ASP 3.12

4.1 INSTRUMENTATION

The major objective of this flight was an experimental study of the effect produced by the telemetering transmitter on the electron density and temperature in the vicinity of a rocket. The probe characteristics were determined with the transmitter "off" and compared with the characteristic with the transmitter "on". The transmitter was keyed at 40 c/s, being "off" for 8 ms and "on" for 17 ms. During the first half of the "on" period the current and voltage values stored during the previous "off" period were transmitted, followed during the second half by the live current and voltage values. The information storage used low leakage capacitors.

The arrangement of instrumentation within the payload is shown in Figure 4-1. Two electrodes are used, both formed by isolating a section of the external surface of the rocket. One electrode is the conical tip of the rocket and the other a circular area on the cylindrical part of the instrumentation section.

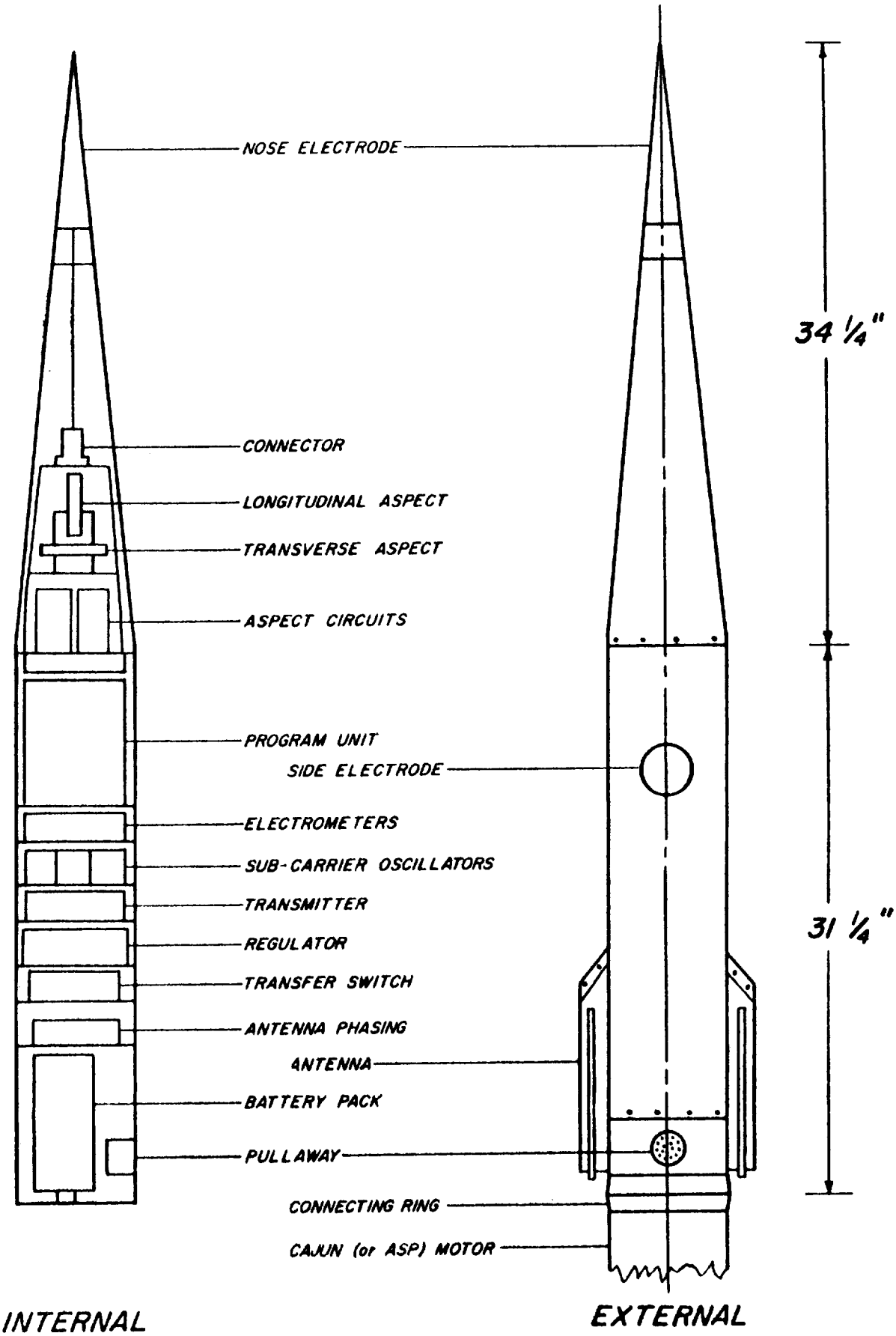

Figure 4-1.

PAYLOAD CONFIGURATION FOR NIKE-ASP 3.12 AND NIKE-CAJUN 10.25

The heart of the system is the electro-mechanical program unit which serves the following purposes: (a) to key the transmitter, (b) to cycle the probe voltage, (c) to feed the storage condenser, (d) to switch electrodes and (e) to apply periodic calibrations.

The telemetering system consists of an FM/FM 2 watt transmitter and three subcarrier oscillators, one each for probe current and probe voltage and one shared between the two aspect sensors.

A sweep voltage is applied between the electrode and ground (the rocket frame) and the current measured by the voltage developed across a resistor, inserted, as shown in Figure 4-2 between the sweep generator and ground. The current to be measured may vary over several orders of magnitude; accordingly, a non-linear load resistor is indicated. After experimenting with diode-switching of load resistors, it was found that a simple solution is provided by a miniature thyrite resistor (General Electric). The thyrites, being semi-conductor devices, are temperature sensitive; for any given voltage a $100^{o}C$ increase in temperature doubles the current. However, this is of no consequence in the present application as the resistor is thermally insulated (potted in foam) and calibrated at ten second intervals. The range of current to be measured is 10^{-8} amp to 10^{-4} amp.

The voltage developed across the thyrite resistor is sufficiently large that no amplification is required and, in fact, a slight loss of voltage in the cathode follower can be tolerated. The input circuit in shown in Figure 4-3.

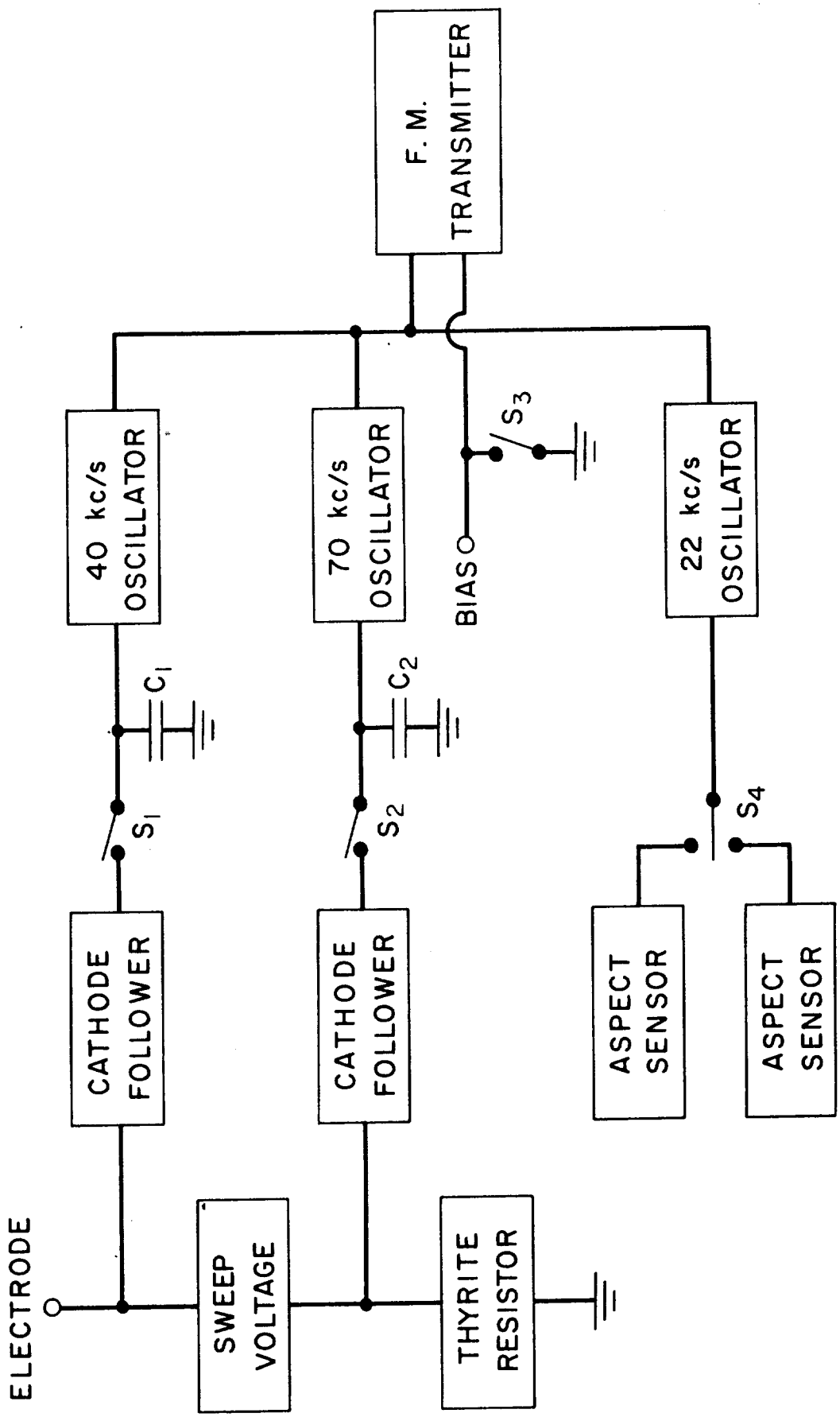

LANGMUIR PROBE INSTRUMENTATION

Figure 4-2.

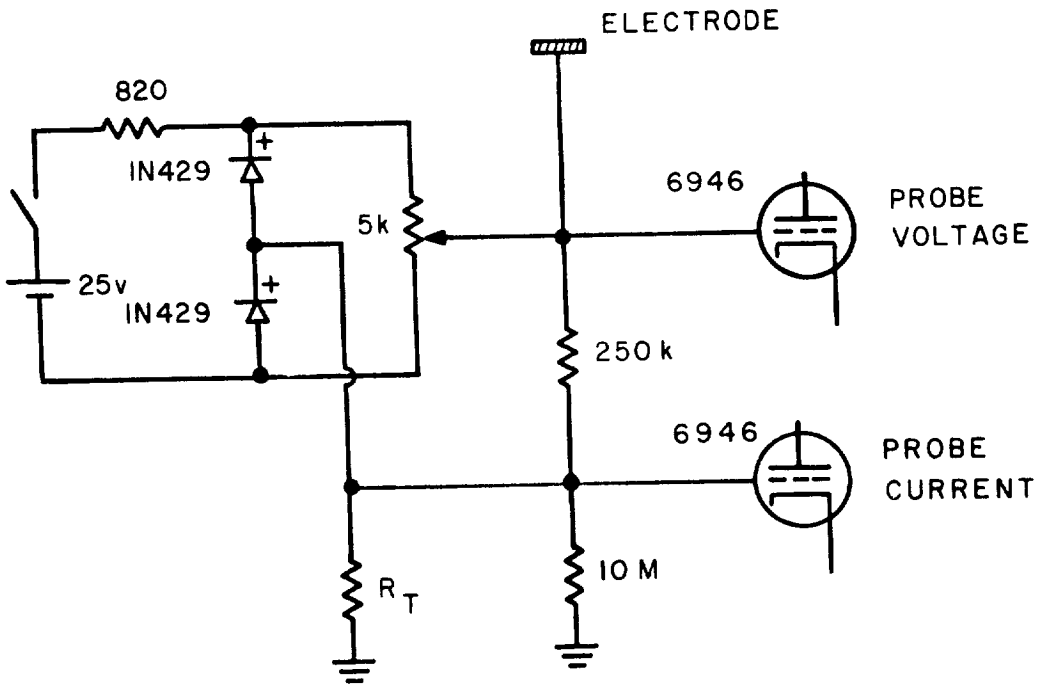

R_T: THYRITE RESISTOR, GE Type 839940IG1

LANGMUIR PROBE INPUT CIRCUIT

Figure 4-3.

The voltage between the probe and rocket frame is less than the sweep voltage by an amount equal to the voltage developed across the thyrite resistor. The sweep voltage is a linear function of time (-9 to +9 volts, two sweeps per second) and thus the actual probe voltage may be derived if the probe current alone is telemetered. However, it is preferred, in the present case, to use an additional channel of telemetry and directly measure the probe potential. This redundancy of information is justified by the reduced effort in data analysis but also provides protection in the event of malfunction of the channel carrying probe current data. Previous experience has shown the value of such a procedure.

The method of storing information is also shown in Figure 4-2. The outputs of the two cathode followers (representing probe current and probe voltage on a zero to +5 volt scale) may, on closing switches S_1 and S_2, be fed directly to the sub-carrier oscillators. This is referred to as "live" information. When the switches are opened, the instantaneous values of voltage are "stored" on the capacitance C_1 and C_2. The operation of such a system depends on the input impedance of the sub-carrier oscillators being very much greater than the output impedance of the cathode follower; in the present case the two impedance are 100 K and 1 K respectively.

Since the system is capable of storing only a single voltage value, the current-voltage characteristic of the probe must be interrupted and transmitted piecemeal. Accordingly, the switches S_1 and S_2 are operating

at 40 c/s giving 20 points on a current-voltage characteristic (sweep time 0.5 sec). The transmitter is switched on, by closing S_3, about 1 msec after S_1 and S_2 have opened thus transmitting the stored information. After a further 8 msec, switches S_1 and S_2 close and live information is transmitted for 9 msec. Then S_5 opens putting the transmitter off the air for 6 msec. This sequence is repeated continuously in normal operation.

Switches S_1, S_2, S_3 and the aspect-sensor switch S_4 are part of the electro-mechanical program unit. In addition, five more switches in the program unit are used to vary the program on consecutive cycles. The complete sequence repeats at intervals of ten seconds and is detailed in Table 4-1. These features have two functions, first to monitor the performance of the instrument in flight and second to assist in the interpretation of the operation of the Langmuir Probe.

4.2 FLIGHT SUMMARY

An attempt to launch the first payload on Nike-Asp 3.12 on 1 June 1960 had been indefinitely postponed shortly before that date until the cause of certain previous rocket failures has been eliminated. Subsequently the use of the Nike-Asp was approved and 3.12 was launched on 22 August 1960 from Wallops Island, Virginia. The flight was unsuccessful due to malfunction of the second stage (Asp). The geophysical instrumentation continued to function up to impact at 322 sec after launch, but the payload did not attain sufficient altitude to penetrate the ionosphere and consequently no scientific results were obtained.

TABLE 4-1

PROGRAM SEQUENCE

Cycle No.	Electrode	Program
1	Nose	Normal*
2	Side	
3	N	Transmitter on continuously
4	S	
5	N	Normal
6	S	
7	N	+7 volt applied to unsampled electrode
8	S	
9	N	Normal
10	S	
11	N	Transmitter on continuously
12	S	
13	N	Normal
14	S	
15	N	+7 volt applied to unsampled electrode with transmitter on continuously
16	S	
17	N	Normal
18	S	
19	50k	Calibration
20	5M	

The complete sequence repeats at 10 second intervals.

*Unless otherwise stated, transmitter is keyed and unsampled electrode is grounded to rocket frame.

Information taken from the post-flight summary is included here:

Identification

Flight number:	NASA 3.12
Wallops Rocket Number:	G2-222 Motor 281-33
Rocket Type:	Nike-Asp
Number of Stages:	2
Place of Firing:	Wallops Island, Virginia
Date of Firing:	22 August 1960
Time of Firing:	12:40:57 E.S.T.

Flight Objectives

The measurement of electron density and temperature in the ionosphere by the Langmuir double probe technique with particular emphasis on the influence of the telemetering transmitter on the electron density and temperature in the vicinity of the rocket.

Flight Information

	Predicted	Observed
Peak Altitude	162 Statute miles	14.5 miles (RS)*
Peak Time	240 seconds	44 seconds (RS)*

*Radar Skin Track

Predicted Data:		Time (sec)	Altitude (ft)	Velocity (ft/sec)
Bottom Stage	Ignition	0	0	0
	Burnout	3.7	34,000	3500
Top Stage	Ignition	18.8	45,000	2200
	Burnout	24.6	70,000	6950
Actual at Break-up		25.6	52,000(RS)*	3800

Impact Data (by Radar Skin Track)

	Time (sec)	Range	Azimuth
Bottom Stage	94	3.3 Stat. mi.	102°
Top Stage	323	5.3 Stat. mi.	102°

Firing Angle (Launcher Setting):

Azimuth from True North: 102°

Elevation above horizontal: 80.3°

Rocket Information

Total Asp Rocket Measured Weight (including payload) - 282½ lbs

Total Rocket Measured C.G. (including payload) - 68 7/16" from nozzle exit

(Propellant included in the above)

Total Rocket Length including booster: 27'

Individual Stage Weights and c.g.'s:

	Weight	C.G. (in)	C.G. Reference	Total Component Length
Payload	59#	16 13/16"	from aft end	60"
Asp Stage 2	223½#	51 5/8	nozzle exit	111"
Adapter	53.56#			15-3/4"
**Nike Stage 1	1333#	6'4 9/16"	nozzle exit	11'2½"

*Radar Skin Track

**Not Weighed

Rocket-Borne Equipment

Upper Air Instrumentation: FM/FM mc 231.4

Sub-carriers: 22KCS (Aspect sensors; sub-commutated)

40KCS (Probe voltage)

70KCS (Probe current)

Telemetry Instrumentation:

FM/FM: 231.4 mc

Ground-Based Equipment

Telemetry Instrumentation: Bomb Tone 3088 KC for time synchronization

Preliminary Results and Comments

Rocket Performance: Below predicted.

Comments: Multiple targets noted by Radar at 26 seconds indicate rocket malfunction during Asp burning.

Propellant quality has been assured as virtually free of voids by X-ray inspection. Cause of break-up is unknown.

Telemetry: Complete data recovery: Type: FM/FM

Comments: No experimental data because of low altitude attained.

Tracking Instrumentation: Adequate tracking: Type - 584

Type - Mod II

Comments: Multiple targets at 26 seconds.

Radar tracked largest target (payload) to about 80,000 feet, lost it, picked it up on descent at about 70,000 feet and tracked to impact.

Upper Air Instrumentation: Payload telemetry operated continuously until splash.

4.3 SHOCK TRANSIENTS AND VIBRATION

The electrometers used in the circuits for measuring probe current and probe voltage are normally considered non-microphonic (Sylvania Gold Brand 3946). However, some microphonics can be recognized on both channels which are attributable to extremely severe environmental conditions. These are identified as shock transients if occurring as large single pulses and as vibration if having appreciable duration and many pulses. This information obtained from the probe current channel is given in Table 4-1. The three shock transients are identified in the table as resulting from (1) separation squibs, (2) second stage ignition and (3) second stage break-up. This last is shown in relation to the magnetometer records in Figure 4-4.

The first two of the four periods of vibration are attributed to rough burning of the first stage; this may be normal, however. The third period occurs toward the end of the coast period but cannot be associated with any particular event. The fourth period begins one second before break-up and continues for slightly more than two seconds although the intensity after break-up is noticeably reduced.

No signals attributable to shock and vibration are observed after 26.8 seconds although the telemetered information continues without loss of signal to impact at 322 seconds.

TABLE 4-2

MICROPHONICS NOTED ON PROBE CURRENT CHANNEL

	Time after launch: seconds	Identification
Shock Transients	3.05	Nike separation mechanism (squibs)
	22.2	Asp ignition
	25.7	Break-up
Vibration	0 - 1.1	Nike burning
	1.8 - 1.9	Nike burning
	16.2 -18.5	Not identified
	24.7 -26.8	Associated with break-up

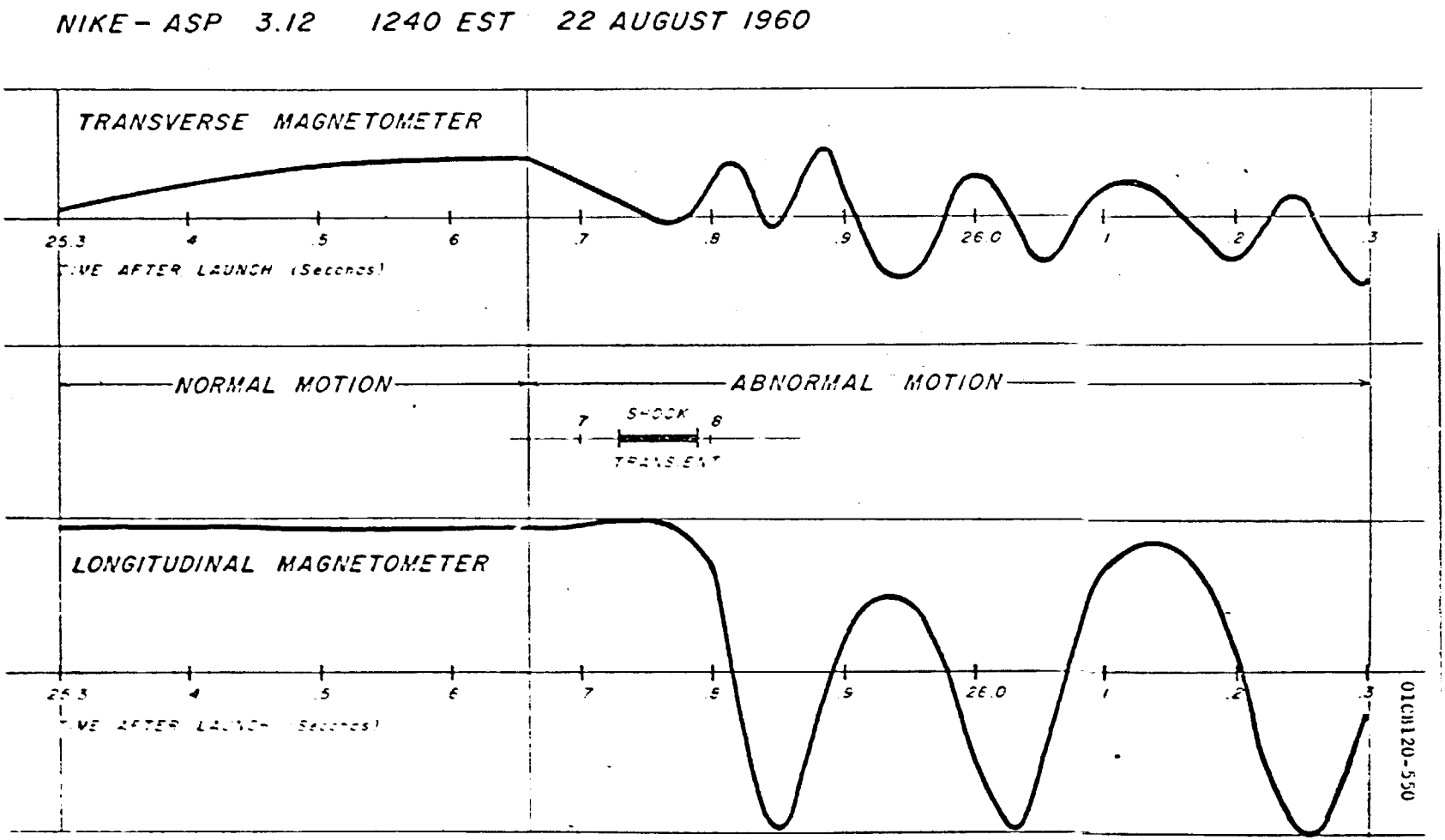
NIKE - ASP 3.12 1240 EST 22 AUGUST 1960
TRANSVERSE MAGNETOMETER
25.3
4
5
6
7
8
9
26.0
1
2
3
NORMAL MOTION
ABNORMAL MOTION
SHOCK
LONGITUDINAL MAGNETOMETER
01CM120-550

Figure 4-4.

4.4 MAGNETOMETER RECORDS

Two magnetometers (Schonstedt type RAM-3) are used in the payload to determine aspect of the vehicle. One is located along the axis of the payload and the other placed transverse to the axis. The outputs of the two magnetometers are sub-commutated on to channel A of the FM/FM telemetry system.

The two most obvious features of the magnetometer records are the beginning of the Asp spin on stage separation at 3.5 seconds, and break-up at 25.7 seconds. During the coasting period (3.5 to 22.2 seconds), the roll rate, as indicated by the transverse sensor decreases from 1.3 rps to 1.0 rps (the nominal roll rate is 3.0 rps). The longitudinal sensor, however, indicates that the Asp was spinning not about its longitudinal axis but about an axis which makes a continuously increasing angle with the longitudinal axis. This angle is about 6^{o} at 10 sec after launch and 10^{o} at 17 sec after launch. This unusual motion appears to damp out after second stage ignition.

A section of the magnetometer records showing the break-up of the rocket at 25.7 seconds after launch is shown in Figure 4-4. The chart speed here is 10 in/sec. The change in motion from normal to abnormal is indicated at 25.66 seconds after launch, corresponding to a change in motion detected by the transverse magnetometer. The shock transient appearing on the probe current channel is also indicated.

A most remarkable feature of this record is the first end-for-end flip of the payload which takes only 0.11 seconds (25.74 to 25.85 seconds after launch). A rough calculation shows that such a motion could be produced by a thrust equal to that of the Asp (7000 lb) acting on the payload at the lower end but perpendicular to the longitudinal axis for a total time of 0.01 seconds. This is the kind of motion which would be expected if the coupling ring between payload and motor were to break while the motor was still under full power.

The very rapid spin indicated by both sensors following break-up slows down, reaching a minimum at about 55 seconds after launch where the rates are 0.17 and 0.45 rps for the longitudinal and transverse sensors, respectively. The spin rates then increase continuously to the end of the record.

4.5 CONCLUSION

Though the flight was not successful in obtaining scientific data, the geophysical instrumentation performed satisfactorily and, as indicated above, revealed some interesting facts concerning the missile behavior.

Prior to this flight it was believed that earlier cases of second stage break-up were due to defective Asp motors, specifically numerous voids (blow-holes) in the propellant. The rocket motor assigned to 3.12 has been selected after X-ray examination as virtually free of voids. However, it did not result in a successful flight.

The flight appears normal up to firing of the separation squibs at 3.05 sec and stage separation at 3.5 sec. During the coast period, the Asp developed a "cork-screw" motion, the angle of attack gradually increasing from nothing at stage separation to 10^{o} at Asp ignition. It is believed that this large angle of attack resulted in the breaking of the coupling ring between payload and motor.

At break-up, the second-stage motor had been burning for 3.5 sec of its nominal burning time of 5.5 sec and would have been approaching maximum thrust. This can explain the rapid tumbling of the payload after break-up.

It is felt that the break-up of the second stage was not necessarily the result of misbehavior of the Asp motor itself but that the flight was already doomed from the moment of booster separation. This, together with the low roll rate during coast and second stage burning (less than one half of the nominal value of 3 rps) would indicate an aerodynamic problem perhaps connected with malfunction of the stage separation mechanism.

SECTION 5

NIKE-CAJUN 10.25

5.1 FLIGHT SUMMARY

Following the failure of the first rocket on this project, Nike-Asp flights were again suspended pending re-evaluation of the vehicle. Due to the long delay already incurred and no immediate prospect of correction of the difficulties, it was decided to fly the payload on a Nike-Cajun. The only modification required was the fabrication of a new coupling ring which attaches the payload to the Cajun Lead-cap. Change of rocket results in a reduced apogee which, for the 60-pound payload, is about 150 km for the Nike-Cajun compared with 220 km for the Nike-Asp.

The rocket was launched from Wallops Island, Virginia, at 11.52 EST on 8 December 1960. It was completely successful.

Information taken from the post-flight summary (with corrections) is included here:

IDENTIFICATION

Flight Number	:	NASA 10.25
Wallops Model Number	:	G2-488
Engine/Motor Numbers	:	1st State 12069
Rocket Type	:	Nike Cajun
Number of Stages	:	Two
Place of Firing	:	Wallops Island, Virginia
Date of Firing	:	8 December 1960
Time of Firing	:	11:52:09 EST
Instrumenting Agency	:	Geophysics Corporation of America

FLIGHT OBJECTIVES

(1) The primary purpose of this flight is the measurement of electron temperature and electron density by the Langmuir double probe technique.

(2) The experiment is also arranged to determine the influence of the telemetering transmitter on the electron temperature and electron density in the vicinity of a rocket.

FLIGHT INFORMATION

	Predicted	Observed
Peak Altitude:	92 statute miles	95.6 statute miles (RS)*
Peak Time :	188 seconds	193 seconds (RS)*

Ignition Data:	Time (sec)	Altitude (ft)	Velocity (ft/sec)
Bottom Stage	0	0	0
Top Stage	approx. 20	43,000	1800
Burnout Data:			
Top Stage	approx. 24	57,000	5500

*RS = Radar Skin Track

Impact Data:	Time (sec)	Impact Location	
		Range	Azimuth
Bottom Stage	N/A	13,500 ft.	50°
Top Stage	379	19.6 statute mi.	50°

Firing Angle (Launcher Setting)

Azimuth from True North (deg): 106°

Elevation above Horizontal : 81°

ROCKET INFORMATION

Individual Stage Weights and c.g.'s:

	Weight (lb)	C.G. (in)	C.C. Reference	Total Component Length
Payload	63			174 in.
Payload + Cajun	264			
(Nike) Stage 1	201	48 1/4	Nozzle Exit Plane	

ROCKET-BORNE EQUIPMENT

Upper Air Instrumentation: 231.4 mc

(1) Langmuir Probe using nose tip electrode and side electrode.

(2) Magnetic Aspect Sensors; one longitudinal, the other transverse to rocket axis.

Telemetry Instrumentation:

FM/FM 231.4 mc

Tracking Instrumentation:

Radar: FPS-16 and MIT Mainland Radar

PRELIMINARY RESULTS AND COMMENTS

Rocket Performance:

Above Predicted

Comments:

The rocket attained a peak altitude of 96 miles being somewhat above the predicted 92 miles. This is in part due to an apparent high launch angle which at the same time resulted in an impact range of 20 miles compared with the predicted 40 miles. In all respects the rocket performance was perfect for the scientific purpose of the flight.

Telemetry:

Complete Data Recovery: FM/FM (Modified)

Comments:

Good trajectory data is essential to the success of this mission. A complete and reliable trajectory was obtained by at least one radar.

PRELIMINARY RESULTS AND COMMENTS (continued)

Upper Air Instrumentation:

The duplicate Langmuir probe experiments performed perfectly. The effect of the ionosphere was first observed at about 50 seconds after launch, through apogee at about 200 seconds and on the way down until 340 seconds; these times correspond to the period the rocket was above about 52 km (apogee 153 km). In the region below about 100 km, the Langmuir probes are measuring atmospheric electrical conductivity; above that height electron density and electron temperature.

The magnetic aspect sensors performed perfectly and indicated the motion of the vehicle. The data are used in interpreting the probe data.

5.2 ROCKET ASPECT

The payload contains two magnetic aspect sensors (Schonstedt type RAM-3), one along the axis of symmetry and one transverse to it. The longitudinal sensor is intended to indicate change in angle of attack of the vehicle while the transverse sensor is primarily intended to show the roll rate of the vehicle. These sensors are included in the payload because of possible dependence of the Langmuir probe measurements on payload orientation.

The Nike-Cajun is nominally a zero spin vehicle but is subject to some rotation during flight. In the present flight, immediately following stage separation (at t + 3.6 sec) the Cajun has a spin period of 1.7 sec. During the subsequent coast period the spin rate decreases to a minimum at about t + 14.5 sec. The spin rate then increases, presumably in the opposite direction of rotation.

The probe electrometer shows noise from t + 20.3 sec to t + 24.2 sec corresponding to Cajun burning. (Similar noise is observed during Nike burning and has been seen on the previous flight Nike-Asp 3.12). The spin rate reaches a maximum of 2.0 rps at t + 23.9 sec i.e. near the end of the Cajun burning period. This spin-up is attributed to a tangential component of thrust such as might be caused by a nozzle imperfection.

Beginning sharply at t + 22.8 sec the longitudinal sensor indicates precession of the vehicle. This is consistent with a tangential component to the thrust. Subsequently the angle of the cone traced by the Cajun axis increases while the period of revolution decreases.

At t + 75 sec (at a height of 87 km) the rocket has stabilized in a slow flat spin having a period of 77 sec while revolving about its own axis with a period of 8.3 sec. This motion continues until quite sharply at t + 310 sec (87 km on descent) the vehicle turns nose down. The spin rate increases to 1.3 rps at t + 363 sec then decreases to impact at t + 379 sec.

The motions of the Cajun were unexpected though fortunately not detrimental to the primary purpose of the flight; in fact the peculiar orientation above 90 km permitted the examination of electron density in the wake of the vehicle, an unexpected bonus.

The total velocity and altitude of the second stage, obtained from FPS-16 radar data are plotted in Figure 5-1. Ignition can be identified at 20.7 sec after launch and burnout at 23.8 sec.

5.3 EFFECT OF THE TELEMETRY TRANSMITTER

The effect of the telemetry transmitter is determined by comparing the current-voltage characteristic of the probe as measured with the transmitter on and with it off. The transmitter (Telechrome 1475B, 231 Mc/s, 3 watt) is modulated by a 31 cps bias voltage so that it is alternately on for 21.8 ms and off for 10.5 ms. (Figures are given as measured during flight). The bias signal is generated in the electro-mechanical program unit which also generates the probe sweep voltage (sweep period 645 ms). A simple switch arrangement in the program unit either feeds live information to the subcarrier oscillators or feeds stored information, the information being held on a condenser. This system was described in Section 4.1 of this report. This method provides a very sensitive test of the effect of the transmitter.

The result of the present flight show quite definitely that the current-voltage characteristic of the probes are identical to the

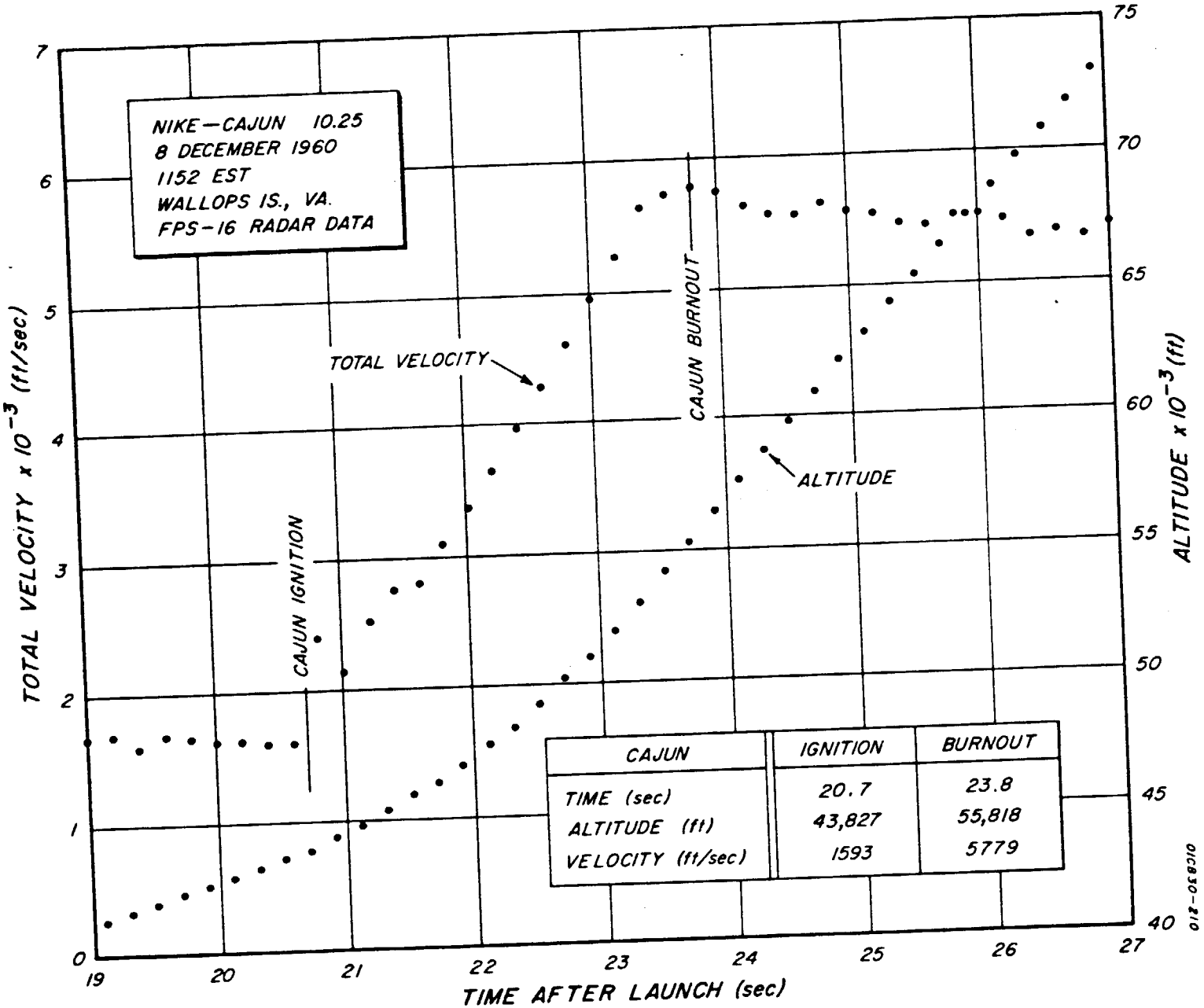
NIKE—CAJUN 10.25
8 DECEMBER 1960
1152 EST
WALLOPS IS., VA.
FPS-16 RADAR DATA
TOTAL VELOCITY
CAJUN BURNOUT
ALTITUDE
CAJUN IGNITION
TOTAL VELOCITY x 10⁻³ (ft/sec)
ALTITUDE x 10⁻³ (ft)
TIME AFTER LAUNCH (sec)
CAJUN | IGNITION | BURNOUT
TIME (sec) | 20.7 | 23.8
ALTITUDE (ft) | 43,827 | 55,818
VELOCITY (ft/sec) | 1593 | 5779
0 1 2 3 4 5 6 7
40 45 50 55 60 65 70 75
19 20 21 22 23 24 25 26 27

Figure 5-1.

accuracy of the measurements, with the transmitter on or off. It is therefore concluded that for the particular arrangement the transmitter does not cause any significant change in electron density or electron temperature. It will be possible in future flights to dispense with the precaution of turning the transmitter off the air. It should be noted that this conclusion does not necessarily apply to transmitters having higher power or lower frequency or both.

5.4 CURRENT-VOLTAGE CHARACTERISTICS

The analysis of the probe current-voltage characteristic involves several steps:

(1) The corresponding current and voltage values are read off the telemetered data.

(2) The contribution of positive ions to the probe current is estimated and subtracted from the total (measured) current to give the electron current.

(3) The electron current is plotted against probe voltage on semi-log paper.

Three important quantities can immediately be read off the semi-log plot, namely electron temperature (from the slope of the linear part), electron saturation current (the value of electron current at the end of the linear part) and finally the rocket potential (equal to but of opposite sign to the probe potential at the end of the linear part).

The analysis of the individual sweeps of the probe voltage is tedious and initially is examined at height intervals of 5 km. The observed i - V plot for the nose electrode at a height of 115 km on ascent is shown in Figure 5-2. The first feature to note is the offset or bias which prevents the curve going through the origin; the current to the electrode is actually zero when the electrode is made 1.0 volt positive with respect to the body. The bias may be regarded as a voltage (for example contact potential) or a current (such as photo emission) but does not, in either case affect the analysis. The second feature of significance is the absence of a sharply defined saturation of current, although a change of slope becomes apparent at about 10 microamp. The next step is to determine electron current. This is shown against voltage on a semi-log plot in Figure 5-3. Now the change in the curve from the exponential rise of current to a pseudo-saturation is more obvious, occurring at a potential of +1.4 volt. At this point the electrode is at space potential. The slope for voltages less than 1.40 volt gives the electron mean energy; a value of 0.12 ± 0.01 volt results. Although this value is greatly in excess of the ambient thermal energy (about 0.03 ev) the linearity of the semi-log plot shows that over a considerable range the energy distribution of the electrons is Maxwellian i.e., they are in equilibrium among themselves but not in equilibrium with the neutral particles and, presumably, ions.

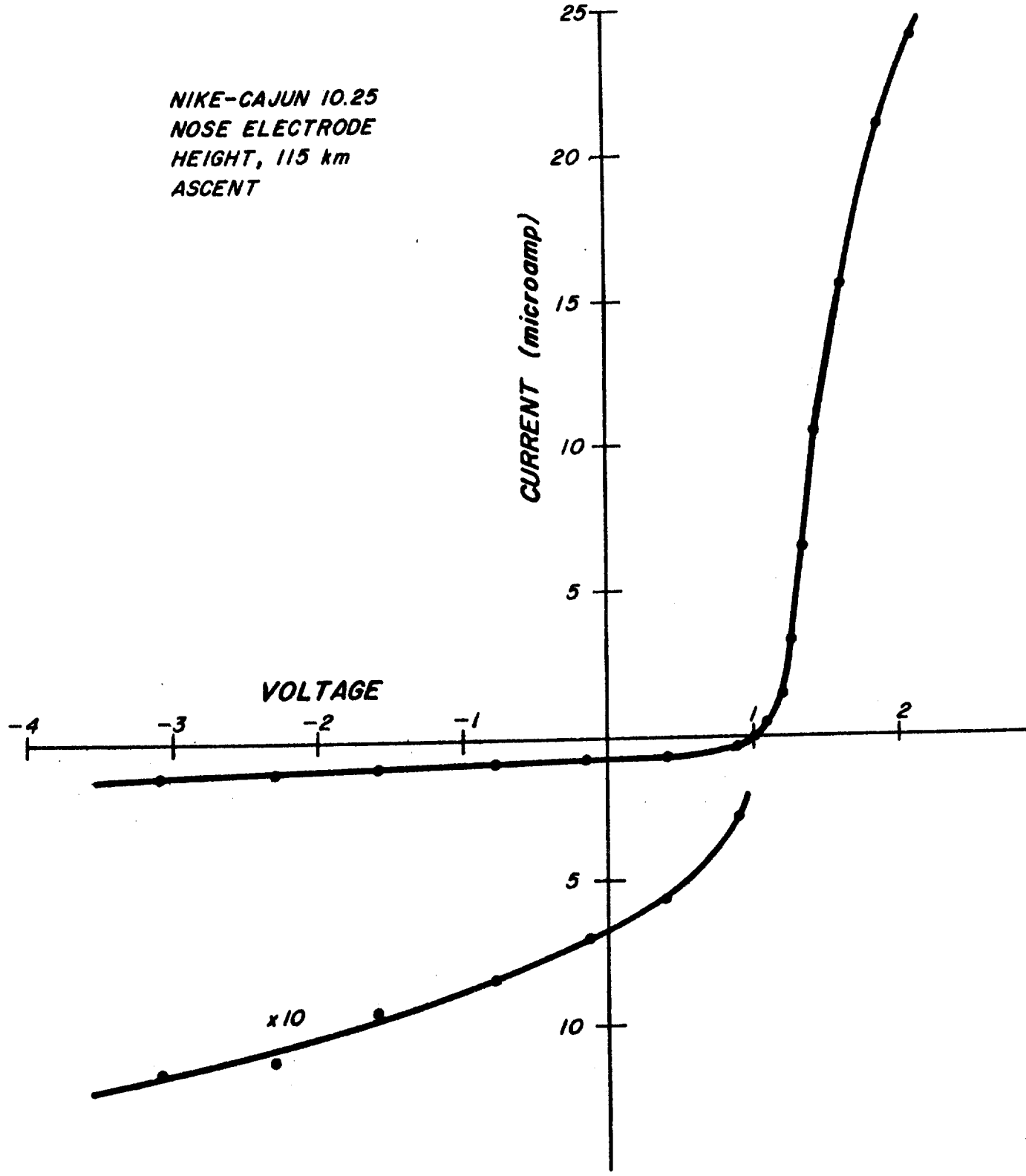

Figure 5-2. **Current-Voltage plot at 115 km**

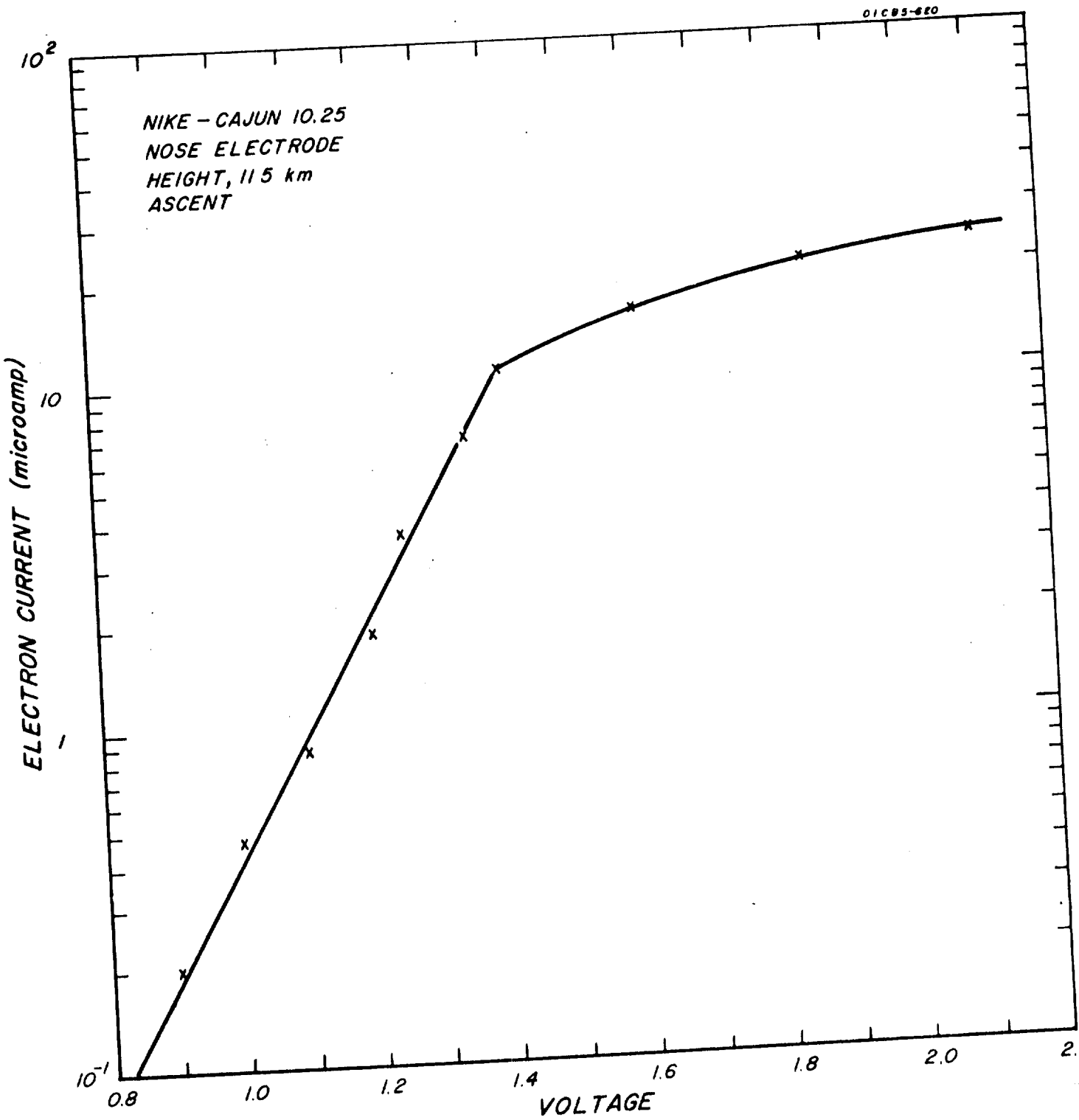

Figure 5-3. Observed semi-log plot of electron current.

The variation of electron mean energy with height is shown in Figure 5-4. There is some indication of an increase with height from about 0.12 volt at 100 km to about 0.14 volt at 150 km. The dashed line shows the electron energy corresponding to ambient temperature (values from 1959 ARDC Model Atmosphere). In this region of the ionosphere the ambient temperature rises rapidly but no such rapid rise is apparent in the observed values of electron mean energy.

The electron current at space potential is seen from the semi-log plot to be 11 micro amp. Since the area of the nose electrode is 196 cm^2 this gives a value for electron random current density of

$$j_e = 5.6 \times 10^{-8} \text{ amp/cm}^2.$$

At the same height the side electrode similarly gives

$$j_e = 5.9 \times 10^{-8} \text{ amp/cm}^2$$

in reasonable agreement with the value from the nose electrode. The electron energy of 0.12 volt corresponds to an electron mean velocity of 2.3×10^7 cm/sec. Hence, using

$$j_e = \tfrac{1}{4} ne\bar{v}$$

we find values of electron density of 6.1×10^4 cm^{-3} from the nose electrode and 6.4×10^4 cm^{-3} from the side electrode. The value of f_oE at Washington, D.C. at this time was 3.3 Mc/s corresponding to a peak electron density in the E-layer of 1.35×10^5 cm^{-3}. Thus the

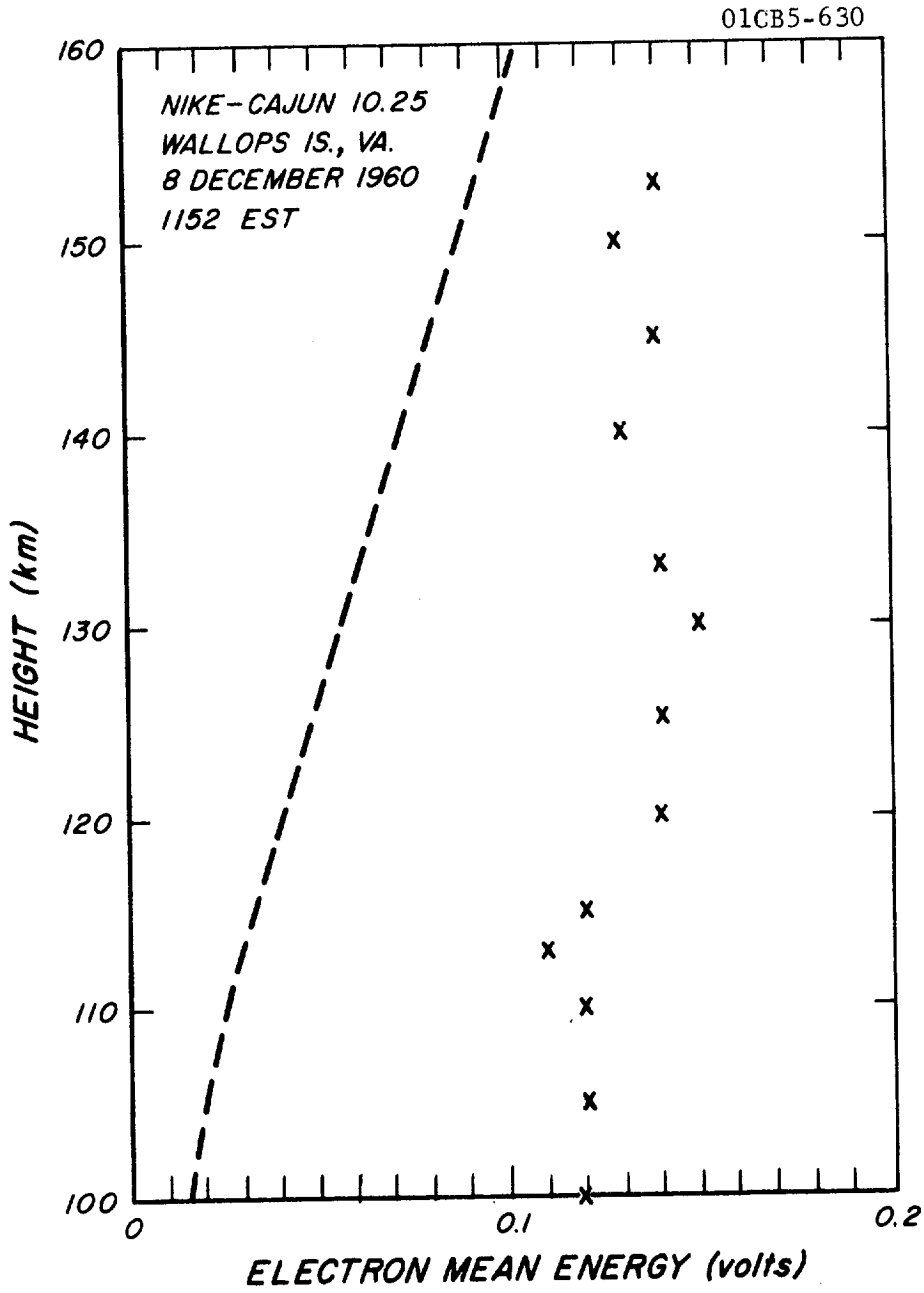

Figure 5-4. Variation of Electron Mean Energy With Height

values deduced from the nose and side electrode are both low by a factor of about 2.1. This is much greater error than the data permit (the data error is about 10 percent) and is a serious factor. Whether it shows a fundamental error in the probe theory or whether some feature of the analysis has been misinterpreted remains to be shown. This need not, however, prevent the use of the probe to study the ionosphere, if necessary only using relative values of electron density.

The potentialities of the probe are best illustrated by considering the current at constant voltage. The voltage chosen for Figure 5-5 is 1.80 volt i.e., 0.40 volt positive with respect to space potential. The values of current were obtained fron the individual sweeps though, of course, the effort can be reduced and the accuracy increased by actually using a fixed probe voltage with an occasional sweep as a check.

In Figure 5-5 the electron density is proportional to probe current above 100 km and perhaps at somewhat lower altitudes but the application of probe theory becomes questionable below 100 km. The ascent and descent values are not entirely consistent but this may be attributed to aging of the electrode or perhaps rocket outgassing on ascent and is not at present attributed to a real change in the electron density. The E-layer shows up clearly with a peak at 110 $\pm$ 1 km (on descent) and a trough of reduced electron density up to 130 km where the value again equals the peak of the E-layer. The minimum in the trough after smoothing is 76 percent on ascent and 84 percent on descent of the corresponding

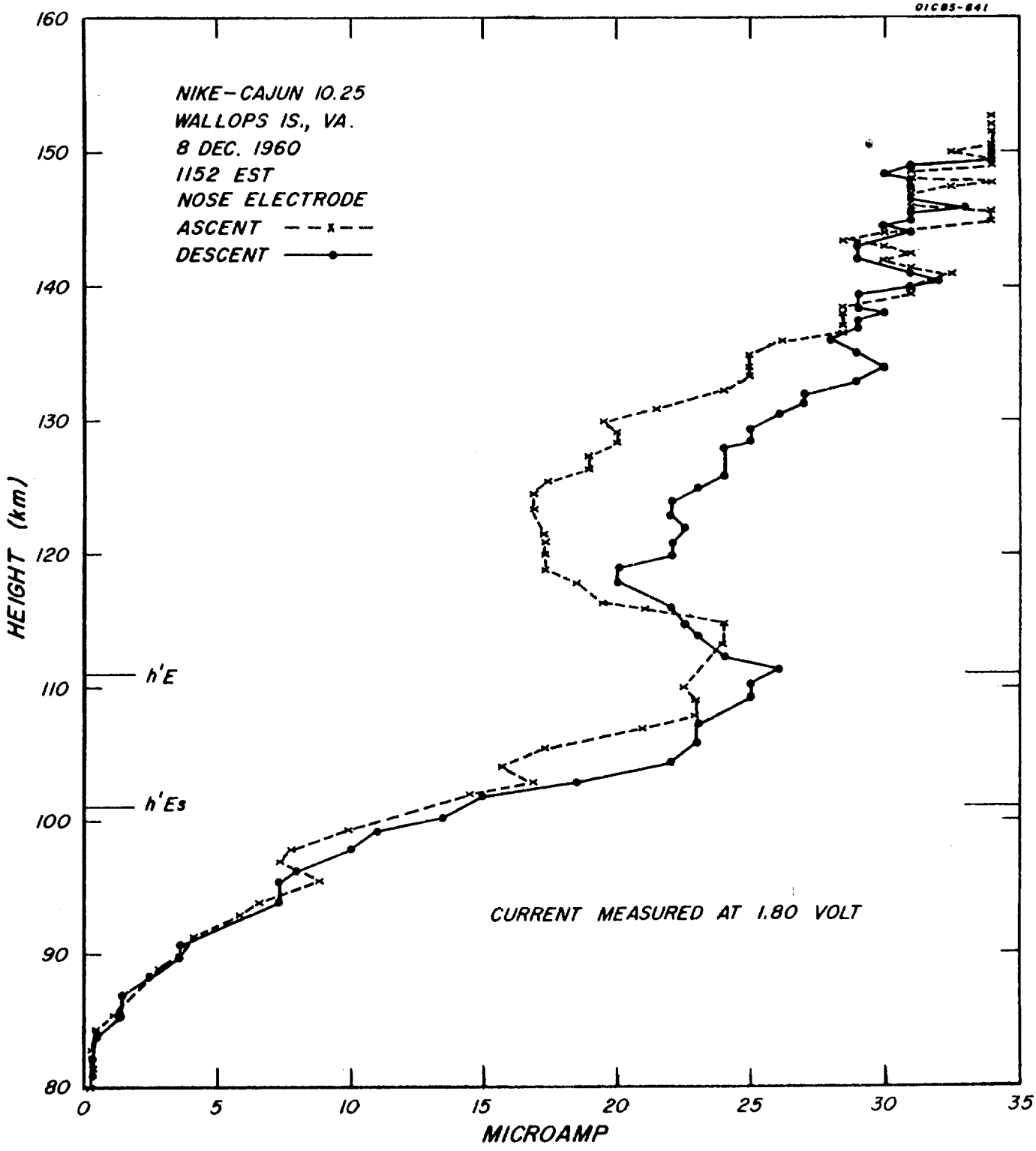

Figure 5-5. **Plot of current measured at a fixed voltage**

value at the peak of the E-layer. The minor fluctuations are attributed to experimental errors arising from the use of a logarithmic device to measure current; however a subsidiary layer near 95 km is observed both on ascent and descent and is probably real. The height resolution is not adequate to show the shape of this layer.

5.5 D-REGION ANALYSIS

The electrometer is sufficiently sensitive that current into the nose electrode is first detected at 54 km on ascent and down to 52 km on descent. In the height range below 90 km the measurement may be interpreted to give conductivity due to positive ions. (See Appendix B) The i-V plots are linear and the slope (di/dV) is proportional to conductivity, the constant of proportionality being $1/(4\pi c)$ where c is a characteristic capacity. In the present case the appropriate capacity is that of the rocket (as a whole) in free space and a value of 55 esu (or cm) computed. Thus, measuring di/dV in microamp per volt the conductivity in esu is

$$\sigma = 1.3 \times 10^3 \frac{di}{dV} .$$

The value of σ is plotted in Figure 5-6, showing good agreement between ascent and descent values in the main features of the variation with height. The positive ion density is next derived using the formula for D. C. conductivity:

$$\sigma = \frac{ne^2}{m\nu}$$

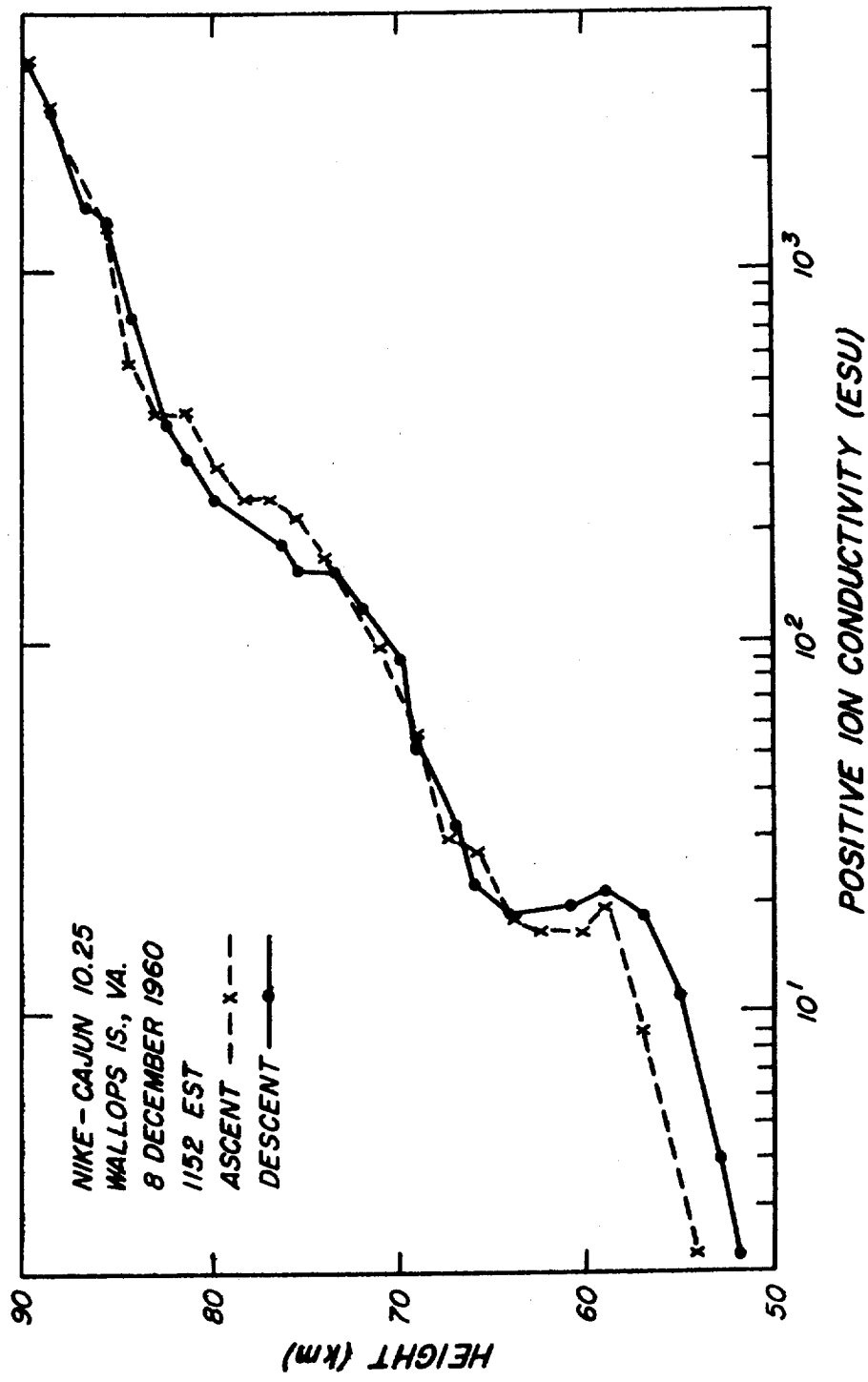

Figure 5-6. Positive Ion Conductivity Versus Height

where m is the mass and ν the collision frequency of the ions. The collision frequency is taken directly from the ARDC 1959 Model Atmosphere and leads to the values of positive ion density shown in Figure 5-7. A very significant layering is evident with peaks at 73 km and 58 km. The major minima of ion density occur at 82 km and 65 km, the upper one corresponding in height with the dust layer responsible for noctilucent clouds.

The electron density in the D region is of considerable interest and although it is not measured directly it may be derived from the positive ion values by assuming a value of λ, the ratio of negative ions to electrons. The absolute value of λ is uncertain to an order of magnitude, but the variation with height (in the region of interest) is inversely proportional to collision frequency. Thus, paradoxically, Figure 5-6 which is actually a plot of conductivity shows the variation of electron density with height in the D-region, a variation which is consistent with the much less definite radio techniques.

5.6 ELECIRON DENSITY IN THE VEHICLE WAKE

An important result was obtained concerning the electron density in the wake of a rocket because of the unexpected altitude of the vehicle in the ionosphere. It was in a slow flat spin (period 77 sec) while rotating on its own axis with a period of 8.3 sec. Thus the electrode on the side of the payload was alternately looking up and down. It is found that the current to this electrode is modulated with

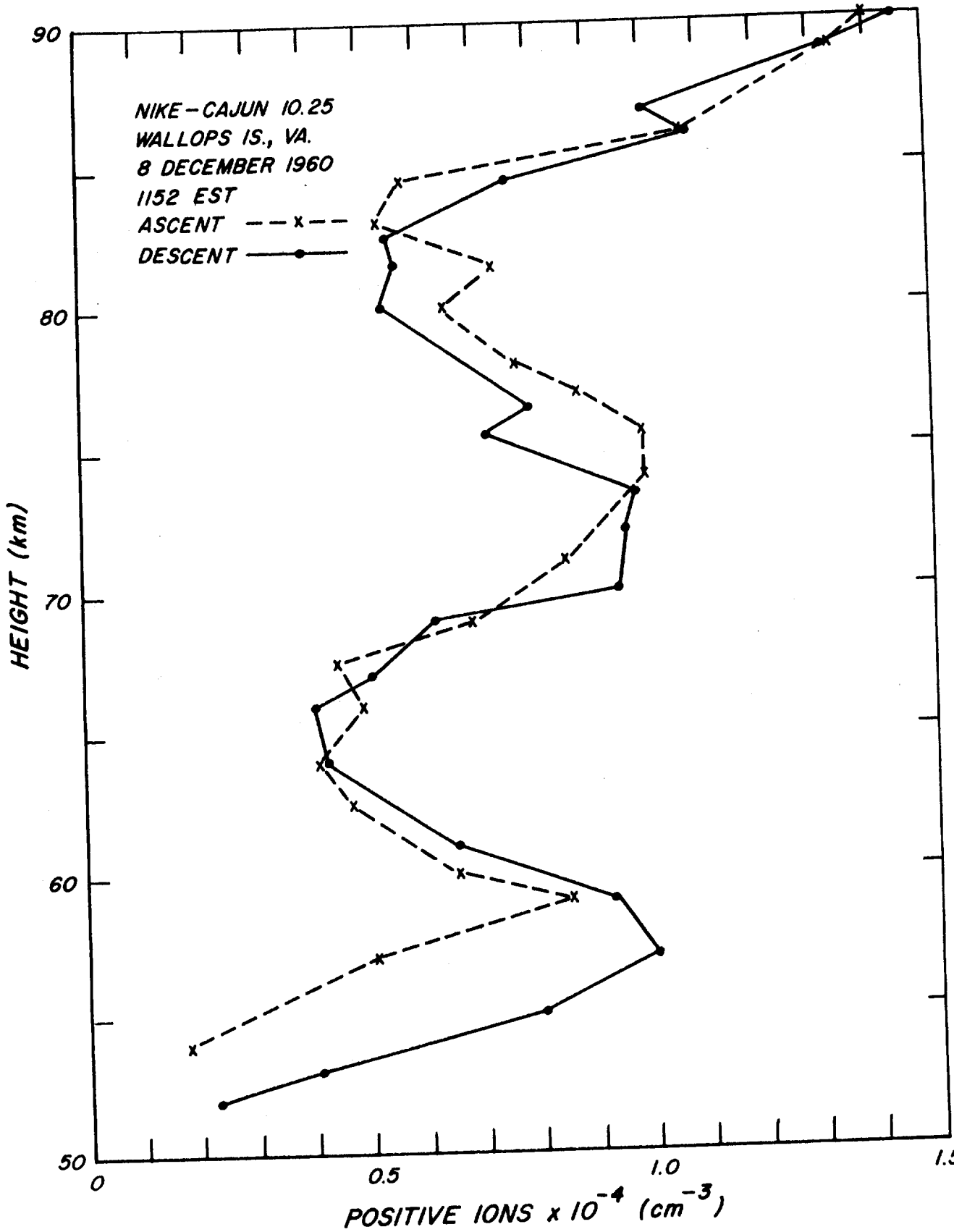

Figure 5-7. Positive Ion Density Versus Height

a period equal to the roll rate and that the minima of current occur on ascent with the electrode looking down, while on descent they occur with the electrode looking up. Thus the minima correspond to the electrode being in the wake of the vehicle. The magnitude of the modulation is greater in the low ionosphere and decreases to apogee. This indicates a rarefaction of electron density in the wake corresponding to that of neutral particles and ions. It will be noted that the velocity of the rocket at 100 km is about 1 km/sec compared with a thermal velocity of the neutral gas of 0.38 km/sec. Thus, at least qualitatively, we see evidence that the requirement of neutrality of the plasma results in electron rarefaction in the wake although the electron mean thermal velocity is much greater than the vehicle velocity.

SECTION 6

NIKE-CAJUN 10.51

6.1 INSTRUMENTATION

The general arrangement of the payload is shown in Figure 6-1. A nose electrode and a side electrode are used simultaneously but independently. The electrodes are alternately connected to a sweep voltage (-5 to +5 volt, duration 0.5 sec) and a fixed voltage (+2.7 volt, duration 0.5 sec), the two electrodes being in opposite phase, i.e., one is being swept while the other is held at a fixed potential, and vice-versa. The fixed voltage is used to determine the fine structure of the electron density on a relative scale while the sweep is necessary for the regular Langmuir probe analysis: to obtain absolute values of electron density and electron energy (temperature). Again, the earlier flight gave a sound basis for this procedure.

The circuit block diagram for these payloads is shown in Figure 6-2. The nose and side electrodes each are allocated one channel of the FM/FM telemetry system. The third channel is fed a mechanical commutator on the same shaft as the potentiometer from which the sweep voltage

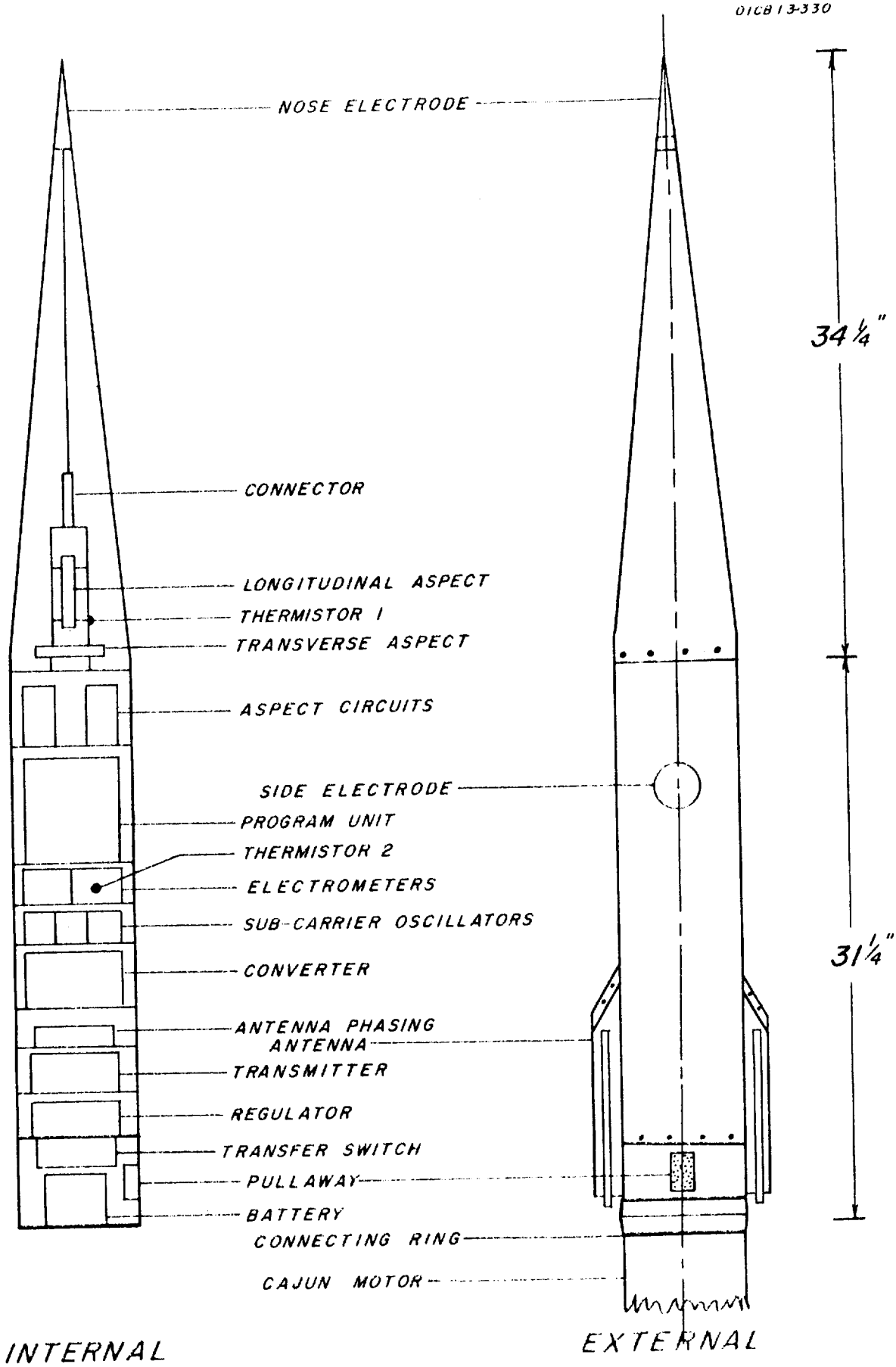

Figure 6-1.

PAYLOAD CONFIGURATION FOR NIKE-CAJUN 10.51 & 10.52

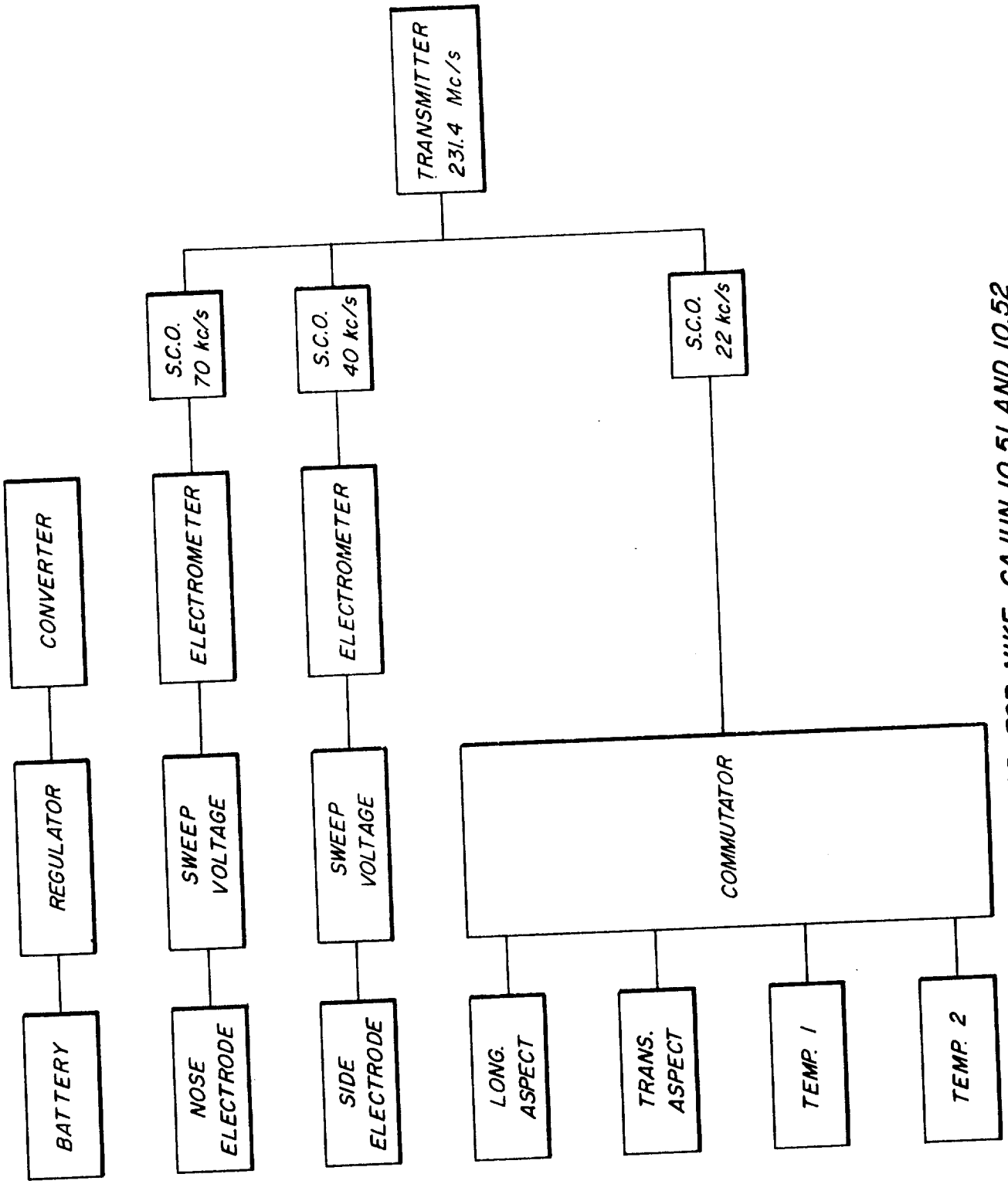

PAYLOAD FOR NIKE-CAJUN 10.51 AND 10.52

Figure 6-2.

is derived. The arrangement of the commutator is shown in Figure 6-3. The sync pulse (1500 c/s, amplitude 0.7 volt peak-to-peak) is added to the 5.0 volt reference to provide synchronization for monitoring purposes before and during the flight.

The two temperature measurements are included for design purposes. One termistor is placed in the nose cone section while the second is mounted on the circuit board of the electrometer and is surrounded by potting compound and a metal box.

The circuit of the Langmuir probe is shown in Figure 6-4 with details of the electrometer in Figure 6-5. A thyrite resistor is used as the feedback element to produce a compressed scale. Ihe calibration curve of a unit having a full scale current of about 20 microamp is shown in Figure 6-6. In payloads 10.51 and 10.52 the full scale current for nose and side electrode is, respectively, 10 and 2 microamp.

The sweep voltage is derived from a motor-driven potentiometer as in the previous flight (Nike-Cajun 10.25). On that flight the probe voltage was transmitted over a separate channel from that used for the probe current. In the present flight, by a very simple arrangement, it has been found possible to transmit the sweep voltage information over the same channel as probe current in such a way as to simplify the data reduction problem increase the accuracy of the electron temperature determination.

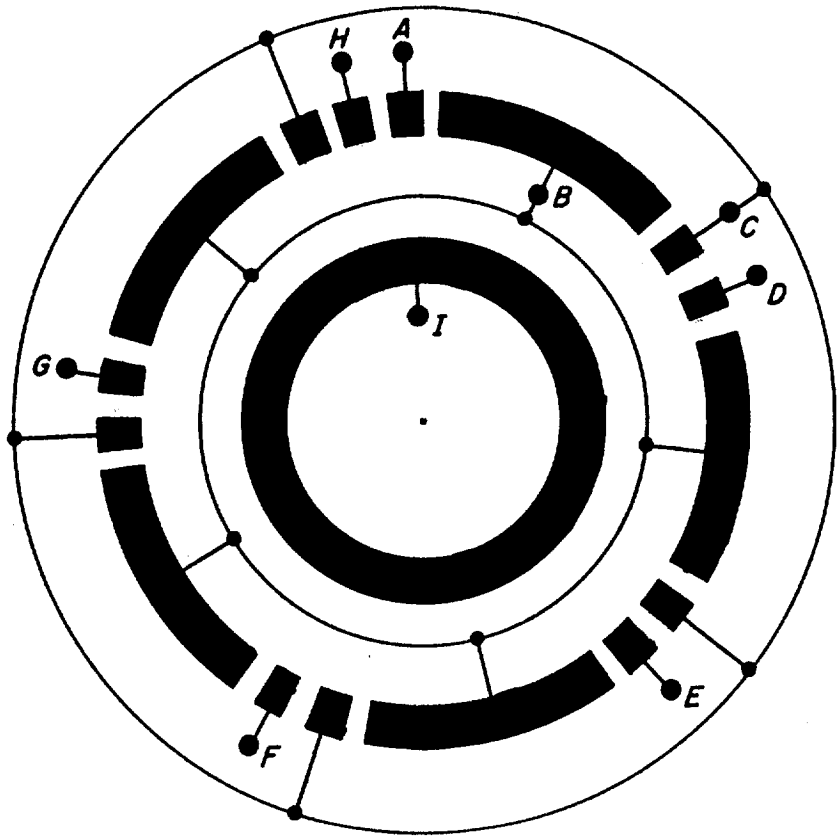

A: 5 volt (ref.) + Sync.
B: Transverse Magnetometer
C: Longitudinal Magnetometer
D: Tr. Magnetometer zero
E: Long. Magnetometer zero
F: 0 volt (ref.)
G: Thermistor 1
H: Thermistor 2
I: Output

COMMUTATOR SEQUENCE: ABCDBCEBCFBCGBCH
SEQUENCE DURATION: 0.5 second (nominal)

COMMUTATOR FOR NIKE-CAJUN 10.51 and 10.52

Figure 6-3.

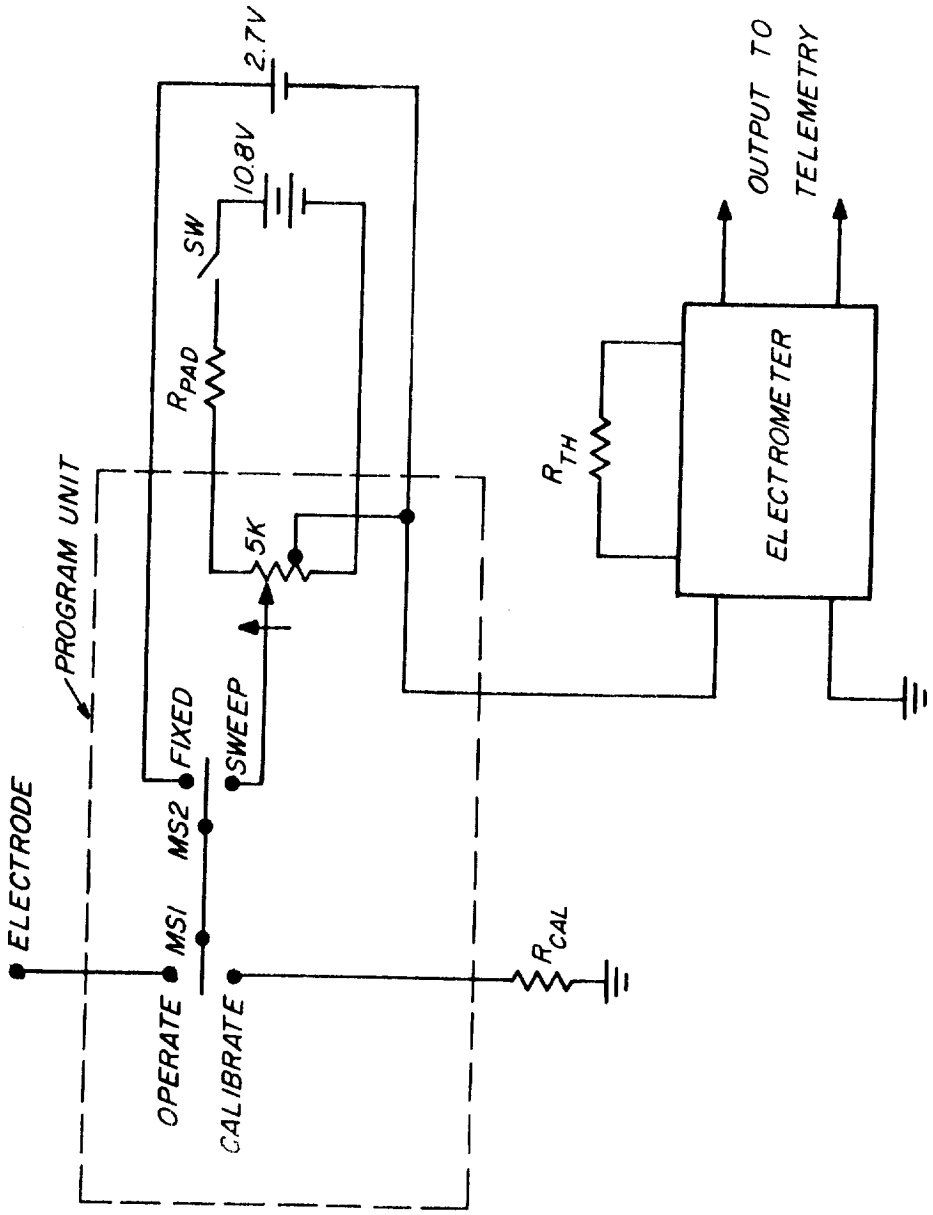

Figure 6-4. LANGMUIR PROBE CIRCUIT

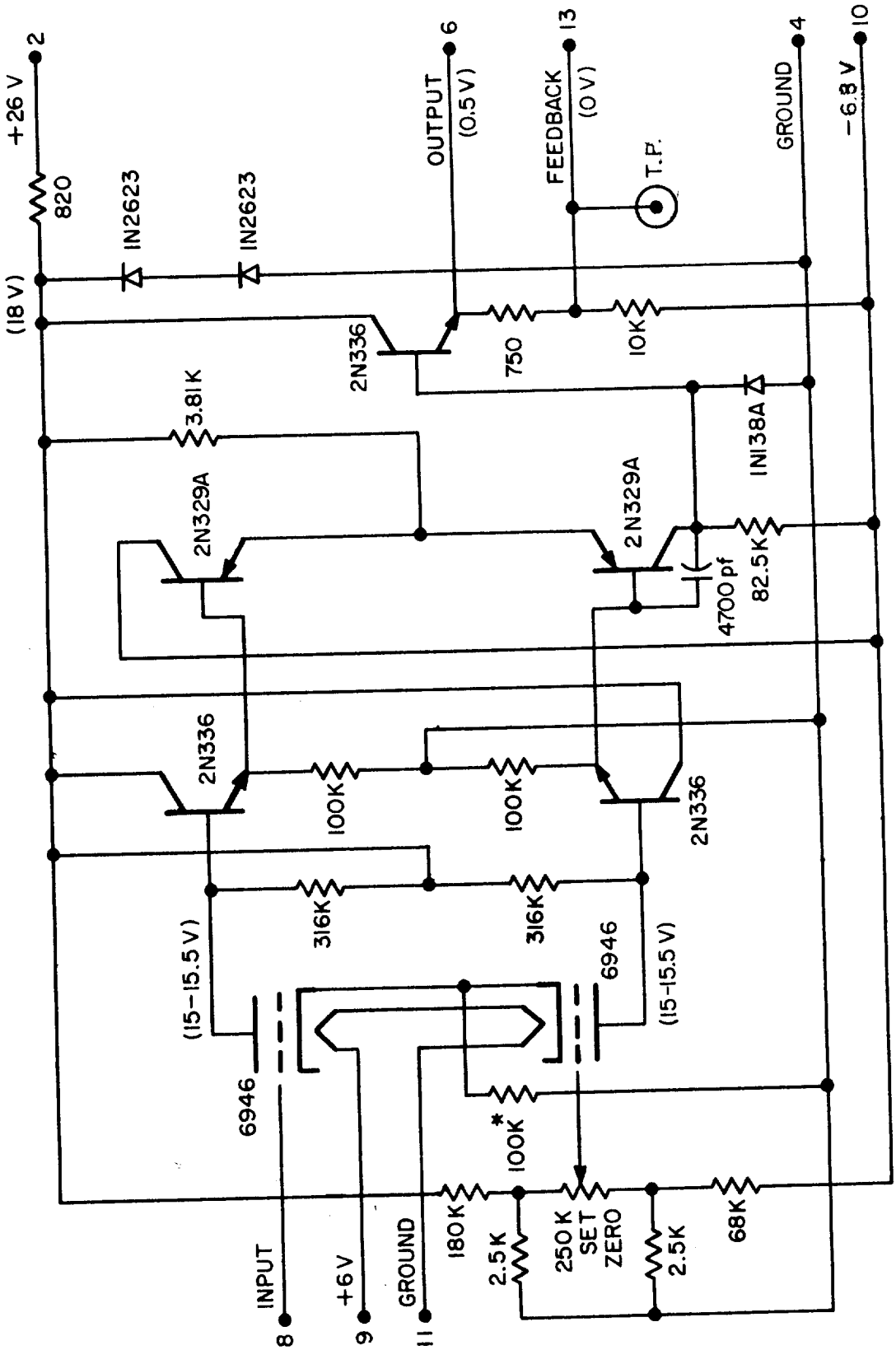

*ADJUST FOR MINIMUM GRID CURRENT AT INPUT

Figure 6-5. ELECTROMETER

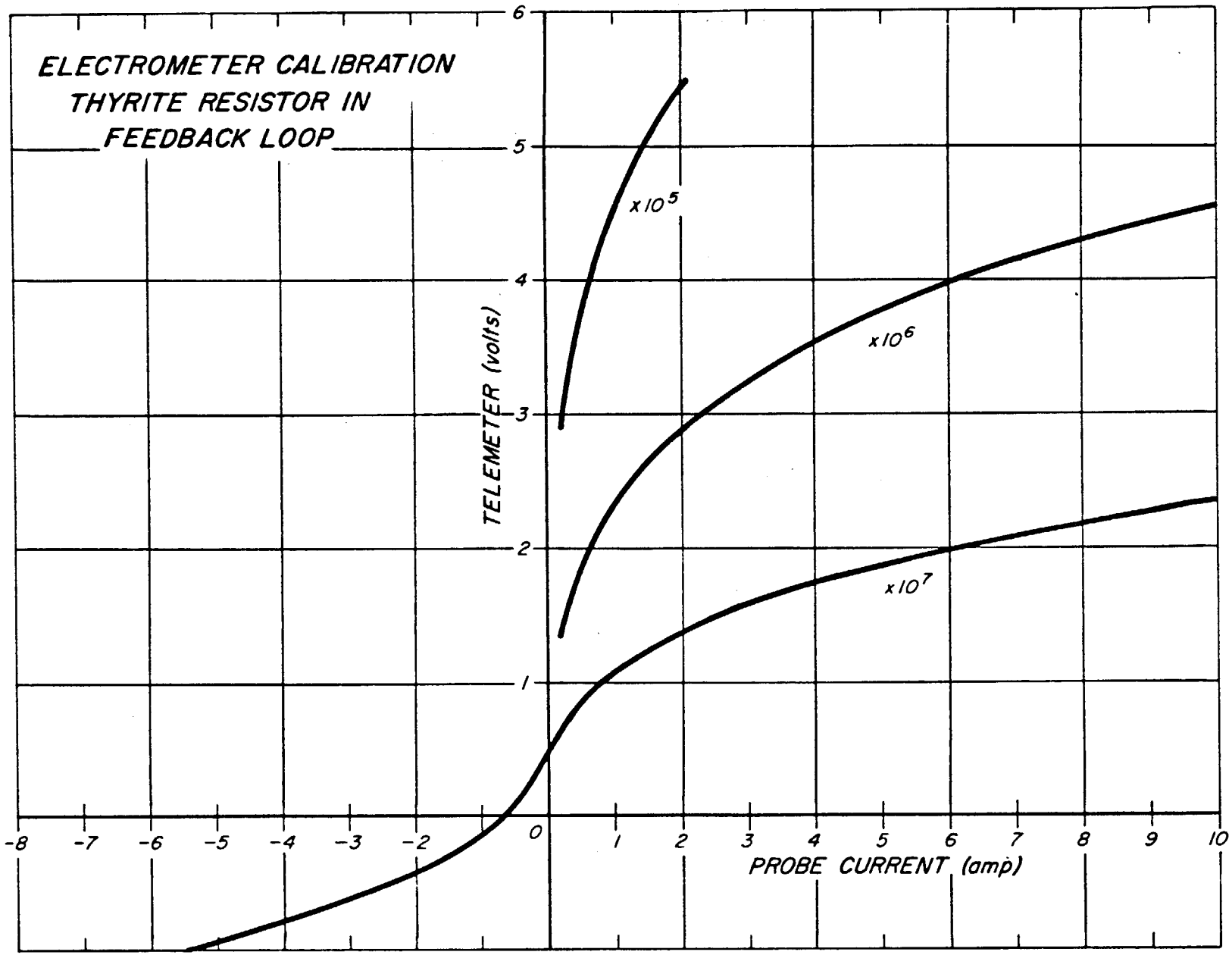
ELECTROMETER CALIBRATION
THYRITE RESISTOR IN
FEEDBACK LOOP
TELEMETER (volts)
PROBE CURRENT (amp)
x10^5
x10^6
x10^7
6
5
4
3
2
1
-8
-7
-6
-5
-4
-3
-2
0
1
2
3
4
5
6
7
8
9
10
0C8184-11

Figure 6-6.

A magnetic pickup (Electro Products type 3015-HTB) generates a 500 c/s (nominal) signal from the D.C. motor which is driving the precision potentiometer. The gear ratio between motor shaft to potentiometer shaft (55 to 1) and voltage applied across the potentiometer are arranged so that each cycle of the magnetic pickup corresponds accurately to a voltage increment of 0.040 volt in sweep voltage. This is true independently of the speed or variation in speed of the motor.

This 500 c/s signal with an amplitude of 50 millivolt is added to the output of each electrometer and the combined signal fed to the respective sub-carrier oscillator. The effect as seen on the telemetry record is equivalent to a marker pulse superimposed on the record of probe current and indicating voltage increments of 0.040 volt.

6.2 FLIGHT SUMMARY

Information taken from the post-flight summary (with corrections) follows:

IDENTIFICATION

Flight Number	:	10.51 CI
Wallops Model Number	:	G2-682
Engine/Motor Numbers	:	1st Stage 36613, 2nd Stage BP15-198-8
Rocket Type	:	Nike-Cajun
Number of Stages	:	Two
Place of Firing	:	Wallops Island, Virginia
Date of Firing	:	17 August 1961
Time of Firing	:	2206R (Eastern Standard Time)
Instrumenting Agency	:	Geophysics Corporation of America

BRIEF OF FLIGHT OBJECTIVES

Measurement of electron density and electron temperature in the lower ionosphere under nighttime conditions using the Langmuir probe technique. Two independent probes are carried, one using a nose tip electrode, the other, an electrode on the side of the payload shell. Two magnetic aspect sensors and two temperature measurements are also in the payload. The corresponding measurements in the daytime ionosphere were successfully obtained on flight NASA 10.25, launched 8 December 1960 from Wallops Island.

FLIGHT INFORMATION (FROM RADAR SKIN TRACK)

	Predicted	Observed
Peak Altitude:	82 statute miles	88 statute miles (141 km)
Peak Time :	178 seconds	185 seconds

FLIGHT INFORMATION (continued)

Ignition Data:	Time (sec)	Altitude (ft.)	Velocity (ft/sec)
Nike Bottom Stage	0	0	0
Cajun Stage	17.5	36,500	1,800
Burnout Data:			
Nike Bottom Stage	3.6	-	-
Cajun Stage	20.6	46,000	5,900

Impact Data:		Impact Location	
		Range	Azimuth
Nike Stage	90	18,000 ft.	98°
Cajun Stage	365	461,400 ft.	94°28'

Firing Angle (Launcher Setting)

Azimuth from True North (deg):	105°	(90° effective)
Elevation above Horizontal :	87.7°	(80° effective)

ROCKET INFORMATION

Total Rocket Measured Weight (Including Payload) 1591 lbs.
Propellant included in the above
Total Rocket Length: 322.2"
Individual Stage Weights and c.g.'s:

	Weight (lbs)	C. G. (in)	C. G. Reference	Total Component Length
Payload	58	-	-	65 1/2"
Cajun Stage 2	199	48 3/8	Nozzle Exit Plane	107.1"
Nike Stage 1	1,334	75 1/4	Nozzle Exit Plane	149.7"

ROCKET-BORNE EQUIPMENT

Upper Air Instrumentation:

Two Langmuir probes (nose and side electrode)
Two magnetic aspect sensors (longitudinal and transverse)
Two thermistors (payload temperatures)

ROCKET-BORNE EQUIPMENT (continued)

Telemetry Instrumentation : FM/FM 231.4 mc
Range Safety Instrumentation : None
Tracking Instrumentation : None
Miscellaneous Instrumentation:

Umbilical connector held by explosive bolt which is fired at 30 seconds before launch. No pyrotechnic devices in payload at launch.

GROUND-BASED EQUIPMENT

Telemetry Instrumentation : FM/FM
Range Safety Instrumentation: None
Tracking Instrumentation : Radar

PRELIMINARY RESULTS AND COMMENTS

Rocket Performance: Above Predicted
Comments:

Both peak height and impact range were above predicted values indicating above average performance of vehicle. The second stage precessed into a very slow flat spin (indicated by the magnetic aspect sensors) after launch. (NOTE: Radar reported extremely strong echo for 4 seconds at 104 seconds confirming the broadside position.) The vehicle completes one revolution in 97 seconds (precession period) while rolling about its longitudinal axis with a period of 21 seconds. The flat spin ends at 290 seconds as the vehicle begins to turn nose down on re-entry. On ascent the most rapid roll rate occurs at about 35 seconds when the roll period is 2.6 seconds.

Telemetry: Complete Data Recovery: Type: FM/FM

Comments: Strong signal from launch to impact. Occasional interference on 22 kc/s channel resulting from momentary malfunction of instrumentation on 40 kc/s channel.

PRELIMINARY RESULTS AND COMMENTS (continued)

Tracking Instrumentation:

Complete Tracking:	Type:	MIT Mainland Radar
	Type:	SPANDAR Radar
Adequate Tracking:	Type:	FPS-16
	Type:	584
	Type:	MOD II

Comments:

Complete tracking by two radars give good agreement. FPS-16 lost at 127 seconds which is about average for this type of vehicle.

Miscellaneous Instrumentation:

Trailing edges of two opposing Cajun fins were notched to increase radar cross section when viewed from rear by FPS-16. However, no improvement in tracking was obtained.

Upper Air Instrumentation:

Excellent data obtained from the Langmuir probe using the nose tip electrode. First measurements were obtained at 64 seconds and continued to 304 seconds (i.e., region above 74 km). The measurements indicate a well-defined E-layer with a broad peak between 95 and 110 km and a narrow layer (1 km thick) of much greater electron density centered at 102.5 km. This is presumably a Sporadic-E layer. Ascent and descent data agreement is excellent. No significant data was obtained from the probe using the side electrode although the internal calibration indicates that the instrument was operating properly.

The magnetic aspect and temperature measurements and the commutator (program unit) operated perfectly. The temperature in the electrometer

(encapsulated in foam) rose continuously from 26°C at launch to 30°C at splash. The temperature in the nose section (uncovered thermistor not touching the payload shell) reached 50°C at 230 seconds. At end of flight temperature has risen to 62°C.

6.3 ROCKET PERFORMANCE

The toal velocity and altitude of the second stage, obtained from FPS-16 radar data, is plotted in Figure 6-7. Ignition can be identifiedat 17.5 seconds after launch and burnout at 20.8 seconds. These times are very close to the nominal values for the igniter and motor. We note also that the performance of the vehicle was greater than predicted in spite of the use of relatively bulky antennas on the payload.

As with the previous rocket (10.25) the second stage precessed into a flat spin. The precessional motion (or coming) as shown by the longitudinal magnetometer is first detected at 35 seconds after launch when the spin period has a minimum value of 2.6 seconds.

On descent the second stage begins to turn nose down at 85 km and the motion is complete at 75 km. These heights are very close to the corresponding heights for payload 10.25.

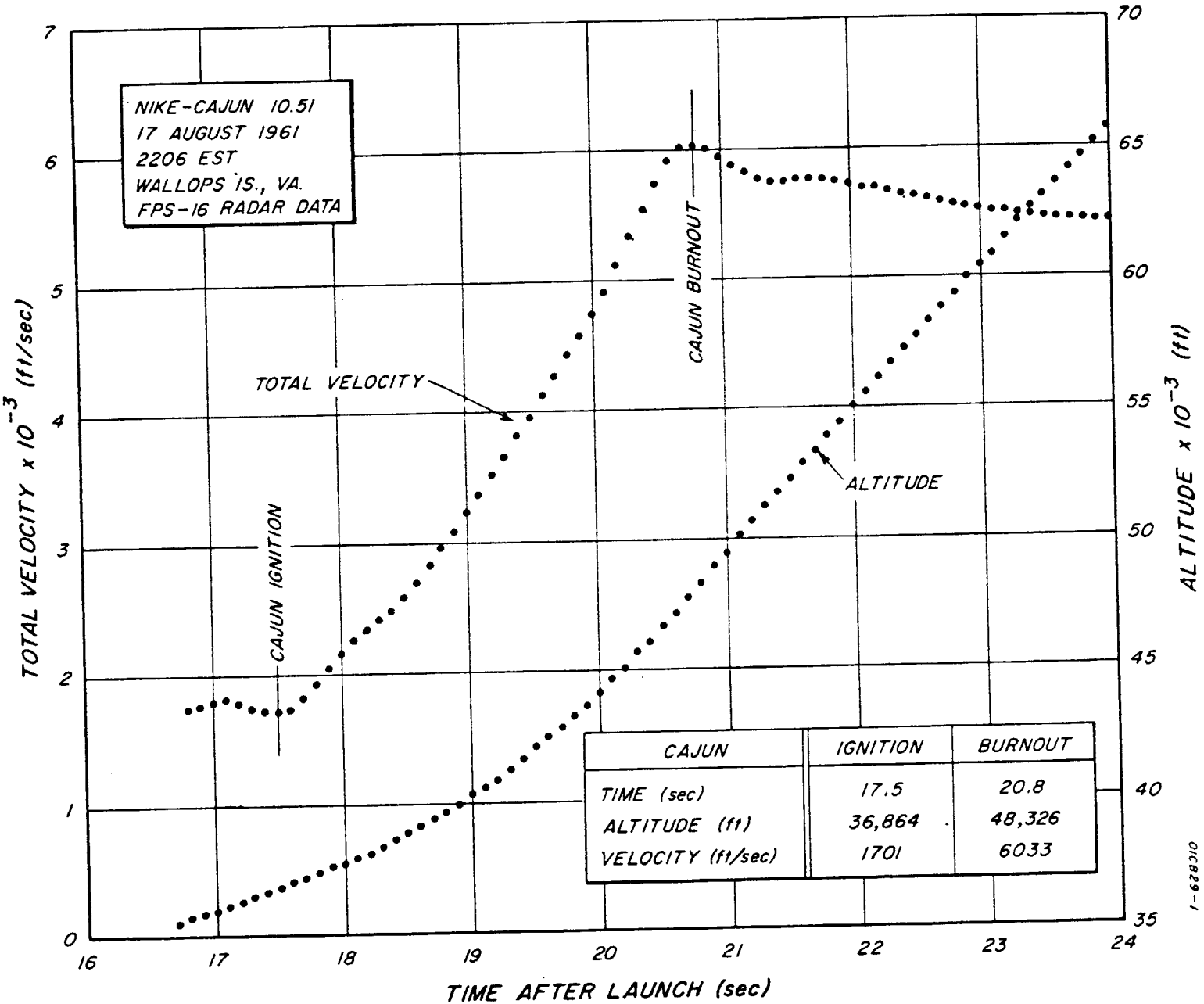

Figure 6-7. Total velocity and altitude showing second stage ignition and burnout.

6.4 PRELIMINARY RESULTS

A basic weakness of the conventional Langmuir probe technique is that each sweep of potential of the electrode leads to only a single value of electron density and electron temperature. This limits the usefulness of the technique in the study of the fine structure of the electron density profile. The sweep duration is limited by two factors: a) the time constant of the current measuring device, and b) the telemetry system itself. We have found it necessary to use a sweep of 0.5 second duration although this could perhaps be reduced to 0.1 second at the expense of elaborating the instrument. However, a resolution of 0.01 second (corresponding to 10 meters at a vehicle velocity of 1 km/sec) is desirable for accurate measurement of the profile of thin layers in the ionosphere. An alternative approach was realized after the flight of 10.25 and the data from that flight used to test the validity of the method. The method was incorporated in the design of the payload under discussion here (10.51) with very satisfactory results.

The method is experimentally very simple but somewhat more difficult to justify on theoretical grounds. It consists of changing the program of the voltage applied to the probing electrode from one of consecutive sweeps to a program in which occasional sweeps are separated by periods of fixed voltage. In 10.51, the program consists of a sweep voltage of -5 to +5 volt (duration 0.5 second) alternating with a fixed voltage of +2.70 volt (duration 0.5 second).

It had been found in the data of 10.25 that the current at a given potential (in that case +1.80 volt) was in a constant ratio with the current measured at space potential. This means that the current to the electrode at fixed voltage is proportional to electron density. (This depends on the observed fact that the electron temperature was nearly constant over the height range of interest.) This can be easily justified on theoretical grounds for two extreme cases: the very small sphere and the infinite plane electrode. It is also apparently true for other geometrical shapes over a limited range of electron density. Thus, it is excellent for studying the fine structure but cannot immediately be justified for obtaining complete profiles of the whole ionosphere.

The record obtained in the D and E-region from 75 to 115 km from the flight of 10.51 is shown in Figure 6-8. Here the calibration has been obtained by reference to individual sweeps (on a high-speed telemetry record), and the compressed scale is obtained by using a thyrite resistor as the feedback element in the electrometer. It should be noted that the ascent and descent profiles are separated in time and horizontal distance; at 102.5 km they are 182 second and 72 km respectively.

The general features of the profiles show a well-defined E-layer in the height range 96 to 107 km with a deep trough above it. At apogee (141 km), there is no sign of an increase of electron density toward the F-region. In the height range 120 to 140 km, the electron density varies irregularly with values of a few hundred per cm^3.

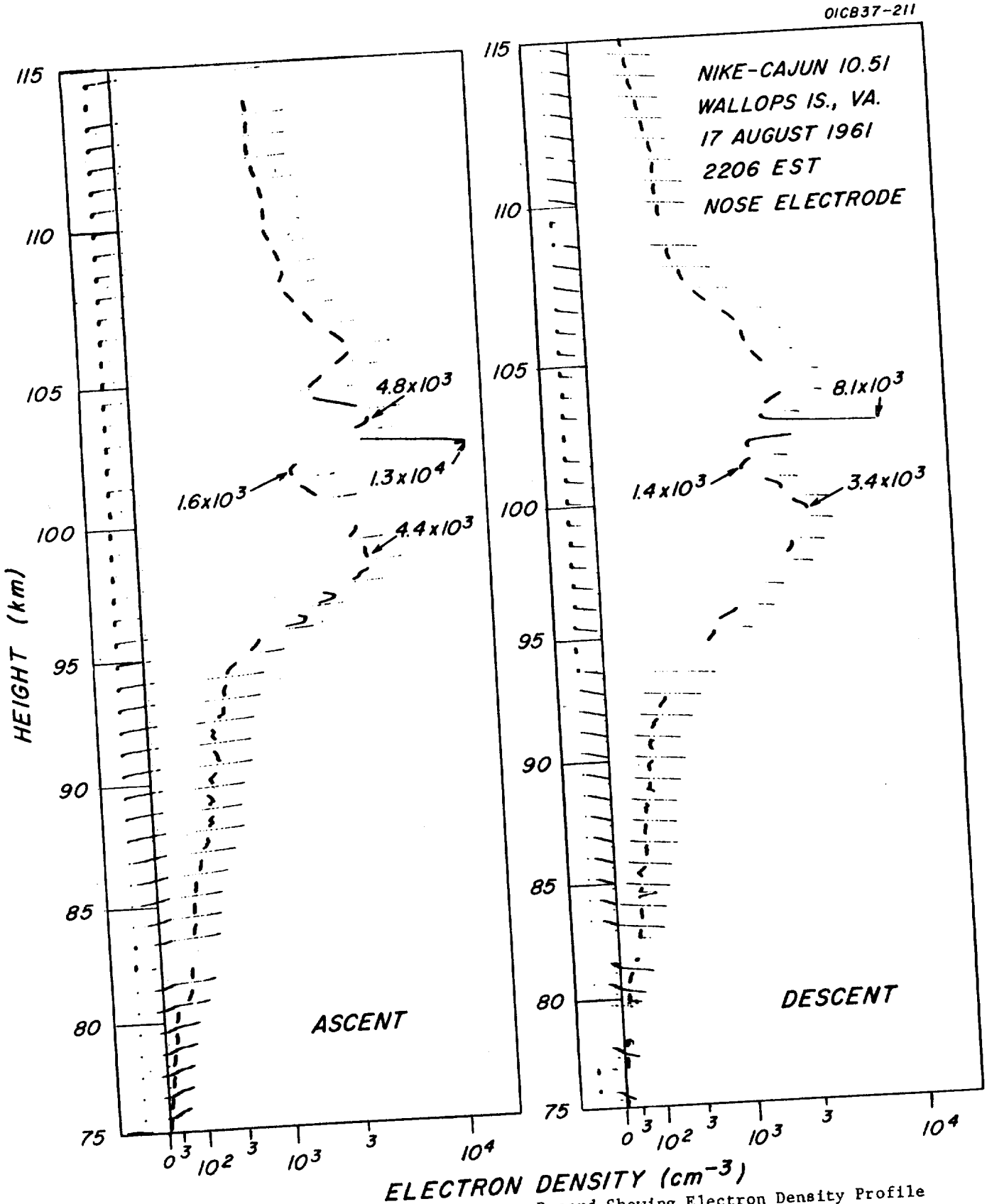

Figure 6-8. Sections of Telemetry Record Showing Electron Density Profile Between 75 and 115 km, 22:06 EST, 17 August 1961

A striking feature of these profiles is the appearance of a thin layer of high electron density at 102.5±0.1 km. The peak was measurable on ascent as $1.3 \times 10^4 cm^{-3}$ but the peak occurred during a voltage sweep on descent and the highest value of electron density that is measured is $8.1 \times 10^3 cm^{-3}$. A composite layer shape obtained by superimposing ascent and descent data shows that the thickness at half the peak electron density is 450 m. This layer has the characteristics of Sporadic-E, an identification which is supported by ionosonde data. However, the Sporadic-E layer as seen on the ionosonde has a constant virtual height of 110±1 km. The difference in height of about 7.5 km is far greater than instrumental errors allow and must be regarded as a serious discrepancy.

In passing, we note that the Sporadic-E, which had been particularly intense for several days prior to this rocket launch, coincided with a period of very little geomagnetic activity (i.e., a very quiet ionosphere), a correllation which has been pointed out by E. K. Smith as a feature of Sporadic-E in temperate latitudes.

Apart from the Sporadic-E layer, the other major structure does not correspond in height for ascent and descent although the range of electron density (1.4×10^3 to $4.8 \times 10^3 cm^{-3}$) is about the same.

Below the main E layer, several features may be noted. A small ledge (i.e., steep gradient) may be seen at 81 km and two small layers at 96 and 97 km. Also the small scale fluctuations in electron density between 87 and 93 km should be noted.

The general variability of electron density at night makes it difficult to obtain reliable values of electron temperature. It is, however, possible to select and analyze sweeps which occurred at times when the electron density was momentarily constant. Only three sweeps have produced good data on electron temperature. The altitudes and values are:

	Height	Electron Energy	Equivalent Temperature
Ascent	98.3 km	0.040±0.01 volt	T_e = 460±100°K
	105.8 km	0.035±0.01 volt	T_e = 410±100°K
Descent	99.5 km	0.035±0.01 volt	T_e = 410±100°K

The electron density in the higher part of the trajectory was too small for temperatures to be determined.

Although lower than daytime measurements of electron temperature, these values are still approximately twice as large as current estimates of the kinetic temperature of the neutral gas.

SECTION 7

NIKE-CAJUN 10.52

7.1 INTRODUCTION

The electron density profile obtained in the flight of Nike-Cajun 10.51 immediately shows the great value of the modified Langmuir probe technique. The payload of Nike-Cajun 10.52 which has been constructed as an identical twin of 10.51 was subsequently changed to allow better resolution of the ionospheric irregularities. The sweep of -2.4 to +2.7 volt (duration 0.5 second) alternates with a period of 1.5 seconds at fixed voltage (+2.7 volt). The time of launch was scheduled for two hours before dawn and launch took place on 27 October 1961 at 0435 EST. The data from this flight shows a well-defined E-layer with a deep trough above. The electron density profile also shows interesting irregularities.

7.2 FLIGHT SUMMARY

Information taken from the post-flight summary follows:

IDENTIFICATION

Flight Number : NASA 10.52 CI
Wallops Model Number: G2-685
Engine/Motor Numbers: 1st Stage 36637, 2nd Stage PV16-6-6
Rocket Type : Nike-Cajun
Number of Stages : Two (2)
Place of Firing : Wallops Island, Virginia
Date of Firing : 27 October 1961
Time of Firing : 0935Z
Instrumenting Agency: Geophysics Corporation of America
Instrumenting Agency Chief Scientist: Dr. L. G. Smith
NASA Rocket Vehicle Manager: J. A. Sterhardt
NASA Project Scientist: R. E. Bourdeau

BRIEF OF SLIGHT OBJECTIVES

The primary purpose of this flight is the measurement of electron temperature and electron density by the Langmuir Probe technique under nighttime conditions in the ionosphere.

FLIGHT INFORMATION*

	Predicted**	Observed
Peak Altitude:	82 statute miles	90.1 statute miles (146 km)
Peak Time :	178 seconds	187 seconds

Ignition Date: (Observed)	Time (sec)	Altitude (ft)	Velocity (ft/sec)
Bottom Stage	0	0	0
Stage 2	16.7	35,600	1,760

*Source: RS = Radar Skin Track

**Prediction based on flight weight - not estimated weight

	Time (sec)	Altitude (ft)	Velocity (ft/sec)
Burnout Data: (Observed)			
Bottom Stage	NA	NA	NA
Stage 2	20.3	48,700	5,890

Impact Data:	Time (sec)	Impact Location	
		Range	Azimuth
Bottom Stage	NA	NA	NA
Stage 2	371	315,700 ft.	86°

Launcher Setting:	Actual	Effective
Azimuth from True North (deg):	97°	90°
Elevation above Horizontal :	76.6°	80°

ROCKET INFORMATION

Second Stage Measured Weight (Including Payload) 260 lbs.
Second Stage Measured C.G. (Including Payload) 65 7/8 NEP
(Propellant included in the above)
Individual Stage Weights and c.g.'s:

	Weight (lbs.)	C.G. (in.)	C.G. (Ref)	Total Component Length
Payload	58			
Stage 1	1,334.5	75 1/4	NEP	
Stage 2	202			107"
Total	1,594.5			

ROCKET-BORNE EQUIPMENT

Telemetry Instrumentation: FM/FM 231.4 mc

GROUND-BASED EQUIPMENT

Telemetry Instrumentation: FM Ground Station 231.4 mc
Tracking Instrumentation: Radar: 584, MOD II, FPS-16, SPANDAR
Special Facilities (Include upper air instrumentation): Ionosonde

PRELIMINARY RESULTS AND COMMENTS

Rocket Performance: Above Predicted
Tracking Instrumentation: Complete Tracking: Type: MOD II, FPS-16, SPANDAR, 584
Upper Air Instrumentation:

Excellent results were obtained from the nose probe of the structure of the D and lower E-region. Measurments were obtained from 62 sec. to 314 sec. (i.e., heights above 73 km). A sharply defined lower edge for the main ionization was found at 88 km. A major peak of electron density (perhaps Sporadic-E) was found at 112 km on ascent and again on descent. Additional peaks of almost equal magnitude were found at 106 km on ascent and at 101 km on descent. The side probe did not give significant data. Magnetometers show a roll rate of 0.4 rps during passage through the ionosphere with no coning. This flight and the preceding one (10.51) show the feasibility of studying Sporadic-E by small sounding rockets.

7.3 ROCKET PERFORMANCE

The total velocity and altitude of the second stage obtained from FPS-16 data is shown in Figure 7-1. Ignition occurs at 16.7 sec after launch and burout at 20.3 sec. These times are slightly earlier than the nominal times of 17.5 and 20.8 seconds but well within the specifications of the ingiter.

The performance of the three Nike-Cajuns launched during this NASA contract show a remarkable consistency in performance. The figures given in Table7-1 are derived from tabulated radar data and may differ slightly from figures given in the post-flight summaries. The variation in trajectory indicated by apogee and impact is largely due to the effect of lower atmosphere winds which result in different effective launch angles.

The motion of Nike-Cajun 10.52 differs from the previous two rockets in one very important respect. Whereas the earlier vehicles had precessed into a slow flat spin, this third vehicle remained nose-up with the relatively rapid spin rate of 0.4 rps, until, at about 85 km on descent, it began to turn nose down. The data from the Langmuir probe shows no effect attributable to the nearly tail-first descent of the vehicle and confirm the decision to use the tip of the nose cone (11^{o} included angle) as the probing electrode in this investigation; it has shown a remarkable independence of vehicle orientation.

An important conclusion to be drawn from these and other flights of Nike-Cajuns is that the spin rate and attitude are unpredictable and due allowance must be made in designing experiments using this vehicle.

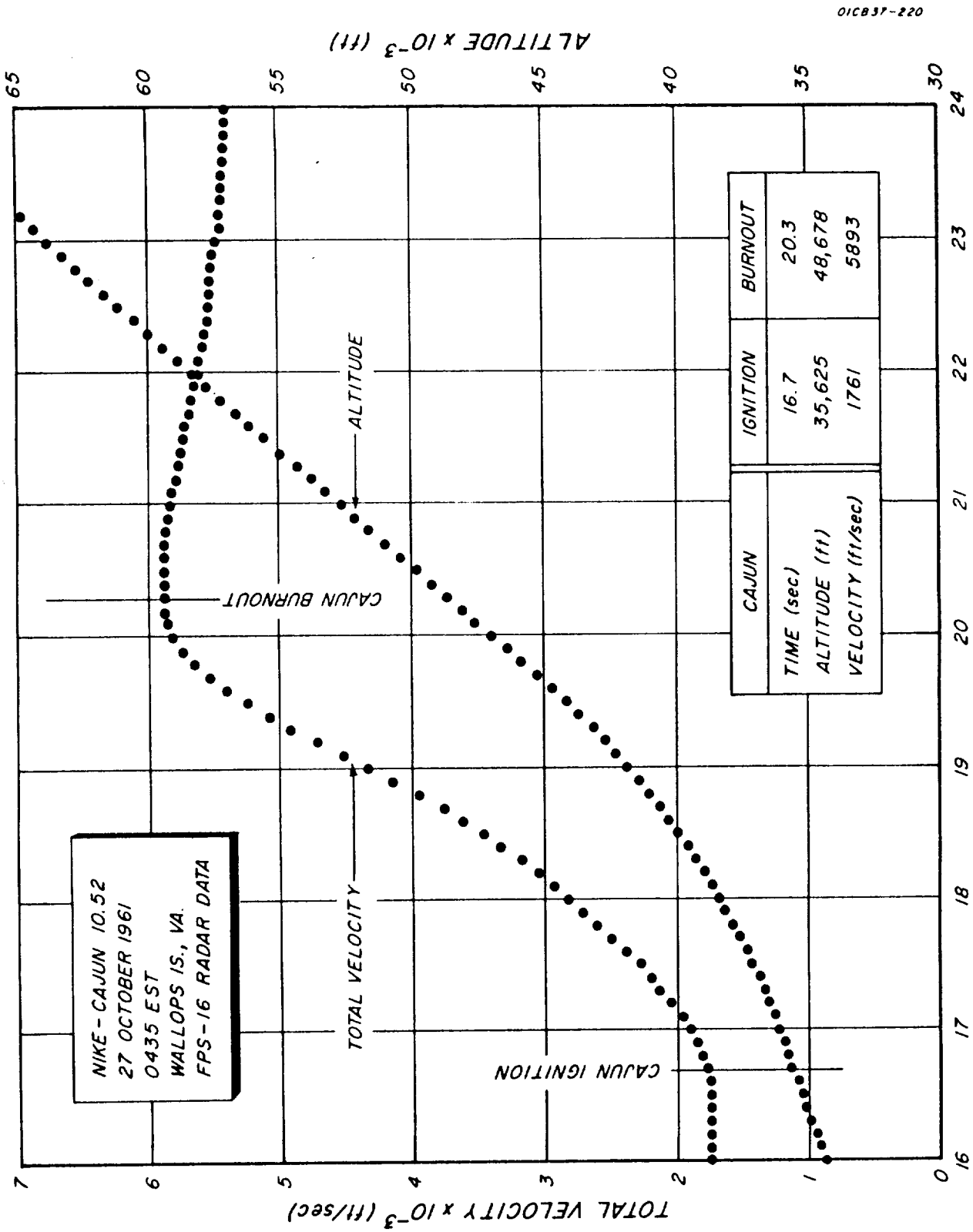

Figure 7-1. Total velocity and altitude showing second stage ignition and burnout.

TABLE 7-1

NIKE-CAJUN PERFORMANCE SUMMARY

NASA Flight Number	10.25	10.51	10.52
Date of Firing	8 December 1960	17 August 1961	27 October 1961
Time of Firing	1152 EST	2206 EST	0435 EST
Payload Weight	60 lb	58 lb	58 lb
Peak Altitude	153 km	141 km	147 km
Peak Time	193 sec	185 sec	188 sec
Impact Range	31.5 km	140 km	96 km
Impact Time	379 sec	365 sec	371 sec
Spin* Period	8.3 sec	21 sec	2.5 sec
Precession* Period	77 sec	97 sec	NONE

*At heights above 85 km

7.4 PAYLOAD TEMPERATURE

The shortage of data on the environment encountered by instruments within the payload prompted the inclusion of thermistors in the payloads of Nike-Cajuns 10.51 and 10.52. One thermistor was included with the electrometer to represent a well-protected position while the second was attached to an aluminum block inside but not touching the nose cone.

The thermistor with the electrometer showed a temperature rise of 3.5°C during the flight. The rise is, however, almost entirely accounted for by internal heating; a pre-flight test showed a temperature rise of 3.0°C during an equal length of time. It is concluded that in the cylindrical section of the payload, a component may be thermally insulated by foam potting compound and a temperature rise of less than 1°C encountered during a typical Nike-Cajun flight.

The rise in temperature of an aluminum block inside the nose cone is shown in Figure 7-2. One side of the aluminum block faced the inside of the nose cone with about 1 inch separation. The other sides of the block were thermally insulated by foam potting compound. The ratio exposed area/mass was increased for the second flight by a factor of about 3.5 resulting in a much greater temperature rise. These data illustrate the value of heat sink in limiting the temperature rise of equipment which cannot be thermally insulated from the nose cone.

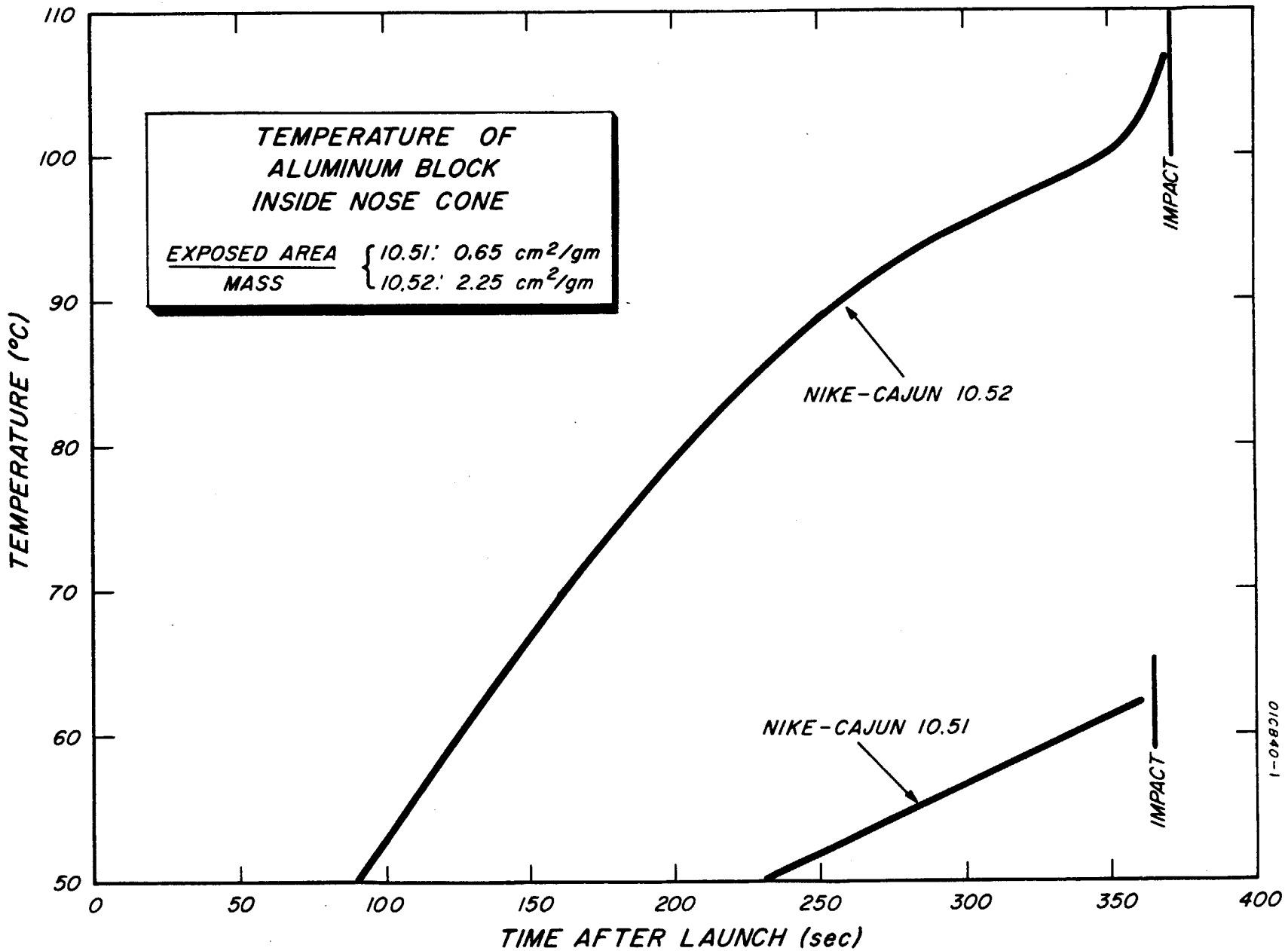

Figure 7-2. Temperature of an Aluminum Block Inside the Nose Cone Showing Effect of Heat Sink

SECTION 8

AEROBEE 4.48

The essential simplicity of the Langmuir probe technique for measurement of electron density and electron temperature make it ideal for inclusion in payloads where the primary is some other related atmospheric property. It was for this purpose that two instrument packages complete with nose tip electrode were designed and built. It was decided to make the configuration compatible with an Aerobee payload because of the relatively large volume which is rarely completely used. The tip electrode, Figure 8-1, having a 20^{o} included angle was designed to replace the standard Aerobee nose tip and the instrument shaped to fit in the conical region adjacent to the tip.

The instrument was finally assigned to Aerobee 4.48. This flight was primarily a flight test of a payload recovery system, a feature not required by the probe since the data is telemetered. The payload carried other scientific experiments but none related to the ionosphere.

The vehicle was launched at 0743 EST from Wallops Island, Virginia, and reached a peak altitude of 200 km. The recovery system performed

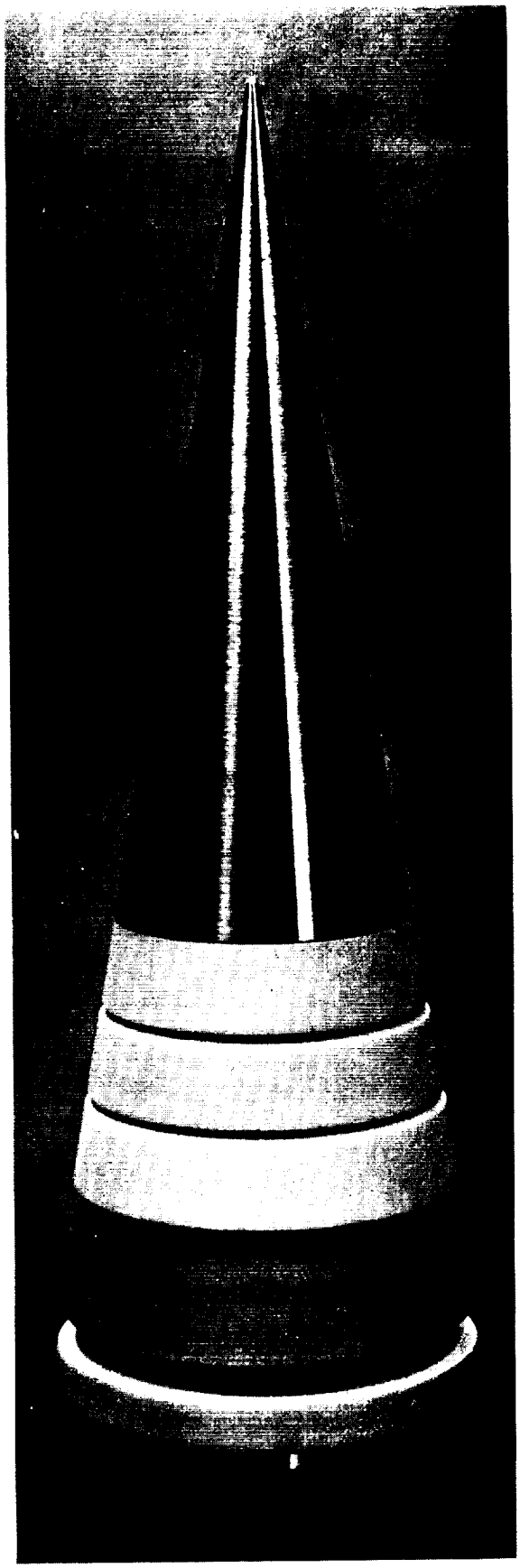

Figure 8-1. Langmuir probe for Aerobee nose tip.

properly and the payload was taken from the sea 27 minutes after launch. The payload had been sealed (for buoyancy) and the instrument package was recovered in perfect condition. In fact, in view of its position in the forward part of the nose cone, it is remarkable that no sign of heat damage could be found.

The most remarkable feature of the data from this flight is the occurrence of a Sporadic-E layer. The Wallops Island ionosonde had recorded E_s present on each observation taken at 5 minute intervals from 0600 to 0845. During the rocket flight the value of fE_s was steady at 5.2 Mc/s. The electron density profile, Figure 8-2, shows a very sharp lower boundary rising from 8.8×10^4 cm^{-3} to 2.5×10^5 cm^{-3}, a factor of 2.8 in 900 m. The upper boundary is less steep. The whole layer is contained in the height range 102.0 to 105.0 km.

The telemetered signal on this flight was poor. However, seven current-voltage sweeps were obtained which were of sufficiently good quality to derive a value of electron temperature. These are given in Table 8-1. Fortunately one of these fell within the Sporodic-E layer and indicated a surprisingly low temperature. The temperatures generally support the increase of electron temperature with height but the data is meager.

An unusual feature of the data on this flight was the low values of probe current observed on descent. The rocket is fired at an effective elevation angle of 88°. This results in the tip probe being within the rarefied region of the vehicle as it descends nearly tail

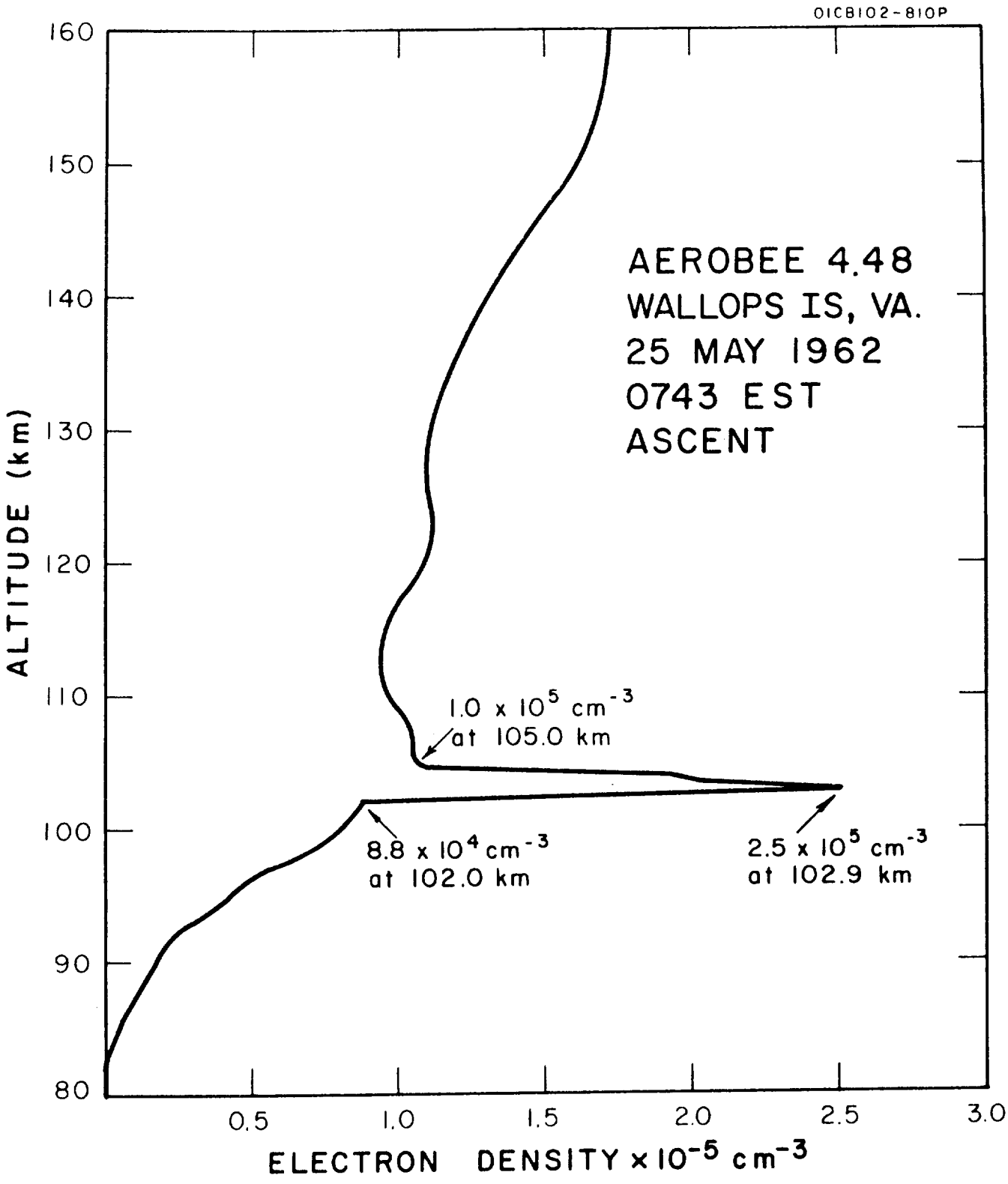

Figure 8-2. Electron density profile.

TABLE 8-1

ELECTRON TEMPERATURE DATA AEROBEE 4.48

Height	Electron Temperature
104 km (in E_s layer)	$300^{\circ}K \pm 100^{\circ}K$
110 km	$700^{\circ}K \pm 100^{\circ}K$
119 km	$350^{\circ}K$
162 km	$1280^{\circ}K$
180 km	$1510^{\circ}K$
196 km	$2100^{\circ}K$
200 km (apogee)	$1620^{\circ}K$

first (actually 4^{o} angle of attack). Thus it is to be expected that the greater the velocity of the vehicle the greater the reduction in current due to rarefaction of the plasma. This interpretation is supported by Figure 8-3 in which the ratio of current measured on descent to that measured on ascent at the same height is plotted against rocket velocity at that height. This rarefaction effect is not observed on the Nike-Cajun flights because of the smaller cone angle (11^{o} instead of 20^{o}) and the lower effective launch angle (80^{o} instead of 88^{o}).

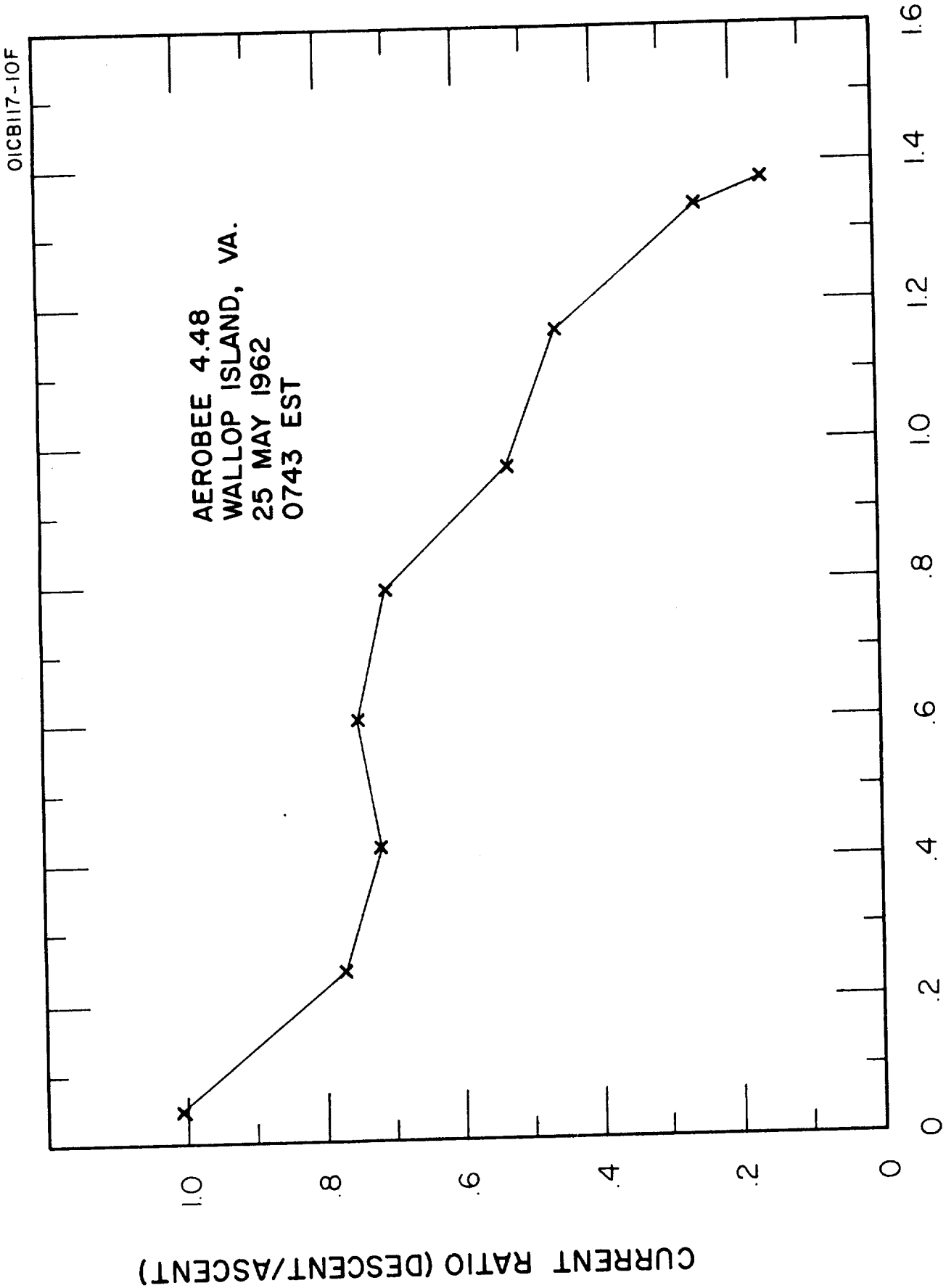

Figure 8-3. Affect of rarefaction in the wake.

SECTION 9

NIKE-APACHE 14.31

An instrument identical with the one flown on Aerobee 4.48 was included in the payload of Nike-Apache 14.31. The only other experiment on this vehicle was a C.W. propogation experiment prepared by S. J. Bauer. The primary objective of the flight was to compare the two techniques by simultaneous measurement of electron density. The propagation experiment used frequencies of 73.6Mc/s and 24.5Mc/s, transmitting from the rocket to a ground station at Wallops Island. The higher frequency transmitted was also used to telemeter the probe signal using an FM/AM system (i.e. using a subcarrier oscillator to amplitude modulate the transmitter carrier).

The use of the FM/AM system resulted in a poor quality telemetry signal. It is realized, in retrospect, that the addition to the payload of a separate telemetry transmitter (costing about $600) using the FM/FM system would have been preferable. As it was the signal was too noisy to allow accurate analysis of the current-voltage characteristics and hence no reliable data on electron temperative was obtained.

The record is clear enough to obtain the probe current at fixed voltage as a function of height.

The rocket was launched from Wallops Island Virginia at 1006 EST in 16 October 1962 and attained a peak height of 166 km. Probe current was first detected at about 55 km altitude remained small up to 65 km then started increasing steadily. At 73.5 km the current suddenly dropped to zero and remained near zero until it suddenly recovered at an altitude of 84.5 km. The current then increases irregularly in general agreement with other day time profiles. The descending portion of the flight gave a poor signal and it is not possible to say denfinitely whether the reduction of probe current between 73.5 km and 84.5 km occurred on descent. The reduction of probe current is associated with RF breakdown of the lower frequency transmitter (power 1.5 watt, nominal). (This was confirmed on a later flight where the transmitter was operated at reduced power during this part of the flight). R.F. breakdown apparently causes the potential of the vehicle to become a few volts negative, (greater than -2.7 volts) so that even with a potential of 2.7 volt applied between probe and rocket body the probe is still slightly negative with respect to the plasma.

The profiles of electron density obtained by the two techniques are shown in Figure 9-1. The scaling factor used for the probe experiment is determined by the Elayer critical frequency to be: 1.15×10^{-6} amp $\equiv$ 1.0×10^{5} electrons/cm^3. The two techniques agree

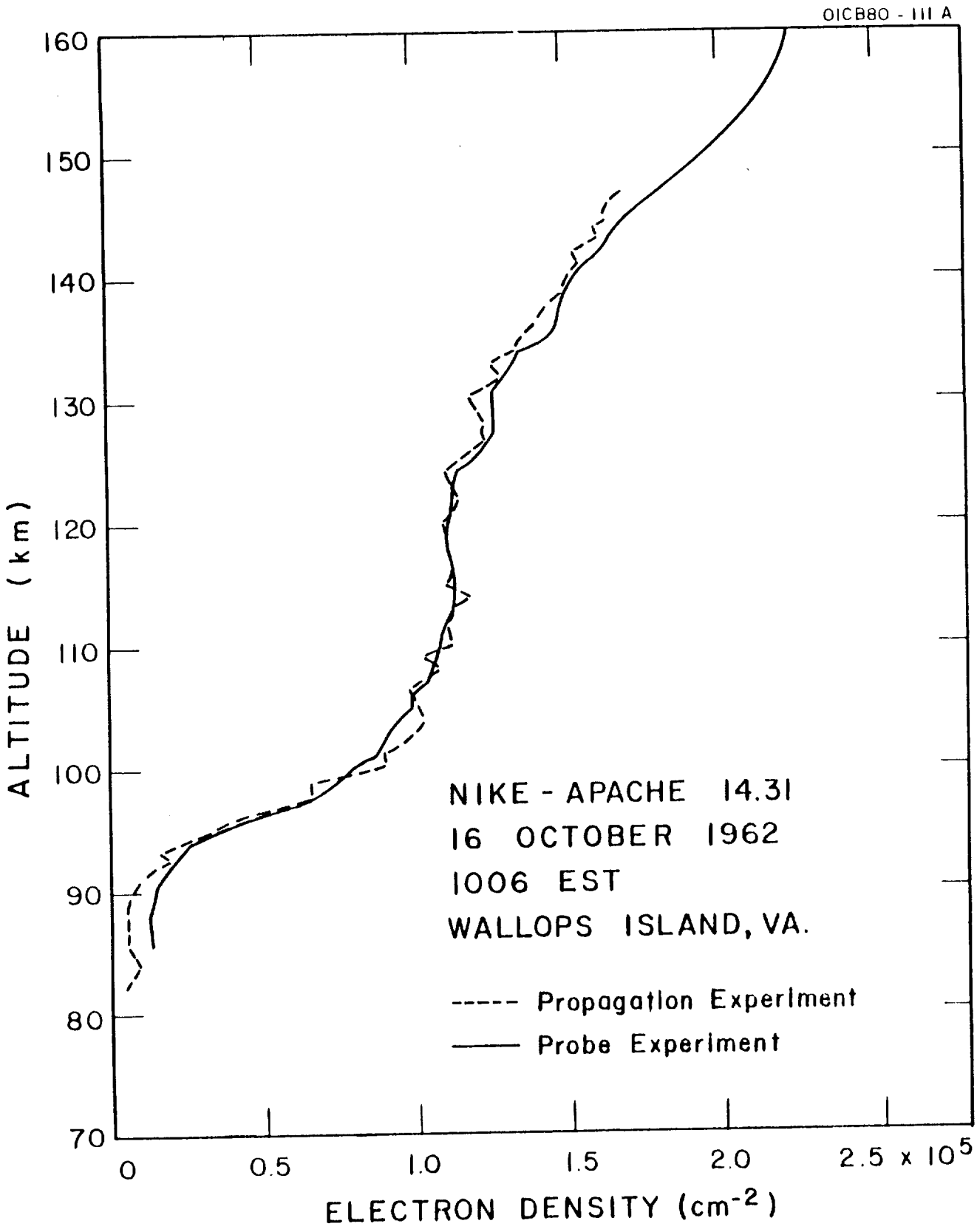

Figure 9-1. Compilation of propagation and probe techniques.

very well as to the general shape of the profile. The propogation experiment appears to show a more irregular profile than does the probe experiment but this is attributable to scatter of the data points and it is felt that the probe experiment gives a more accurate representation of the detailed structure of the region.

Below 90 km the probe current is higher, by a factor of two, than would be indicated by the scaling factor. The difference is too large to be an experimental error. Assuming that the electron density indicated by the propogation experiment is correct the discrepancy may be interpreted to mean either (a) that the scaling factor is not the same below 90 km as the one above that height or (b) that the probe current is not exactly proportional to electron density over a wide range of electron density.

SECTION 10

CONCLUSIONS AND RECOMMENDATIONS

The most significant deviation from Langmuir probe theory which has been encountered concerns the actual value of the electron random current density. The observations indicate values that are lower than the theoretical values by a factor approaching an order of magnitude. Some uncertainty is introduced by the difficulty of identifying exactly the point at plasma potential but this is not enought to account for the low electron current. It is believed that the explanation of the discrepancy can be attributed to the effect of the earth's magnetic field. This point is by no means cleared up and, pending further evidence, either experimental or theoretical, the probe is being used in an empirical manner. The measurement of electron temperature is remarkably independent of such factors as electrode geometry and the geomagnetic field and the technique is used with confidence.

The lowest height to which the Langmuir probe mode of operation is valid has not been established definitely. The high gas density and low electron density below 90 km the simple probe theory in the

D region but there is no clear indication in the actual measurements where the height limit is to be placed. In fact acceptable profiles of electron density down to 50 km are obtained by ignoring the restrictions and applying Langmuir probe theory. The significance of the D region in radio communication, particularly under conditions of high absorption (radio blackout), make the D. C. probe an important instrument for use in the lowest region of the ionosphere and further investigation of its use is indicated.

The most direct approach is to compare the probe with an independant technique carried on the same rocket. One possibility is to use the C. W. propogation technique, essentially repeating the flight of Nike-Apache 14.31. In order to get sufficiently high electron densities in the D region the experiment would be restricted to a polar blackout condition. It is feasible to compare the two techniques as low as 60 km under favorable circumstances.

In the normal D region it is possible that a differential absorption experiment will give a significant check on the operation of a D. C. probe. It has already been proposed to combine the two experiments on a payload and it is hoped to launch the first rocket during early 1964.

The D. C. probe is an extremely valuable instrument for sounding rockets in the ionosphere. It is very simple in construction, requiring no changes in a standard payload housing and consequently

is highly reliable. The greatest advantage of the instrument vis-a-vis other methods of measuring electron density in the ionosphere is the ability to resolve fine structure in the ionosphere. This shows up most strikingly the steep gradients that are typical of Sporadic E layers but has also revealed many other irregularities of the electron density profile.

It appears that irregularities are characteristic of the ionosphere up to 90 km during the day and up to 120 km at night. Their existance may be implied from data obtained with partial reflection sounders. They make possible the ionospheric scatter method of radio communication.

The two nighttime flights established the feasibility of a direct measurement of the height of Sporadic E layers. This has been exploited on a subsequent project (NASw-489) which is, in part, a study of the role of wind shear in the formation of Sporadic E layers. Using the D. C. probe on Nike-Cajuns (10.99, 10.108 and 10.109) launched shortly before the wind structure was measured using the sodium vapor technique it was found that layering tended to be associated with a particular type of wind structure. However not all features of the structure of the E region at night can be attributed to the action of wind shear. Other phenomena must be involved. One that is considered to be important is the action of meteors. This requires further investigation.

The D. C. probe is also being used in a project (NASw-500), now in progress, which is an investigation of the ionosphere during a solar eclipse. The payload in this case included instrumentation to measure solar radiation: a narrow band of ultraviolet including Lyman-α (1216A) and a band of X-rays (44-60A). The payloads (Nike-Apache 14.86 and 14.87) have been flown to test the equipment and a series of six will be launched at Fort Churchill during the solar eclipse of 20 July 1963. The primary objective of the investigation is a determination of the rate coefficient for the loss process for electrons in the D and E regions.

A related experiment which it is felt should be the next project to be undertaken is a study of the transition regions at sunset and sunrise. This has become more important in view of the rather unexpected structure found at night. It is not possible to explain the change of structure in terms of a recombination (or attachment) process. A series of electron density profiles around sunset and around sunrise would provide basic information for determining the nature of the processes involved.

It is believed that this project has established a basis for using the Langmuir probe technique the ionosphere and has shown the value of the instrument in rocket investigation.

APPENDIX A

DOUBLE PROBE MEASUREMENT OF CONDUCTIVITY

The rocket carrying an electron probe is, in general, not at the same potential as the plasma in which it is immersed. This leads to the so-called "floating double probe" method of measurement, developed by Johnson and Malter for the Langmuir probe, and derived below for conductivity measurements.

Consider a double probe system, Figure B-1a, consisting of a small spherical electrode A_1 and a large spherical electrode A_2, immersed in a plasma with polar conductivities σ_- and σ_+. A potential V is applied between the electrodes (the polarity being such that the small electrode is positive with respect to the large electrode) and a current I observed to flow between them. V and I are the two quantities measured experimentally.

The current of negative ions (including any electrons) into A_1 must equal the current of positive ions into A_2. An equilibrium condition is reached at which A_1 is at a potential V_1, and A_2 at a potential V_2, both measured with respect to the plasma potential; V_1 being positive and V_2 negative, Figure B-1b. Thus

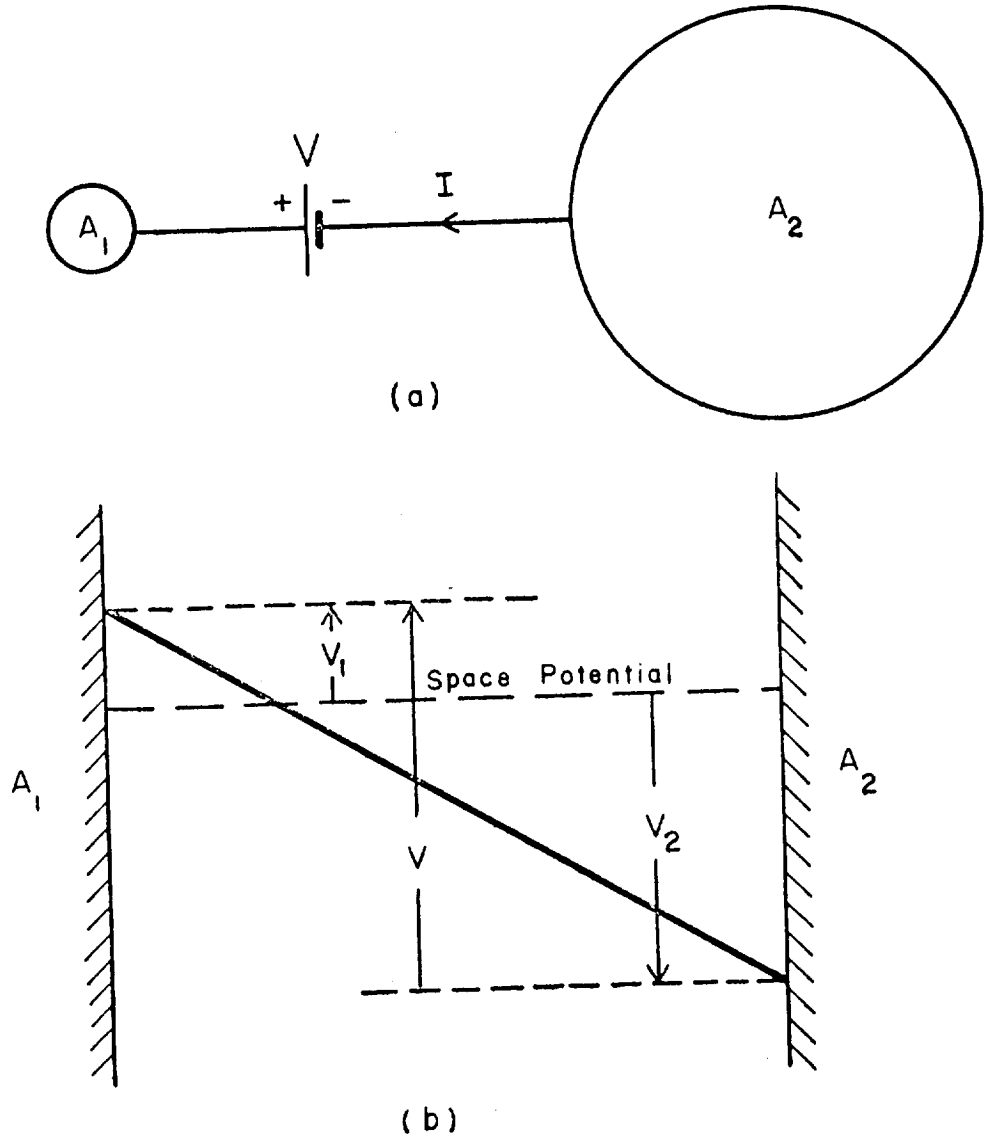

Double probe measurement of conductivity

Figure B-1.

$$V_1 - V_2 = V \tag{B-1}$$

By a theorem in electrostatics, if an electrode (of arbitrary shape) having a capacity C is immersed in a medium of conductivity σ, then, in the absence of space charge (electrode effect), the resistance R (potential divided by current into the electrode) is given by

$$C\,R = \frac{1}{4\pi\sigma} \tag{B-2}$$

This may be easily verified for the case of a spherical electrode.

In the double probe system, we have, therefore, at electrode A_1,

$$\frac{C_1 V_1}{I} = \frac{1}{4\pi\sigma_-} \tag{B-3}$$

where C_1 is the capacity of the isolated electrode A_1. Similarly for electrode A_2

$$-\frac{C_2 V_2}{I} = \frac{1}{4\pi\sigma_+} \tag{B-4}$$

where C_2 is the capacity of the isolated electrode A_2.

Combining (B-3) and (B-4)

$$\frac{V_1}{V_2} = -\frac{C_2}{C_1} \cdot \frac{\sigma_+}{\sigma_-} \tag{B-5}$$

Thus, from B-1

$$V_1 = \left(\frac{C_2 \sigma_+}{C_2\sigma_+ + C_1\sigma_-}\right) V \qquad \text{(B-6)}$$

$$V_2 = \left(\frac{C_1 \sigma_-}{C_2\sigma_+ + C_1\sigma_-}\right) V \qquad \text{(B-7)}$$

Substituting B-6 in B-5 and rearranging, we obtain, finally,

$$\left(\frac{I}{V}\right)_+ = \frac{4\ C_1C_2\sigma_+\sigma_-}{C_2\sigma_+ + C_1\sigma_-} \qquad \text{(B-8)}$$

The subscript is added to the ratio (I/V) to indicate this formula applies to positive values of V. The corresponding equation for negative values of V is

$$\left(\frac{I}{V}\right)_- = \frac{4\pi C_1C_2\sigma_+\sigma_-}{C_1\sigma_+ + C_2\sigma_-} \qquad \text{(B-9)}$$

If the ratio (I/V) is measured for positive and negative values of V and C_1 and C_2 are known (but unequal), it is possible to obtain σ_+ and σ_- using Equation B-8 and B-9. This is the basis of the double probe measurement of conductivity.

Two special cases are of particular interest:

(a) When σ_+ and σ_- are approximately equal (as when $\lambda = N_-/N_o$ is very large), then, assuming $C_2 \gg C_1$, the slopes of the I-V plots become .

$$\left(\frac{I}{V}\right)_+ = 4\pi C_1 \sigma_- \tag{B-10}$$

and

$$\left(\frac{I}{V}\right)_- = 4\pi C_1 \sigma_+ \tag{B-11}$$

Thus the positive and negative polar conductivities may be measured separately and only C_1 need be known accurately.

(b) When σ_- is much greater than σ_+ (as when λ is small), the equations become, approximately,

$$\left(\frac{I}{V}\right)_+ = 4\pi C_2 \sigma_+ \tag{B-12}$$

$$\left(\frac{I}{V}\right)_- = 4\pi C_1 \sigma_+ \tag{B-13}$$

In this case, for either polarity, the current is determined by the positive polar conductivity and the negative conductivity is not measured.

It will be noted that the slope for negative voltages is the same whether the negative component of the plasma consists of negative ions or electrons (or both). Thus the value of positive polar conductivity may be experimentally determined without any knowledge of λ for the plasma.

It is possible that the composition of the plasma may be determined by considering the ratio $(I/V)_+/(I/V)_-$:

For (a) (no electrons):

$$\frac{(I/V)_+}{(I/V)_-} = \frac{\sigma_-}{\sigma_+}$$

Whereas for (b) (no negative ions):

$$\frac{(I/V)_+}{(I/V)_-} = \frac{C_2}{C_1}$$

The latter is a (known) constant of the experiment. Thus a comparison of slopes for positive and negative voltages provides an experimental method of distinguishing the two cases and perhaps of evaluating λ.

The theory predicts a linear current-voltage characteristic, although with different slopes for positive and negative voltages. It is to be expected, however, that in practice this will be true only for sufficiently small currents. For larger currents the formation of space charge at the electrodes will reduce the slope. The characteristics will thus become curved as though towards a saturation current though not reaching one. An analysis of such an electrode effect by J.J. Thompson leads to a relation of the form

$$V = A\,I + B\,I^2$$

which is linear for small I but parabolic for large I.

Another important factor to be considered is the effect of photoemission from the surface of either electrode. The magnitude of the effect is not known with certainty, but in the D-region is probably about 2×10^{-9} amp per cm^2 for a surface normal to the solar radiation. This current flows when the electrode is negative with respect to space potential. The photoelectric current I_e (from the negative electrode) can easily be incorporated in the theory given above. The result is that the current-voltage characteristic is now broken into two linear parts corresponding to $I \geqslant I_e$ and $I \leqslant I_e$, Figure B-2. For $I \geqslant I_e$ the slope is as given before (B-8), while for $I \leqslant I_e$ the slope is greater, being

$$\frac{I}{V}_{+} = 4\pi C_1 \sigma_-$$

Again, these relations must be modified to incorporate the electrode effect.

The analysis has been presented above for unequal spheres physically separated but electrically connected. This geometrical arrangement is inconvenient for rocket launch especially if measurements are to be made below the D-region where atmospheric drag is considerable. It is proposed to use the double-probe conductivity method with the electrode arrangement already developed for the Langmuir probe experiment. In this the major part of the payload section and rocket casing form the larger electrode while the small electrode is alternately either a circular disc

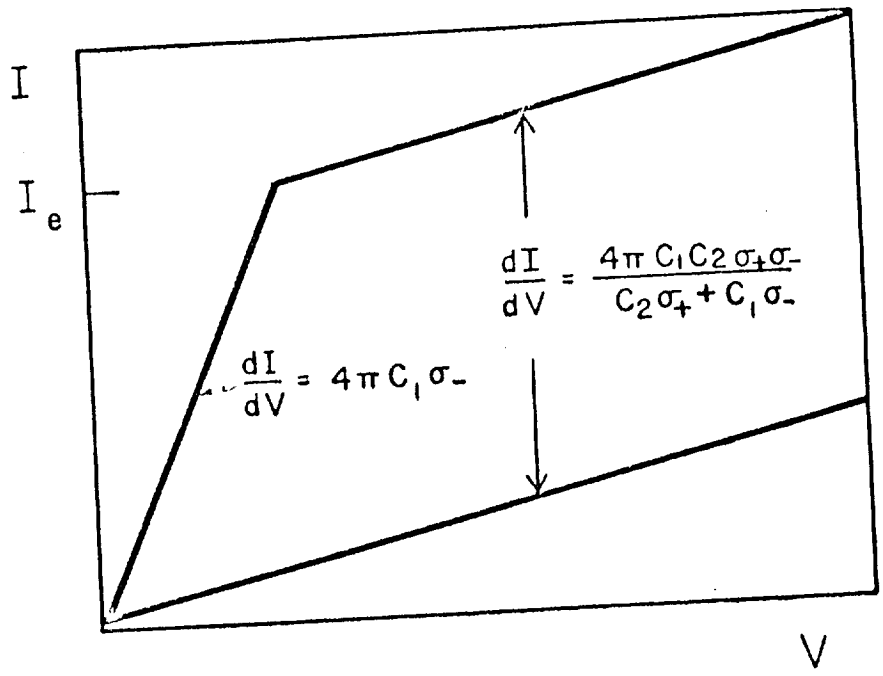

Effect of photoemission on I - V plot

Figure B-2.

(5 cm diameter) in the rocket skin or the top 25 cm of the nose cone. In this arrangement the aerodynamic shape of the rocket is preserved and a relatively simple construction evolved.

This geometrical arrangement makes for complication in determining the appropriate values of capacity to be substituted in Equations (B-8) and (B-9). A rough value can be obtained by assigning a characteristic length to each electrode, an average radius. For more accurate work, a calibration experiment must be performed by inserting the rocket in a wind tunnel or by using a model in an electrolytic tank. Initially, however, the validity of the technique can be rested by studying the variation with height of the (I/V) slopes for positive and negative voltages. This experiment can conveniently be combined with a Langmuir probe experiment.